BSIMSOIv4.6.0 MOSFET MODEL

Users' Manual

BSIM GROUP

May 2017

Department of Electrical Engineering and Computer Sciences

University of California, Berkeley, CA 94720

B4SOI Developers:

- Tapas Dutta
- Chetan Kumar Dabhi
- Shivendra Singh Parihar
- Chetan Gupta
- Harshit Agrawal
- Prof. Yogesh Singh Chauhan

Previous BSIMSOI/BSIMPD Developers:

- Mr. Hui Wan
- Dr. Xuemei Xi
- Dr. Samuel Fung
- Dr. Dennis Sinitsky
- Dr. Stephen Tang
- Dr. Pin Su
- Dr. Weidong Liu
- Dr. Robert Tu
- Prof. Mansun Chan
- Prof. Ping K. Ko
- Prof. Chenming Hu
- Dr. Wenwei Yang
- Dr. Chung-Hsun Lin
- Dr. Tanvir Hasan Morshed
- Dr. Darsen Lu
- Dr. Angada B. Sachid
- Dr. Navid Paydavosi
- Prof. Ali Niknejad
- Prof. Chenming Hu

BSIMSOIv4.x web site with BSIM source code and documents**:**

http://bsim.berkeley.edu/models/bsimsoi

Acknowledgement:

Chapter 1: Introduction

BSIMSOI is an international standard model for SOI (Silicon-On-Insulator) circuit design [20, 21]. This model is formulated on top of the BSIM3 framework [1]. It shares the same basic equations with the bulk model so that the physical nature and smoothness of BSIM3v3 are retained. Most parameters related to general MOSFET operation (non-SOI specific) are directly imported from BSIM3v3 to ensure parameter compatibility.

BSIMPD [18] is the Partial-Depletion (PD) mode of BSIMSOI. Many enhanced features are included in BSIMPD through the joint effort of the BSIM Team at UC Berkeley and IBM Semiconductor Research and Development Center (SRDC) at East Fishkill. In particular, the model has been tested extensively within IBM on its state-of-the-art high speed SOI technology.

BSIMPD, a derivative of BSIM3SOIv1.3 [2], has the following features and enhancements:

- Real floating body simulation in both I-V and C-V. The body potential is determined by the balance of all the body current components.

- An improved parasitic bipolar current model. This includes enhancements in the various diode leakage components, second order effects (high-level injection and Early effect), diffusion charge equation, and temperature dependence of the diode junction capacitance.

- An improved impact-ionization current model. The contribution from BJT current is also modeled by the parameter *Fbjtii*.

- A gate-to-body tunneling current model, which is important to thin-oxide SOI technologies.

- Enhancements in the threshold voltage and bulk charge formulation of the high positive body bias regime.

- Instance parameters (*Pdbcp, Psbcp, Agbcp, Aebcp, Nbc*) are provided to model the parasitics of devices with various body-contact and isolation structures [17].

- An external body node (the 6th node) and other improvements are introduced to facilitate the modeling of distributed body-resistance [17].

- Self heating. An external temperature node (the 7th node) is supported to facilitate the simulation of thermal coupling among neighboring devices.

- A unique SOI low frequency noise model, including a new excess noise resulting from the floating body effect [3].

- Width dependence of the body effect is modeled by parameters (*K1, K1w1, K1w2*).

- Improved history dependence of the body charges with two new parameters, (*Fbody, DLCB*).

- An instance parameter *Vbsusr* is provided for users to set the transient initial condition of the body potential.

- The new charge-thickness capacitance model introduced in BSIM3v3.2 [4], capMod=3, is included.

In BSIMSOIv4.0, based on BSIMSOIv3.2 [26] and BSIMv4.5.0 bulk model [27], we included the following features:

1. A scalable stress effect model for process induced stress effect, device performance becoming thus a function of the active area geometry and the location of the device in the active area;

2. Asymmetric current/capacitance model S/D diode and asymmetric S/D resistance;

3. Improved GIDL model with BSIM4 GIDL compatibility;

4. Noise model Improvements:

   1) Improved width/length dependence of flicker noise

   2) SPICE2 thermal noise model is introduced as TNOIMOD=2 with parameter NTNOI that adjusts the magnitude of the noise density

   3) Body contact resistance induced thermal noise

   4) Thermal noise induced by the body resistance network

   5) Shot noises induced by Ibs and Ibd separated

5. A two resistance body resistance network introduced for RF simulation;

6. Threshold voltage model enhancement:

   1) Long channel DIBL effect model added

   2) Channel-length dependence of body effect improved

7. Drain induced threshold shift (DITS) model introduced in output conductance;

8. Improved model accuracy in moderate inversion region with BSIM4 compatible Vgsteff;

9. Multi-finger device with instance parameter NF;

10. A new instance parameter AGBCPD to improve gate current for body contact;

11. A new instance parameter DELVTO representing threshold voltage variation;

12. FRBODY is both instance/model parameter.

    In BSIMSOIv4.1, the following features are added:

1. A new material model (mtrlMod);

2. Asymmetric GIDL/GISL model and new GIDL/GISL model (gidlMod);

3. A new impact-ionization current model;

4. An improved Coulombic scattering model for high k/metal gate;

5. An improved body-contact model to characterize the opposite-type gate;

6. A new ΔV_{bi} model to simplify the parameter extraction;

7. A new VgsteffCV model for C-V, which is similar to Vgsteff in I-V;

8. A new gate current component in body contact region;

9. An improved DITS model with more flexibility and better fit.

    BSIMSOIv4.2 up to v4.5 benefits from an extensive review of the code by the CMC members. A significant number of code implement issues/ errors are resolved and fixed in these versions through close interaction with many user companies. The voltage, temperature and charge derivatives are reviewed and improved as well. We believe users will greatly benefit from the improvements introduced in the latest version. In BSIMSOIv4.4 two new features were added (Vb check in SOIMOD=2 and fringe capacitance model enhancement), compared to BSIMSOIv4.3.1. The correlated thermal noise model along with many other improvements is introduced in version 4.5.0.

Note that BSIMSOIv4.6.0 model might not be backward compatible with its previous versions (BSIMSOIv4.4.0 or below).

Chapter 2: MOS I-V Model

A typical PD SOI MOSFET structure is shown in Fig. 2.1. The device is formed on a thin SOI film of thickness T_{si} on top of a layer of buried oxide with thickness T_{box}. In the floating body configuration, there are four external biases which are gate voltage (V_g), drain voltage (V_d), source voltage (V_s) and substrate bias (V_e). The body potential (V_b) is iterated in circuit simulation. If a body contact is applied, there will be one more external bias, the body contact voltage (V_p).
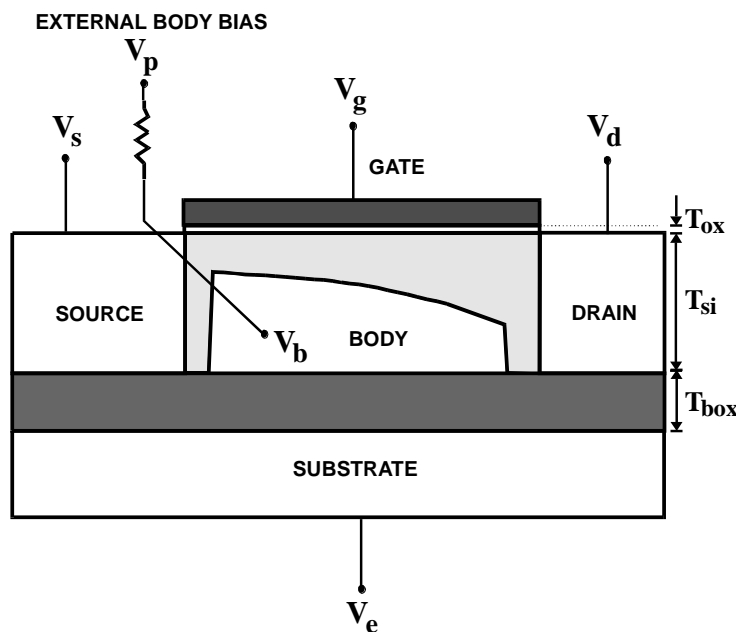
Fig. 2.1   Schematic of a typical PD SOI MOSFET.

Since the backgate (V_e) effect is decoupled by the neutral body, PD SOI MOSFETs have similar characteristics as bulk devices. Hence most PD SOI models reported [5, 6] were

developed by adding some SOI specific effects onto a bulk model. These effects include parasitic bipolar current, self-heating and body contact resistance.

BSIMPD is formulated on top of the BSIM3v3 framework. In this way, a lot of physical effects which are common in bulk and SOI devices can be shared. These effects are reverse short channel effect, poly depletion, velocity saturation, DIBL in subthreshold and output resistance, short channel effect, mobility degradation, narrow width effect and source/drain series resistance [1, 4].

2.1. Floating Body Operation and Effective Body Potential

In BSIMPD, the floating body voltage is iterated by the SPICE engine. The result of iteration is determined by the body currents [7, 18]. In the case of DC, body currents include diode current, impact ionization, gate-induced drain leakage (GIDL), oxide tunneling and body contact current. For AC or transient simulations, the displacement currents originated from the capacitive coupling are also contributive.

To ensure a good model behavior during simulations, the iterated body potential V_{bs} is bounded by the following smoothing function

$$T_1 = V_{bsc} + 0.5\left[V_{bs} - V_{bsc} - \delta + \sqrt{(V_{bs} - V_{bsc} - \delta)^2 - 4\delta V_{bsc}} \right], \ V_{bsc} = -5V \tag{2.1}$$

$$V_{bsh} = \phi_{s1} - 0.5\left[\phi_{s1} - T_1 - \delta + \sqrt{(\phi_{s1} - T_1 - \delta)^2 + 4\delta T_1} \right], \ \phi_{s1} = 1.5V \tag{2.2}$$

Here the body potential V_{bsh} is equal to the V_{bs} bounded between (V_{bsc}, ϕ_{s1}), and is used in the threshold voltage and bulk charge calculation. To validate the popular square root expression $\sqrt{\phi_s - V_{bsh}}$ in the MOSFET model, V_{bsh} is further limited to $0.95\phi_s$ to give the following effective body potential

$$V_{bseff} = \phi_{s0} - 0.5\left[\phi_{s0} - V_{bsh} - \delta + \sqrt{(\phi_{s0} - V_{bsh} - \delta)^2 + 4\delta V_{bsh}} \right], \ \phi_{s0} = 0.95\phi_s \tag{2.3}$$

2.2. Threshold Voltage in the High Vbs Regime

2.2.1. Linear Extrapolation for the Square-Root Expression

Using the V_{bseff} which is clamped to the surface potential ϕ_s, the square-root dependence $\sqrt{\phi_s - V_{bseff}}$ of the threshold voltage is ensured to behave properly during simulations [20]. However the real body potential may be larger than the surface potential in state-of-the-art PD SOI technologies. To accurately count the body effect in such a high body bias regime, we extend the square-root expression by

$$sqrtPhisExt = \sqrt{\phi_s - V_{bseff}} + s(V_{bsh} - V_{bseff}), \quad s = -\frac{1}{2\sqrt{\phi_s - \phi_{s0}}} \qquad (2.4)$$

where a linear extrapolation is employed for $V_{bsh} \geq 0.95\phi_s$. Notice that $sqrtPhisExt = \sqrt{\phi_s - V_{bseff}}$ for $V_{bsh} \leq 0.95\phi_s$.

2.2.2. Width Dependence of the Body Effect

In BSIMPD, the body effect coefficient K_1 is replaced by

$$K_{1eff} = K_1 \left(1 + \frac{K_{1w1}}{W'_{eff} + K_{1w2}} \right) \qquad (2.5)$$

to model the width dependence of the body effect. Notice that K_{1eff} approaches K_1 asymptotically as the effective channel width W'_{eff} increases. While the body effect coefficient will be determined by the parameters (K_{1w1}, K_{1w2}) when W'_{eff} becomes small so that the contribution from the channel-stop doping should be taken into account.

The complete equation of the threshold voltage V_{th} can be found in the Appendix C.

2.3. Bulk Charge Effect in the High Vbs Regime

The bulk charge factor in BSIMSOI4.0 is given as

$$A_{bulk} = 1 + \left(\frac{K_{1ox} \cdot \sqrt{1 + LPEB/L_{eff}}}{2\sqrt{(\phi_s + Ketas) - \frac{V_{bsh}}{1 + Keta \cdot V_{bsh}}}} \left(\frac{A_0 L_{eff}}{L_{eff} + 2\sqrt{T_{si}X_{dep}}} \left(1 - A_{gs}V_{gsteff} \left(\frac{L_{eff}}{L_{eff} + 2\sqrt{T_{si}X_{dep}}} \right)^2 \right) + \frac{B_0}{W'_{eff} + B_1} \right) \right) \qquad (2.6)$$

to accommodate the model behavior in the high body bias regime, which is important in PD SOI. The parameter *Ketas* acts like an effective increment of the surface potential, which can be used to adjust the A_{bulk} rollup with the body potential V_{bsh}. While the other parameter *Keta* is used to tune the rate of rollup with V_{bsh}. By using this new expression, the non-physical drain current roll-off due to the dramatic A_{bulk} rollup at high body bias can be avoided [20].

2.4. Asymmetric and Bias-Dependent Source/Drain Resistance Model

The total parasitic resistance at the source/drain terminal consists of two parts: (a) Bias independent and (b) Bias dependent. BSIMSOIv4.6 offers three different options to model parasitic resistance with variations on the way the bias dependent and bias independent parts of the parasitic resistance are handled . These options can be exercised by the switch RDSMOD as described below:

(a)RDSMOD=0: Bias dependent part of parasitic resistance is internal to the model, while bias independent part is external to the model. Additional nodes are created. This is same as BSIM3 model.

(b)RDSMOD=1: Both bias dependent and bias independent parts of parasitic resistances are external to the model. This option allows the source extension resistance Rs(V) and the drain extension resistance Rd(V) to be external and asymmetric (i.e. Rs(V) and Rd(V) can be connected between the external and internal source and drain nodes, respectively; furthermore, Rs(V) does not have to be equal to Rd(V)). This feature makes accurate RF CMOS simulation possible.

(c)RDSMOD=2: Both bias dependent and bias independent parts of parasitic resistances are internal to the model. This option assumes symmetric source/drain resistances. No additional nodes are created in this option.

The expressions for source/drain series resistances are as follows:

• *rdsMod* = 0 (Bias Independent External Series Resistance, Bias Dependent Internal Resistance)

$$R_{ds}(V) = R_{dsw} \frac{1 + P_{rwg} \cdot V_{gsteff} + P_{rwb} \cdot \left(\sqrt{\emptyset_s - V_{bseff}} - \sqrt{\emptyset_s} \right)}{\left(10^6 W'_{eff} \right)^{WR}}$$

$$R_s = R_{s,geo}, \quad R_d = R_{d,geo}$$

• **rdsMod** = 1 (External Rd(V) and Rs(V))

$$R_s(V) = \frac{RSWMIN + RSW \cdot \left[-PRWB \cdot V_{bs} + \dfrac{1}{1 + PRWG \cdot \left(V_{gs} - V_{fbsd}\right)}\right]}{\left(1e6 \cdot W_{eff}\right)^{WR} \cdot NF}$$

$$R_d(V) = \frac{RDWMIN + RDW \cdot \left[-PRWB \cdot V_{bd} + \dfrac{1}{1 + PRWG \cdot \left(V_{gd} - V_{fbsd}\right)}\right]}{\left(1e6 \cdot W_{eff}\right)^{WR} \cdot NF}$$

Where, $V_{fbsd} = \dfrac{k_B T}{q} \ln\left(\dfrac{N_{gate}}{10^{20}}\right)$ for NGATE larger than 0, otherwise, $V_{fbsd} = 0$.

• **rdsMod** = 2 (Bias Dependent Internal Resistance, $R_{ds}(V)$)

$$R_{ds}(V) = R_{s,geo} + R_{dsw} \frac{1 + P_{rwg} \cdot V_{gsteff} + P_{rwb}\left(\sqrt{\phi_s - V_{bseff}} - \sqrt{\phi_s}\right)}{\left(10^6 \cdot W'_{eff}\right)^{WR}} + R_{d,geo}$$

Where, The resistance $R_{s,geo}$ and $R_{d,geo}$ are simply calculated as the sheet resistance (RSH) times the number of squares (NRS, NRD):

$R_{s,geo}$ = NRS*RSH

$R_{d,geo}$ = NRD*RSH

2.5.   Single Drain Current Equation

After improving the V_{th} and A_{bulk} behavior in the high body bias regime, we can describe the MOSFET drain current by the same equation as BSIM3v3. The effective drain voltage V_{dseff} and effective gate overdrive voltage V_{gsteff} (i.e., effective $V_{gse} - V_{th}$ in Appendix C-5) introduced in BSIM3v3 [1] are employed to link subthreshold, linear and saturation operation regions into a single expression as

$$I_{ds,MOSFET} = \frac{I_{ds0}}{1 + \dfrac{R_{ds}I_{dso}}{V_{dseff}}}\left(1 + \frac{V_{ds} - V_{dseff}}{V_A}\right)$$

$$\beta = \mu_{eff} C_{ox} \frac{W_{eff}}{L_{eff}}$$

$$I_{dso} = \frac{\beta V_{gsteff}\left(1 - A_{bulk}\dfrac{V_{dseff}}{2\left(V_{gsteff} + 2v_t\right)}\right)V_{dseff}}{1 + \dfrac{V_{dseff}}{E_{sat}L_{eff}}}$$
(2.7)

Where, V_{dseff} is the effective source-drain bias (Appendix C-8), R_{ds} is the source/drain series resistance, μ_{eff} is the mobility (Users are suggested to check the details in Chap. 10 and Appendix C), E_{sat} is the critical electrical field at which the carrier velocity becomes saturated and V_A accounts for channel length modulation (CLM) and DIBL as in BSIM3v3. The substrate current body effect (SCBE) [8, 9] on V_A is not included because it has been taken into account explicitly by the real floating body simulation determined by the body currents, which will be detailed in the next chapter.

Chapter 3: Body Currents Model

Body currents determine the body potential and therefore the drain current through the body effect. Beside the impact ionization current considered in BSIM3v3, diode (bipolar) current, GIDL, oxide tunneling and body contact current are all included in the BSIMPD model [Fig. 3.1] to give an accurate body-potential prediction in the floating body simulation [18].

3.1. Diode and Parasitic BJT Currents

In this section we describe various current components originated from **B**ody-to-**S**ource/**D**rain (B-S/D) injection, recombination in the B-S/D junction depletion region, **S**ource/**D**rain-to-**B**ody (S/D-B) injection, recombination current in the neutral body, and diode tunneling current.
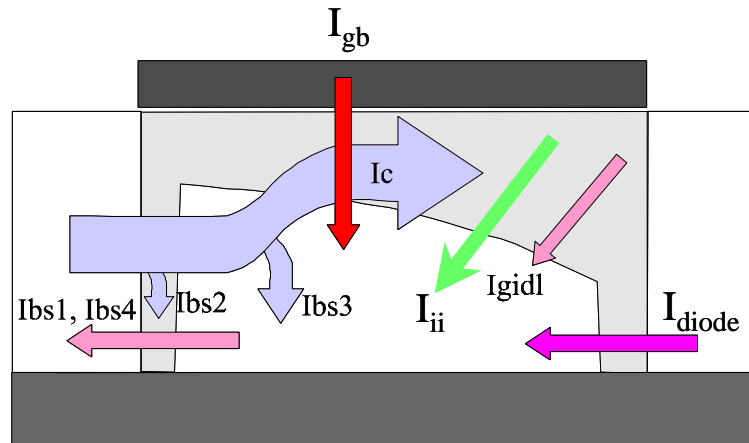
Fig. 3.1   Various current components inside the body.

The backward injection current in the B-S/D diode can be expressed as

$$I_{bs1} = W_{dios} T_{si} j_{difs} \left(\exp\left(\frac{V_{bs}}{n_{diodes} V_t} \right) - 1 \right)$$

$$I_{bd1} = W_{diod} T_{si} j_{difd} \left(\exp\left(\frac{V_{bd}}{n_{dioded} V_t} \right) - 1 \right)$$

(3.1)

Here $n_{diodes}, j_{difs}, W_{dios}, n_{dioded}, j_{difd}, W_{diod}$ are the non-ideality factor, the saturation current, the effective B-S diode width and the B-D diode width, respectively.

The carrier recombination and trap-assisted tunneling current in the space-charge region is modeled by

$$I_{bs2} = W_{dios} T_{si} j_{recs} \left(\exp\left(\frac{V_{bs}}{0.026 n_{recfs}} \right) - \exp\left(\frac{V_{sb}}{0.026 n_{recrs}} \frac{V_{rec0s}}{V_{rec0s} + V_{sb}} \right) \right)$$

$$I_{bd2} = W_{diod} T_{si} j_{recd} \left(\exp\left(\frac{V_{bd}}{0.026 n_{recfd}} \right) - \exp\left(\frac{V_{db}}{0.026 n_{recrd}} \frac{V_{rec0d}}{V_{rec0d} + V_{db}} \right) \right)$$

(3.2)

Here $n_{recfs}, n_{recrs}, j_{recs}, n_{recfd}, n_{recrd}, j_{recd}$ are non-ideality factors for forward bias and reverse bias, the saturation current, respectively. Note that the parameters V_{rec0s}, V_{rec0d} are provided to model the current roll-off in the high reverse bias regime.

The reverse bias tunneling current, which may be significant in junctions with high doping concentration, can be expressed as

$$I_{bs4} = W_{dios} T_{si} j_{tuns} \left(1 - \exp\left(\frac{V_{sb}}{0.026 n_{tuns}} \frac{V_{tun0s}}{V_{tun0s} + V_{sb}} \right) \right)$$

$$I_{bd4} = W_{diod} T_{si} j_{tund} \left(1 - \exp\left(\frac{V_{db}}{0.026 n_{tund}} \frac{V_{tun0d}}{V_{tun0d} + V_{db}} \right) \right)$$

(3.3)

where j_{tuns}, j_{tund} are the saturation currents. The parameters n_{tuns}, n_{tund} and V_{tun0s}, V_{tun0d} are provided to better fit the data.

The recombination current in the neutral body can be described by

$$I_{bs3} = (1 - \alpha_{bjt}) I_{ens} \left[\exp\left(\frac{V_{bs}}{n_{diodes} V_t} \right) - 1 \right] \frac{1}{\sqrt{E_{hlis} + 1}}$$

$$I_{bd3} = (1 - \alpha_{bjt}) I_{end} \left[\exp\left(\frac{V_{bd}}{n_{dioded} V_t} \right) - 1 \right] \frac{1}{\sqrt{E_{hlid} + 1}}$$

$$I_{ens} = W'_{eff} T_{si} j_{bjts} \left[L_{bjt0} \left(\frac{1}{L_{eff}} + \frac{1}{L_n} \right) \right]^{N_{bjt}}$$

$$I_{end} = W'_{eff} T_{si} j_{bjtd} \left[L_{bjt0} \left(\frac{1}{L_{eff}} + \frac{1}{L_n} \right) \right]^{N_{bjt}}$$

$$E_{hlis} = A_{hlis\_eff} \left[\exp\left(\frac{V_{bs}}{n_{diodes} V_t} \right) - 1 \right]$$

$$E_{hlid} = A_{hlid\_eff} \left[\exp\left(\frac{V_{bd}}{n_{dioded} V_t} \right) - 1 \right]$$

$$\alpha_{bjt} = \exp\left[-0.5 \left(\frac{L_{eff}}{L_n} \right)^2 \right] \tag{3.4}$$

Here α_{bjt} is the bipolar transport factor, whose value depends on the ratio of the effective channel length L_{eff} and the minority carrier diffusion length L_n. j_{bjts} and j_{bjtd} are the saturation currents, while the parameters L_{bjt0} and N_{bjt} are provided to better fit the forward injection characteristics. Notice that E_{hlis} and E_{hlid}, determined by the parameter A_{hlis} and A_{hlid}, stand for the high level injection effect in the B-S/D diode, respectively.

The parasitic bipolar transistor current is important in transient body discharge, especially in pass-gate floating body SOI designs [7]. The BJT collector current is modeled as

$$I_c = \alpha_{bjt} I_{en} \left\{ \exp\left[\frac{V_{bs}}{n_{diodes} V_t} \right] - \exp\left[\frac{V_{bd}}{n_{dioded} V_t} \right] \right\} \frac{1}{E_{2nd}}$$

$$E_{2nd} = \frac{E_{ely} + \sqrt{E_{ely}^2 + 4 E_{hli}}}{2} \tag{3.5}$$

$$E_{ely} = 1 + \frac{V_{bs} + V_{bd}}{V_{Abjt} + A_{ely} L_{eff}}$$

$$E_{hli} = E_{hlis} + E_{hlid}$$

where E_{2nd} is composed of the Early effect E_{ely} and the high level injection roll-off E_{hli}. Note that $E_{2nd} \to E_{ely}$ as $E_{ely} >> E_{hli}$. While $E_{2nd} \to \sqrt{E_{hli}}$ as $E_{hli} >> E_{ely}$, in which case the Early voltage $V_{Abjt} + A_{ely}L_{eff}$ is high.

To sum up, the total B-S current is $I_{bs} = \sum_{i=1}^{4} I_{bsi}$, and the total B-D current is $I_{bd} = \sum_{i=1}^{4} I_{bdi}$.

The total drain current including the BJT component can then be expressed as

$$I_{ds,total} = I_{ds,MOSFET} + I_c \tag{3.6}$$

3.2. New Impact Ionization Current Equation

IiiMod = 0

An accurate impact ionization current equation is crucial to the PD SOI model since it may affect the transistor output characteristics through the body effect [11]. Hence in BSIMPD we use a more recent expression [22] to formulate the impact ionization current I_{ii} as

$$I_{ii} = \alpha_0 (I_{ds,MOSFET} + I_{ii\_BJT}) \exp\left(\frac{V_{diff}}{\beta_2 + \beta_1 V_{diff} + \beta_0 V_{diff}^2} \right)$$

Here, when IiiMod = 0, I_{ii_BJT} is defined as:

$$I_{ii\_BJT} = F_{bjtii} I_c$$

$$V_{diff} = V_{ds} - V_{dsatii}$$

$$V_{dsatii} = VgsStep + \left[V_{dsatii0}\left(1 + T_{ii}\left(\frac{T}{T_{nom}} - 1 \right) \right) - \frac{L_{ii}}{L_{eff}} \right]$$

$$VgsStep = \left(\frac{E_{satii}L_{eff}}{1 + E_{satii}L_{eff}} \right)\left(\frac{1}{1 + S_{ii1}V_{gsteff}} + S_{ii2} \right)\left(\frac{S_{ii0}V_{gst}}{1 + S_{iid}V_{ds}} \right) \tag{3.7}$$

Here the $F_{bjtii} I_c$ term represents the contribution from the parasitic bipolar current. Notice that the classical impact ionization current model [12] adopted in BSIM3v3 is actually a special case of Eqn. (3.6) when $(\beta_0, \beta_1, \beta_2) = (-1,0,0)$. However, the dependence of $\log(I_{ii}/I_{ds})$ on the drain

overdrive voltage V_{diff} is quite linear [22] for state-of-the-art SOI technologies due to thermally assisted impact ionization [23]. In this case, $(\beta_0, \beta_1, \beta_2) \cong (0,0,1)$.

The extracted saturation drain voltage V_{dsatii} depends on the gate overdrive voltage V_{gst} and L_{eff}. One can first extract the parameters $(V_{dsatii0}, L_{ii})$ by the V_{dsatii} - L_{eff} characteristics at $V_{gst} = 0$. All the other parameters $(E_{satii}, S_{ii1}, S_{ii2}, S_{ii0}, S_{iid})$ can then be determined by the plot of V_{dsatii} versus V_{gs} for different L_{eff}. Notice that a linear temperature dependence of $V_{dsatii0}$ with the parameter T_{ii} is also included.

IiiMod = 1

When **IiiMod = 0**, the two component currents $I_{ds,MOSFET}$ and I_c have a same bias dependence for impact ionization rate. This approximation generally won't cause accuracy problem because the MOSFET drain current is the major contribution on impact ionization current in the interested operation regions. While SOI MOSFET device operates in subthreshold to accumulation regions, parasitic BJT effect starts to dominant nodal drain current at high drain bias. In order to model I_{ii} better, **IiiMod =1** is introduce to treat $I_{ds,MOSFET}$ and I_c separately. It means that these two components have the different impact ionization rate [30].

Here $I_{ds,MOSFET}$ still uses the old impact ionization model. The BJT contribution is expressed in Equ (3.8). The temperature dependence is also improved.

$$I_{ii\_BJT} = \frac{CBJTII + EBJTII \cdot L_{eff}}{L_{eff}} I_C (V_{bci} - V_{bd}) \exp\left(-ABJTII \cdot (V_{bci} - V_{bd})^{(MBJTII-1)}\right) \quad (3.8)$$

$$V_{bci} = VBCI\left(1 + TVBCI\left(\frac{T}{TNOM} - 1\right)\right)$$

where *ABJTII*, *CBJTII*, *EBJTII*, *MBJTII*, *VBCI* and *TVBCI* are model parameters and explained in Appendix B.

3.3. Gate Induced Source/Drain Leakage Current

gidlMod = 0

GISL/GIDL can be important in SOI device because it can affect the body potential in the low V_{gs} and high V_{ds} regime.

The formula for GIDL current is:

$$I_{GIDL} = AGIDL \cdot W_{diod} \cdot Nf \cdot \frac{V_{ds} - V_{gse} - EGIDL + V_{fbsd}}{3 \cdot T_{oxe}} \cdot \exp\left(-\frac{3 \cdot T_{oxe} \cdot BGIDL}{V_{ds} - V_{gse} - EGIDL}\right) \cdot \frac{V_{db}^3}{CGIDL + V_{db}^3}$$

(3.9)

Where, *AGIDL*, *BGIDL*, *CGIDL*, and *EGIDL* are model parameters and explained in Appendix A. *CGIDL* accounts for the body-bias dependence of *IGIDL and IGISL*. Here V_{gse} accounts for poly depletion effect.

Following BSIM4, BSIMSOI4.1 also introduces GISL current. In order to model asymmetric source/drain, GISL model has another set of parameters: *AGISL*, *BGISL*, *CGISL*, and *EGISL*.

$$I_{GISL} = AGISL \cdot W_{dios} \cdot Nf \cdot \frac{-V_{ds} - V_{gse} - EGISL + V_{fbsd}}{3 \cdot T_{oxe}} \cdot \exp\left(-\frac{3 \cdot T_{oxe} \cdot BGISL}{-V_{ds} - V_{gse} - EGISL}\right) \cdot \frac{V_{sb}^3}{CGISL + V_{sb}^3}$$

(3.10)

gidlMod = 1

In this new model, the basic idea is to decouple V_{ds} and V_{gs} dependence by introducing an extra parameter *rgidl*. The body bias dependence part is also revised. Here, *KGIDL* and *FGILD* are V_{bs} dependent parameters.

$$I_{GIDL} = AGIDL \cdot W_{diod} \cdot Nf \cdot \frac{V_{ds} - RGIDL \cdot V_{gse} - EGIDL + V_{fbsd}}{3 \cdot T_{oxe}} \qquad (3.11)$$

$$\times \exp\left(-\frac{3 \cdot T_{oxe} \cdot BGIDL}{V_{ds} - V_{gse} - EGIDL}\right) \cdot \exp\left(\frac{KGIDL}{V_{ds} - FGIDL}\right)$$

$$I_{GISL} = AGISL \cdot W_{dios} \cdot Nf \cdot \frac{-V_{ds} - RGISL \cdot V_{gse} - EGISL + V_{fbsd}}{3 \cdot T_{oxe}}$$

$$\times \exp\left(-\frac{3 \cdot T_{oxe} \cdot BGISL}{-V_{ds} - V_{gse} - EGISL}\right) \cdot \exp\left(\frac{KGISL}{-V_{bs} - FGISL}\right)$$

Here $V_{fbsd} = 0$ when mtrlMod = 0.

3.4. Oxide Tunneling Current

For thin oxide (below 20Å), oxide tunneling is important in the determination of floating-body potential [20]. In BSIMPD the following equations are used to calculate the tunneling current density J_{gb}:

In inversion,

$$
\begin{aligned}
J_{gb} &= A \frac{V_{gb} V_{aux}}{T_{ox}^2} \left(\frac{T_{oxref}}{T_{oxqm}} \right)^{N_{tox}} \exp\left(\frac{-B\left(\alpha_{gb1} - \beta_{gb1}|V_{ox}|\right)T_{ox}}{1 - |V_{ox}|/V_{gb1}} \right) \\
V_{aux} &= V_{EVB} \ln\left(1 + \exp\left(\frac{|V_{ox}| - \varphi_g}{V_{EVB}} \right) \right) \\
A &= \frac{q^3}{8\pi h \phi_b} \\
B &= \frac{8\pi \sqrt{2m_{ox}} \phi_b^{3/2}}{3hq} \\
\phi_b &= 4.2eV \\
m_{ox} &= 0.3m_0
\end{aligned}
\tag{3.12}
$$

In accumulation,

$$
\begin{aligned}
J_{gb} &= A \frac{V_{gb} V_{aux}}{T_{ox}^2} \left(\frac{T_{oxref}}{T_{oxqm}} \right)^{N_{tox}} exp\left(\frac{-B\left(\alpha_{gb2} - \beta_{gb2}|V_{ox}|\right)T_{ox}}{1 - |V_{ox}|/V_{gb2}} \right) \\
V_{aux} &= V_{ECB} V_t \, ln\left(1 + exp\left(-\frac{V_{gb} - V_{fb}}{V_{ECB}} \right) \right) \\
A &= \frac{q^3}{8\pi h \phi_b} \\
B &= \frac{8\pi \sqrt{2m_{ox}} \phi_b^{3/2}}{3hq} \\
\phi_b &= 3.1eV \\
m_{ox} &= 0.4m_0
\end{aligned}
\tag{3.13}
$$

Igb is evaluated in IgbMod=1. IgbMod=0 turns it off. Please see Appendix B for model parameter descriptions.

In BSIMSOI4.1, the instance parameter A_{gbcp2} represents the parasitic gate-to-body overlap area due to the body contact. This parameter applies for the opposite-type gate, which is shown Fig. 4.4. In order to account the tunneling current in this region, I_{g_agbcp2} is introduced as following:

$$I_{g\_agbcp2} = A \times A_{agbcp2} \min(V_{gp} - V_{fb2}, 0) \times V_{gp\_eff} T_{oxRatio}$$
$$\exp\left[-B \times T_{oxqm}\left(AIGBCP2 - BIGBCP2 \times V_{gp\_eff}\right)\left(1 + CIGBCP2 \times V_{gp\_eff}\right)\right] \qquad (3.14)$$

$$V_{gp\_eff} = 0.5 \times \left[\sqrt{\left(V_{gp} - V_{fb2}\right)^2 + \delta^2} - \left(V_{gp} - V_{fb2}\right) - \delta\right]$$

$$\delta = 0.01$$

3.5. Gate-to-Channel Current (I_{gc0}) and Gate-to-S/D (I_{gs} and I_{gd})

I_{gc0}, determined by ECB for NMOS and HVB (Hole tunneling from Valence Band) for PMOS at $V_{ds}=0$, is formulated as

$$Igc0 = W_{eff} L_{eff} \cdot A \cdot T_{oxRatio} \cdot V_{gse} \cdot V_{aux}$$
$$\cdot \exp\left[-B \cdot TOXE\left(AIGC - BIGC \cdot V_{oxdepinv}\right) \cdot \left(1 + CIGC \cdot V_{oxdepinv}\right)\right] \qquad (3.15)$$

where $A = 4.97232$ A/V^2 for NMOS and 3.42537 A/V^2 for PMOS, $B = 7.45669e11$ (g/F-s^2)$^{0.5}$ for NMOS and $1.16645e12$ (g/F-s^2)$^{0.5}$ for PMOS, and

$$V_{aux} = NIGC \cdot v_t \cdot \log\left(1 + \exp\left(\frac{V_{gse} - VTH0}{NIGC \cdot v_t}\right)\right) \qquad (3.16)$$

I_{gs} and I_{gd} -- I_{gs} represents the gate tunneling current between the gate and the source diffusion region, while I_{gd} represents the gate tunneling current between the gate and the drain diffusion region. I_{gs} and I_{gd} are determined by ECB for NMOS and HVB for PMOS, respectively.

$$I_{gs} = W_{eff} DLCIG \cdot A \cdot T_{oxRatioEdge} \cdot V_{gs} \cdot V_{gs}' \qquad (3.17)$$
$$\cdot \exp\left[-B \cdot TOXE \cdot POXEDGE \cdot \left(AIGS - BIGS \cdot V_{gs}'\right) \cdot \left(1 + CIGS \cdot V_{gs}'\right)\right]$$

and

$$I_{gd} = W_{eff} DLCIGD \cdot A \cdot T_{oxRatioEdge} \cdot V_{gd} \cdot V_{gd}' \tag{3.18}$$
$$\cdot \exp\left[-B \cdot TOXE \cdot POXEDGE \cdot \left(AIGD - BIGD \cdot V_{gd}'\right) \cdot \left(1 + CIGD \cdot V_{gd}'\right)\right]$$

where $A = 4.97232$ A/V^2 for NMOS and 3.42537 A/V^2 for PMOS, $B = 7.45669e11$ (g/F-s^2)$^{0.5}$ for NMOS and $1.16645e12$ (g/F-s^2)$^{0.5}$ for PMOS, and

$$T_{oxRatioEdge} = \left(\frac{TOXREF}{TOXE \cdot POXEDGE}\right)^{NTOX} \cdot \frac{1}{\left(TOXE \cdot POXEDGE\right)^2} \tag{3.19}$$

$$V_{gs}' = \sqrt{\left(V_{gs} - V_{fbsd}\right)^2 + 1.0e - 4} \tag{3.20}$$

$$V_{gd}' = \sqrt{\left(V_{gd} - V_{fbsd}\right)^2 + 1.0e - 4} \tag{3.21}$$

V_{fbsd} is the flat-band voltage between gate and S/D diffusions calculated as

If NGATE > 0.0

$$V_{fbsd} = \frac{k_B T}{q} \log\left(\frac{NGATE}{NSD}\right) + VFBSDOFF \tag{3.22}$$

Else $V_{fbsd} = 0.0$.

3.5.1 Partition of I_{gc}

To consider the drain bias effect, I_{gc} is split into two components, I_{gcs} and I_{gcd}, that is $I_{gc} = I_{gcs} + I_{gcd}$, and

$$Igcs = Igc0 \cdot \frac{PIGCD \cdot V_{dseff} + \exp\left(-PIGCD \cdot V_{dseff}\right) - 1 + 1.0e - 4}{PIGCD^2 \cdot V_{dseff}^2 + 2.0e - 4} \tag{3.23}$$

and

$$Igcd = Igc0 \cdot \frac{1 - \left(PIGCD \cdot V_{dseff} + 1\right) \cdot \exp\left(-PIGCD \cdot V_{dseff}\right) + 1.0e - 4}{PIGCD^2 \cdot V_{dseff}^2 + 2.0e - 4} \tag{3.24}$$

where I_{gc0} is I_{gc} at V_{ds}=0.

If the model parameter *PIGCD* is not specified, it is given by

$$PIGCD = \frac{B \cdot TOXE}{V_{gsteff}^{\,2}} \left(1 - \frac{V_{dseff}}{2 \cdot V_{gsteff}} \right)$$

(3.25)

Igc is evaluated in IgcMod=1. IgcMod=0 turns it off.

3.6. Body Contact Current

In BSIMPD, a body resistor is connected between the body (B node) and the body contact (P node) if the transistor has a body-tie. The body resistance is modeled by

$$R_{bp} = \left(R_{body} \frac{W_{eff}'}{L_{eff}} \right) // \left(R_{halo} \frac{W_{eff}'}{2} \right), \quad R_{bodyext} = R_{bsh} N_{rb}$$

(3.26)

Here R_{bp} and $R_{bodyext}$ represent the intrinsic and extrinsic body resistance respectively. R_{body} is the intrinsic body sheet resistance, R_{halo} accounts for the effect of halo implant, N_{rb} is the number of square from the body contact to the device edge and R_{bsh} is the sheet resistance of the body contact diffusion.

The body contact current I_{bp} is defined as the current flowing through the body resistor:

$$I_{bp} = \frac{V_{bp}}{R_{bp} + R_{bodyext}}$$

(3.27)

where V_{bp} is the voltage across the B node and P node. Notice that $I_{bp} = 0$ if the transistor has a floating body.

3.6. Body Contact Parasitics

The effective channel width may change due to the body contact. Hence the following equations are used:

$$W_{eff} = W_{drawn} - N_{bc}dW_{bc} - (2 - N_{bc})dW$$

$$W_{eff}^{'} = W_{drawn} - N_{bc}dW_{bc} - (2 - N_{bc})dW^{'}$$

$$W_{diod} = W_{eff}^{'} + P_{dbcp}$$

$$W_{dios} = W_{eff}^{'} + P_{sbcp}$$

(3.28)

Here dW_{bc} is the width offset for the body contact isolation edge. N_{bc} is the number of body contact isolation edge. For example: $N_{bc} = 0$ for floating body devices, $N_{bc} = 1$ for T-gate structures and $N_{bc} = 2$ for H-gate structures. P_{dbcp} / P_{sbcp} represents the parasitic perimeter length for body contact at drain/source side. The body contact parasitics [17] may affect the I-V significantly for narrow width devices [20].

After introducing all the mechanisms that contribute the body current, we can express the nodal equation (KCL) for the body node as

$$\left(I_{bs} + I_{bd}\right) + I_{bp} - I_{ii} - \left(I_{dgidl} + I_{sgisl}\right) - I_{gb} = 0$$

(3.29)

Eqn. (3.18) is important since it determines the body potential through the balance of various body current components. The I-V characteristics can then be correctly predicted after this critical body potential can be well anchored.

Chapter 4: MOS C-V Model

BSIMPD approaches capacitance modeling by adding SOI-specific capacitive effect to the C-V model of BSIM3v3. Similar to the I-V case, the body charges belonged to the floating body node will be our emphasis. The model incorporates features listed below with the SOI-specific features bold-faced and italicized.

- Separate effective channel length and width for IV and CV models.

- The CV model is not piece-wise (i.e. divided into inversion, depletion, and accumulation). Instead, a single equation is used for each nodal charge covering all regions of operation. This ensures continuity of all derivatives and enhances convergence properties. Just like in BSIM3v3, the inversion and body capacitances are continuous at the threshold voltage.

- In BSIMSOI4.1, a new model selector vgstcvMod is introduced for the Vgsteff calculation. When vgstcvMod = 0, it is the old code. Nothing has been changed; even Qinv/Cgs/Cgd etc., are untouched for the backward compatibility. Thus users are suggested to choose vgstcvMod =1 or 2. Here, vgstcvMod = 1 fixes the bug in vgstcvMod = 0 (For more details, please check the BSIMSOI4.1 release note). vgstcvMod = 2 adopts a new Vgsteff, which is similar to that in IV model. Body effect and DIBL are automatically incorporated in the capacitance model.

- Intrinsic capacitance model has two options. The capMod = 2 option yields capacitance model based on BSIM3v3 short channel capacitance model. The capMod = 3 option is the new charge-thickness model from BSIM3v3.2 [4].

- Front gate overlap capacitance is comprised of two parts: 1) a bias independent part which models the effective overlap capacitance between the gate and the heavily doped source/drain, and 2) a gate bias dependent part between the gate and the LDD region.

- Bias independent fringing capacitances are added between the gate and source as well as the gate and drain. A sidewall source/drain to substrate (under the buried oxide) fringing capacitance is added.

- A source/drain-buried oxide-Si substrate parasitic MOS capacitor is added.

- Body-to-back-gate coupling is added.

- Parasitic gate capacitance model is improved by the new body contact model.

A good intrinsic charge model is important in bulk MOSFETs because intrinsic capacitance comprises a sizable portion of the overall capacitance, and because a well behaved charge model is required for robust large circuit simulation convergence. In analog applications there are devices biased near the threshold voltage. Thus, a good charge model must be well-behaved in transition regions as well. To ensure proper behavior, both the I-V and C-V model equations should be developed from an identical set of charge equations so that C_{ij}/I_d is well behaved.

A good physical charge model of SOI MOSFETs is even more important than in bulk. This is because transient behavior of the floating body depends on capacitive currents [18]. Also, due to the floating body node, convergence issues in PD SOI are more volatile than in bulk, so that charge smoothness and robustness are important. An example is that a large negative guess of body potential by SPICE during iterations can force the transistor into depletion, and a smooth transition between depletion and inversion is required. Therefore the gate/source/drain/backgate to body capacitive coupling is important in PD SOI.

4.1. Charge Conservation
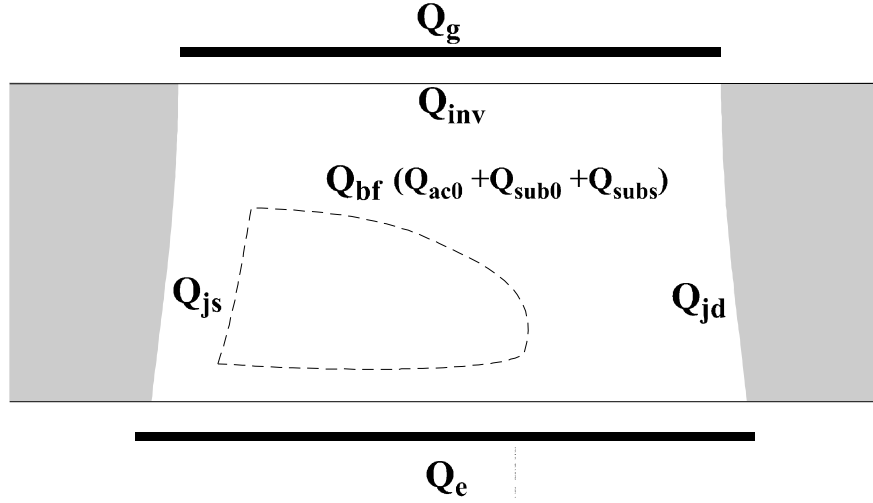
Fig. 4.1   Intrinsic charge components in BSIMPD CV model

To ensure charge conservation, terminal charges instead of terminal voltages are used as state variables. The terminal charges Q_g, Q_d, Q_s, Q_b, and Q_e are the charges associated with the **g**ate, **d**rain, **s**ource, **b**ody, and substrat**e** respectively. These charges can be expressed in terms of inversion charge (Q_{inv}), front gate body charge (Q_{Bf}), source junction charge (Q_{js}) and drain junction charge (Q_{jd}). The intrinsic charges are distributed between the nodes as shown in Fig. 4.1. The charge conservation equations are:

$$Q_{Bf} = Q_{ac0} + Q_{sub0} + Q_{subs}$$

$$Q_{inv} = Q_{inv,s} + Q_{inv,d}$$

$$Q_g = -\left(Q_{inv} + Q_{Bf}\right)$$

$$Q_b = Q_{Bf} - Q_e + Q_{js} + Q_{jd} \tag{4.1}$$

$$Q_s = Q_{inv,s} - Q_{js}$$

$$Q_d = Q_{inv,d} - Q_{jd}$$

$$Q_g + Q_e + Q_b + Q_s + Q_d = 0$$

The front gate body charge (Q_{Bf}) is composed of the accumulation charge (Q_{ac0}) and the bulk charge (Q_{sub0} and Q_{subs}), which may be divided further into two components: the bulk charge at V_{ds}=0 (Q_{sub0}), and the bulk charge induced by the drain bias (Q_{subs}) (similar to δQ_{sub} in BSIM3v3).

All capacitances are derived from the charges to ensure charge conservation. Since there are 5 charge nodes, there are 25 (as compared to 16 in BSIM3v3) components. For each component:

$C_{ij} = \dfrac{dQ_i}{dV_j}$, where i and j denote transistor nodes. In addition, $\sum\limits_{i} C_{ij} = \sum\limits_{j} C_{ij} = 0$.

4.2. Intrinsic Charges

BSIMPD uses similar expressions to BSIM3v3 for Q_{inv} and Q_{Bf}. First, the bulk charge constant A_{bulkCV} is defined as

$$A_{bulkCV} = A_{bulk0}\left(1 + \left(\frac{CLC}{L_{active}}\right)^{CLE}\right) \tag{4.2}$$

where

$$A_{bulk0} = A_{bulk}\left(V_{gsteff} = 0\right) \tag{4.3}$$

This is done in order to empirically fit V_{dsatCV} to channel length. Experimentally,

$$V_{dsatIV} < V_{dsatCV} < V_{dsatIV}\big|_{L\to\infty} = \frac{V_{gsteffCV}}{A_{bulk}} \tag{4.4}$$

vgstcvMod = 0 or 1

The effective CV V_{gst} is defined as

$$V_{gsteffCV} = nv_t \ln\left(1 + \exp\left[\frac{V_{gs} - V_{th}}{nv_t}\right]\exp\left[-\frac{delvt}{nv_t}\right]\right) \tag{4.5}$$

vgstcvMod = 0 and 1 use the same $V_{gsteffCV}$ definition. As mentioned above, the only difference between vgstcvMod = 0 and 1 is that Mod =1 fixes the bug in the code. Users are suggested to choose vgstcvMod =1 or 2.

vgstcvMod = 2

This new $V_{gsteffCV}$ follows that in IV model. There are two new model parameters MINVCV and VOFFCV, which are binnable.

$$V_{gsteffCV} = \frac{nv_t \ln\left[1 + \exp(\frac{m^{*CV}(V_{gs\_eff} - V_{th} - delvt)}{nv_t})\right]}{m^{*CV} + nC_{ox}\sqrt{\frac{2\Phi_s}{q\varepsilon_{si}N_{dep}}} \exp(-\frac{(1-m^{*CV})(V_{gs\_eff} - V_{th} - delvt) - V_{offCV}}{nv_t})} \quad (4.6)$$

$$m^{*CV} = 0.5 + \frac{\arctan(MINVCV)}{\pi}$$

Then we can calculate the CV saturation drain voltage

$$V_{dsatCV} = V_{gsteffCV} / A_{bulkCV} . \quad (4.7)$$

Define effective CV V_{ds} as

$$V_{dsCV} = V_{dsatCV} - \frac{1}{2}(V_{dsatCV} - V_{ds} - \delta + \sqrt{(V_{dsatCV} - V_{ds} - \delta)^2 + 4\delta V_{dsatCV}}) \quad (4.8)$$

Then the inversion charge can be expressed as

$$Q_{inv} = -W_{active}L_{active}C_{ox}\left(\left(V_{gsteffCV} - \frac{A_{bulkCV}}{2}V_{dsCV}\right) + \frac{A_{bulkCV}^2 V_{dsCV}^2}{12\left(V_{gsteffCV} - \frac{A_{bulkCV}}{2}V_{dsCV}\right)}\right) \quad (4.9)$$

where W_{active} and L_{active} are the effective channel width and length in CV, respectively. The channel partition can be set by the *Xpart* parameter. The exact evaluation of source and drain charges for each partition option is presented in Appendix C.

A parameter V_{FBeff} is used to smooth the transition between accumulation and depletion regions. The expression for V_{FBeff} is:

$$V_{FBeff} = V_{fb} - 0.5\left(\left(V_{fb} - V_{gb} - \delta\right) + \sqrt{\left(V_{fb} - V_{gb} - \delta\right)^2 + \delta^2}\right) \quad (4.10)$$

where $V_{gb} = V_{gs} - V_{bseff}$, $V_{fb} = V_{th} - \phi_s - K_{1eff}\sqrt{\phi_s - V_{bseff}}$.

The physical meaning of the function is the following: it is equal to V_{gb} for $V_{gb} < V_{FB}$, and equal to V_{FB} for $V_{gb} > V_{FB}$. Using V_{FBeff}, the accumulation charge can be calculated as

$$Q_{ac0} = -F_{body} W_{active} L_{activeB} C_{ox} (V_{FBeff} - V_{fb})$$ (4.11)

where $L_{activeB} = L_{active} - DLCB$. Notice that the parameters F_{body} and $DLCB$ are provided to give a better fit for the SOI-specific history dependence of the body charge [14].

The gate-induced depletion charge and drain-induced depletion charge can be expressed as

$$Q_{sub0} = -F_{body} W_{active} L_{activeB} C_{ox} \frac{K_{1eff}^2}{2} \left(-1 + \sqrt{1 + \frac{4(V_{gs} - V_{FBeff} - V_{gsteffCV} - V_{bseff})}{K_{1eff}^2}} \right)$$ (4.12)

$$Q_{subs} = F_{body} W_{active} L_{activeB} K_{1eff} C_{ox} (1 - A_{bulkCV}) \left[\frac{V_{dsCV}}{2} - \frac{A_{bulkCV} V_{dsCV}^2}{12(V_{gsteffCV} - A_{bulkCV} V_{dsCV}/2)} \right]$$ (4.13)

respectively.

Finally, the back gate body charge can be modeled by

$$Q_e = F_{body} W_{active} L_{activeBG} C_{box} (V_{es} - V_{fbb} - V_{bseff})$$ (4.14)

where $L_{activeBG} = L_{activeB} + 2\delta L_{bg}$. The parameter δL_{bg} is provided to count the difference of $L_{activeB}$ and $L_{activeBG}$ due to the source/drain extension in the front channel.

For capMod=3, the flat band voltage is calculated from the bias-independent threshold voltage, which is different from capMod=2. For the finite thickness formulation, refer to Section 4.6 and Chapter 7 of BSIM4.6.2 Users' Manual.

4.3. Source/Drain Junction Charges

Beside the junction depletion capacitance considered in BSIM3v3, the diffusion capacitance, which is important in the forward body-bias regime [20], is also included in BSIMPD. The source/drain junction charges Q_{jswg} / Q_{jdwg} can therefore be expressed as

$$Q_{jswg} = Q_{bsdep} + Q_{bsdif}$$
$$Q_{jdwg} = Q_{bddep} + Q_{bddif}$$

(4.15)

The depletion charges Q_{bsdep}/Q_{bddep} have similar expressions as in BSIM3v3 [Appendix C].

While the diffusion charges Q_{bsdif}/Q_{bddif} can be modeled by

$$Q_{bsdif} = \tau \frac{W_{eff}{}'}{N_{seg}} T_{si} J_{sbjt} \left[1 + L_{dif0}\left(L_{bj0}\left(\frac{1}{L_{eff}} + \frac{1}{L_n}\right)\right)\right]^{N_{dif}} \left[\exp\left(\frac{V_{bs}}{n_{dios}V_t}\right) - 1\right] \frac{1}{\sqrt{E_{hlis}+1}}$$

$$Q_{bddif} = \tau \frac{W_{eff}{}'}{N_{seg}} T_{si} J_{dbjt} \left[1 + L_{dif0}\left(L_{bj0}\left(\frac{1}{L_{eff}} + \frac{1}{L_n}\right)\right)\right]^{N_{dif}} \left[\exp\left(\frac{V_{bd}}{n_{diod}V_t}\right) - 1\right] \frac{1}{\sqrt{E_{hlid}+1}}$$

(4.16)

The parameter τ represents the transit time of the injected minority carriers in the body. The parameters L_{dif0} and N_{dif} are provided to better fit the data.

4.4. Extrinsic Capacitances

Expressions for extrinsic (parasitic) capacitances that are common in bulk and SOI MOSFETs are taken directly from BSIM3v3. They are source/drain-to-gate overlap capacitance and source/drain-to-gate fringing capacitance. Additional SOI-specific parasitics added are substrate-to-source sidewall capacitance C_{essw}, and substrate-to-drain sidewall capacitance C_{edsw}, substrate-to-source bottom capacitance (C_{esb}) and substrate-to-drain bottom capacitance (C_{edb}) [Fig. 4.2].
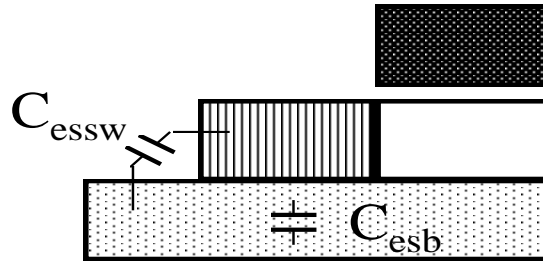
Fig. 4.2   SOI MOSFET extrinsic charge components. C_{essw} is the substrate-to-source sidewall capacitance. C_{esb} is the substrate-to-source bottom capacitance.

In SOI, there is a parasitic source/drain-buried oxide-Si substrate parasitic MOS structure with a bias dependent capacitance. If $V_{s,d}=0$, this MOS structure might be in accumulation. However, if $V_{s,d}=V_{dd}$, the MOS structure is in depletion with a much smaller capacitance, because the Si substrate is lightly doped. The bias dependence of this capacitance is similar to high frequency MOS depletion capacitance as shown in Fig. 4.3. It might be substantial in devices with large source/drain diffusion areas. BSIMPD models it by piece-wise expressions, with accurately chosen parameters to achieve smoothness of capacitance and continuity to the second derivative of charge. The substrate-to-source bottom capacitance (per unit source/drain area) C_{esb} is:

$$C_{esb} = \begin{cases} C_{box} & if & V_{se} < V_{sdfb} \\ C_{box} - \dfrac{1}{A_{sd}}\left(C_{box} - C_{min}\right)\left(\dfrac{V_{se} - V_{sdfb}}{V_{sdth} - V_{sdfb}}\right)^2 & elseif & V_{se} < V_{sdfb} + A_{sd}\left(V_{sdth} - V_{sdfb}\right) \\ C_{min} + \dfrac{1}{1 - A_{sd}}\left(C_{box} - C_{min}\right)\left(\dfrac{V_{se} - V_{sdth}}{V_{sdth} - V_{sdfb}}\right)^2 & elseif & V_{se} < V_{sdth} \\ C_{min} & else & \end{cases} \tag{4.17}$$

Physical parameters V_{sdfb} (flat-band voltage of the MOS structure) and V_{sdth} (threshold voltage of the MOS structure) can be easily extracted from measurement. C_{min} should also be extracted from measurement, and it can account for deep depletion as well. A_{sd} is a smoothing parameter. The expression for C_{edb} is similar to C_{esb}. Fig. 4.3 shows the comparison of the model and measured C_{esb}.
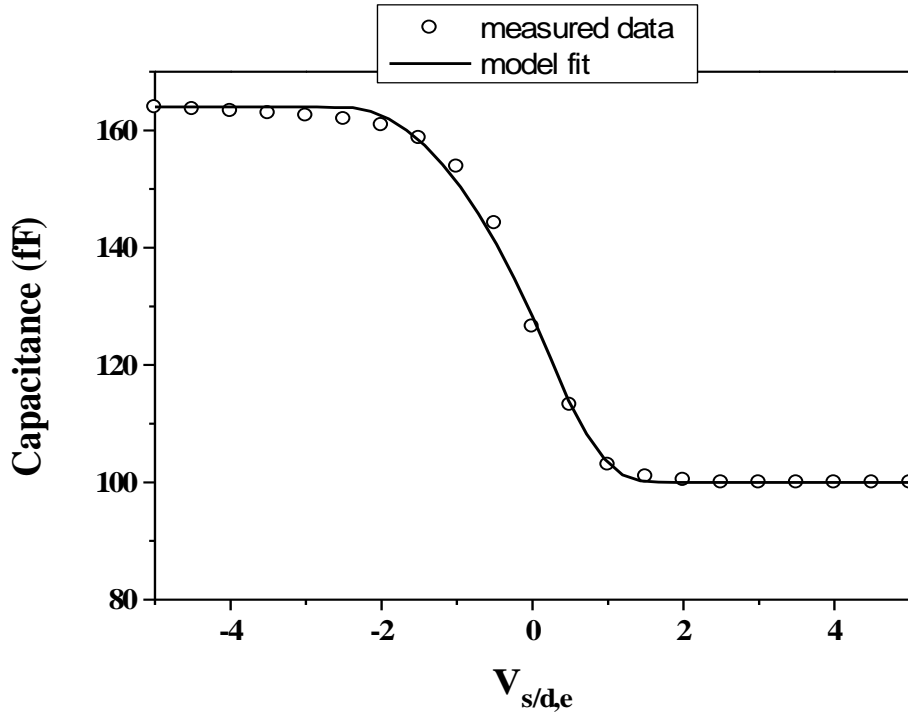
Fig. 4.3   Bottom source/drain to substrate capacitance for a PD SOI MOSFET.

Finally, the sidewall source/drain to substrate capacitance (per unit source/drain perimeter length) can be expressed by

$$C_{s/d,esw} = C_{sdesw} \log\left(CfrCoeff \cdot \left(1 + \frac{T_{si}}{T_{box}} \right) \right) \tag{4.18}$$

which depends on the silicon film thickness T_{si} and the buried oxide thickness T_{box}. The parameter C_{sdesw} represents the fringing capacitance per unit length. *CfrCoeff* has a default value = 1, and is limited to a value of 2 (introduced in v4.4).

4.5.   Body Contact Parasitics

The parasitic capacitive coupling due to the body contact is considered in BSIMPD. The instance parameter A_{gbcp} represents the parasitic gate-to-body overlap area due to the body contact, and A_{ebcp} represents the parasitic substrate-to-body overlap area. The effect may be significant for small area devices [CV part in Appendix C].

   Note: There are four instance parameters used to calculate parasitic capacitances associated with body contacts. They are: psbcp, pdbcp, agbcp and aebcp. It is worth pointing out that psbcp and pdbcp represent additional gate perimeter to the source and drain and must be specified on a per finger basis, while agbcp and aebcp represent addition gate area and addition area of body over the box and must be specified on a total transistor basis.

   BSIMSOI4.1 also considers the P$^+$ implantation for body contact (as shown in Figure 4.4), which will induce parasitic P$^+$-poly gate/NMOS.
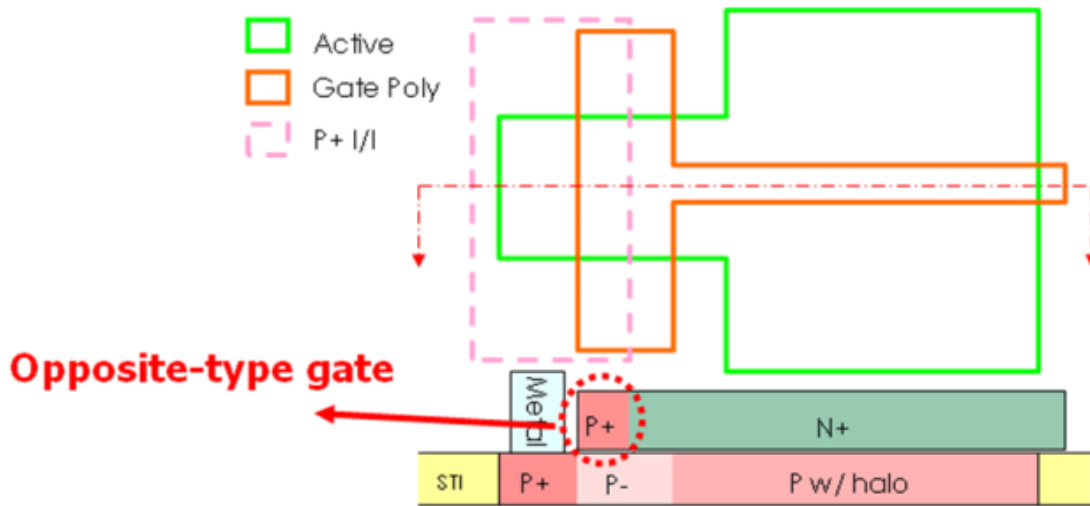
Fig. 4.4   Parasitic capacitance in opposite-type gate.

   In BSIMSOI4.0, the instance parameter A$_{gbcp}$ represents the parasitic gate-to-body overlap area due to the body contact. This parameter only applies for the same-type gate. For the opposite-type gate, the charge will be overestimated by A$_{gbcp}$. Charge model has to be modified to include the effect of P$^+$/P region in this case.

   The higher V$_{FB}$ in the P$^+$/P region lowers the gate charge and the net gate charge is the sum of N$^+$/P and P$^+$/P regions as shown below. One new instance parameter A$_{gbcp2}$ is introduced to account for the opposite-type parasitic capacitance. The final charge could be expressed as

following:

$$\text{Total Charge} = WL \times N^+ / NMOS + A_{gbcp} \times N^+ / NMOS + A_{gbcp2} \times P^+ / NMOS \tag{4.19}$$
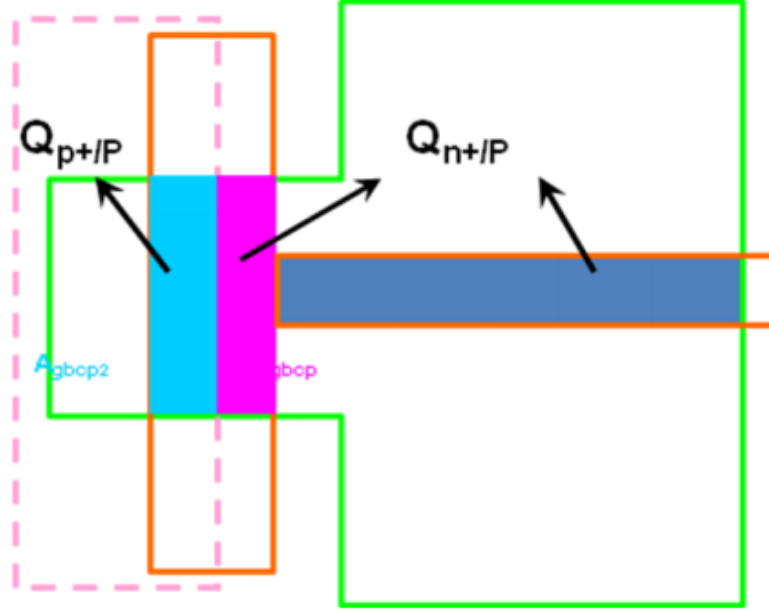
Fig. 4.5   The total charge in the opposite-type gate.

Note: In this case**,** there is a new instant parameters agbcp2, which is similar to agbcp and specified on a total transistor basis.

4.6   Finite Thickness Formulation

The finite thickness formulation is similar to that in BSIM4.

mtrlMod=0

The charge thickness introduces a capacitance in series with C_{ox}, resulting in an effective C_{oxeff}. Based on numerical self-consistent solution of Shrŏdinger, Poisson and Fermi-Dirac equations, universal and analytical X_{DC} models have been developed. C_{oxeff} can be expressed as:

$$C_{oxeff} = \frac{C_{oxp} \cdot C_{cen}}{C_{oxp} + C_{cen}} \tag{4.20}$$

where

$$C_{cen} = \varepsilon_{si} / X_{DC} \tag{4.21}$$

(i) X_{DC} for accumulation and depletion

The DC charge thickness in the accumulation and depletion regions can be expressed by

$$X_{DC} = \frac{1}{3} L_{debye} \exp\left[ACDE \cdot \left(\frac{NDEP}{2 \times 10^{16}} \right)^{-0.25} \cdot \frac{V_{gse} - V_{bseff} - V_{FBeff}}{TOXP} \right] \tag{4.22}$$

where L_{debye} is Debye length, and X_{DC} is in the unit of cm and $(V_{gse}$ - V_{bseff} - $V_{FBeff}) / TOXP$ is in units of MV/cm. For numerical stability, (4.22) is replaced by (4.23)

$$X_{DC} = X_{max} - \frac{1}{2}\left(X_0 + \sqrt{X_0^2 + 4\delta_x X_{max}} \right) \tag{4.23}$$

where

$$X_0 = X_{max} - X_{DC} - \delta_x \tag{4.24}$$

and $X_{max} = L_{debye} / 3; = 10^{-3} TOXE$.

(ii) X_{DC} of inversion charge

The inversion charge layer thickness can be formulated as

$$X_{DC} = \frac{ADOS \times 1.9 \times 10^{-9} \text{ m}}{1 + \left(\dfrac{V_{gsteff} + 4(VTH0 - VFB - \Phi_s)}{2TOXP} \right)^{0.7 \times BDOS}} \tag{4.25}$$

Here, the density of states parameters *ADOS* and *BDOS* are introduced to control the charge centroid. Their default values are one.

Through the *VFB* term, equation (4.25) is found to be applicable to N[+] or P[+] poly-Si gates and even other future gate materials.

(iii) Body charge thickness in inversion

In inversion region, the body charge thickness effect is modeled by including the deviation of the surface potential Φ_S (bias-dependence) from $2\ \Phi_B$

$$\varphi_\delta = \Phi_s - 2\Phi_B = v_t \ln\left(1 + \frac{V_{gsteffCV} \cdot (V_{gsteffCV} + 2K_{1ox}\sqrt{2\Phi_B})}{MOIN \cdot K_{1ox}^2 v_t} \right) \tag{4.26}$$

The channel charge density is therefore derived as

$$q_{inv} = -C_{oxeff} \cdot \left(V_{gsteff,CV} - \varphi_\delta \right)_{eff} \tag{4.27}$$

mtrlMod $= 1$

In this case, *TOXP* should be iteratively calculated by *EOT* first:

$$TOXP = EOT - \frac{3.9}{EPSRSUB} \times X_{DC}\Big|_{V_{gs}=VDDEOT, V_{ds}=V_{bs}=0} \tag{4.28}$$

With the calculated *TOXP*, X_{DC} could be obtained at different gate voltage, just like mtrlMod=0.

Chapter 5: Temperature Dependence and Self-Heating

Self-heating in SOI is more important than in bulk since the thermal conductivity of silicon dioxide is about two orders of magnitude lower than that of silicon [15]. It may degrade the carrier mobility, increase the junction leakage [20], enhance the impact ionization rate [24], and therefore affect the output characteristics [16] of floating-body SOI devices.

5.1. Temperature Dependence

The temperature dependence of threshold voltage, mobility, saturation velocity and series resistance in BSIMSOI is identical to BSIM3v3. However a different temperature dependence of diode characteristics is adopted in BSIMSOI4.0:

$$j_{sbjt} = i_{sbjt} \exp\left[\frac{-E_g(300K)}{n_{diodes}V_t} X_{bjt}\left(1 - \frac{T}{T_{nom}}\right)\right]$$

$$j_{dbjt} = i_{dbjt} \exp\left[\frac{-E_g(300K)}{n_{dioded}V_t} X_{bjt}\left(1 - \frac{T}{T_{nom}}\right)\right]$$

$$j_{sdif} = i_{sdif} \exp\left[\frac{-E_g(300K)}{n_{diodes}V_t} X_{dif}\left(1 - \frac{T}{T_{nom}}\right)\right]$$

$$j_{ddif} = i_{ddif} \exp\left[\frac{-E_g(300K)}{n_{dioded}V_t} X_{dif}\left(1 - \frac{T}{T_{nom}}\right)\right]$$

$$j_{srec} = i_{srec} \exp\left[\frac{-E_g(300K)}{n_{recf0s}V_t} X_{rec}\left(1 - \frac{T}{T_{nom}}\right)\right]$$

$$j_{drec} = i_{drec} \exp\left[\frac{-E_g(300K)}{n_{recf0d}V_t} X_{rec}\left(1 - \frac{T}{T_{nom}}\right)\right]$$

$$j_{stun} = i_{stun} \exp\left[X_{tun}\left(\frac{T}{T_{nom}} - 1\right)\right]$$

$$j_{dtun} = i_{dtun} \exp\left[X_{tun}\left(\frac{T}{T_{nom}} - 1 \right) \right] \qquad (5.1)$$

$$n_{recrs} = n_{recr0s}\left[1 + nt_{recr}\left(\frac{T}{T_{nom}} - 1 \right) \right]$$

$$n_{recrd} = n_{recr0d}\left[1 + nt_{recr}\left(\frac{T}{T_{nom}} - 1 \right) \right]$$

$$n_{recfs} = n_{recf0s}\left[1 + nt_{recf}\left(\frac{T}{T_{nom}} - 1 \right) \right]$$

$$n_{recfd} = n_{recf0d}\left[1 + nt_{recf}\left(\frac{T}{T_{nom}} - 1 \right) \right]$$

The parameters $i_{sbjt}, i_{dbjt}, i_{sdif}, i_{ddif}, i_{srec}, i_{drec}, i_{stun}, i_{dtun}$ are diode saturation currents at the nominal temperature T_{nom}, and the parameters $X_{bjt}, X_{dif}, X_{rec}, X_{tun}$ are provided to model the temperature dependence. Notice that the non-ideality factors $n_{recfs}, n_{recfd}, n_{recrs}, n_{recrd}$ are also temperature dependent.

5.2. Self-Heating Implementation

BSIMPD/BSIMSOI models the self-heating by an auxiliary $R_{th}C_{th}$ circuit as shown in Fig. 5.1 [18]. The temperature node (T node) will be created in SPICE simulation if the self-heating selector *shMod* is ON and the thermal resistance is non-zero. The T node is treated as a voltage node and is connected to ground through a thermal resistance R_{th} and a thermal capacitance C_{th}:

$$R_{th} = \frac{R_{th0}}{W'_{eff} + W_{th0}}, \; C_{th} = C_{th0}(W'_{eff} + W_{th0}) \qquad (5.2)$$

where R_{th0} and C_{th0} are normalized thermal resistance and capacitance, respectively. W_{th0} is the minimum width for thermal resistance calculation [19]. Notice that the current source is driving a current equal to the power dissipated in the device.

$$P = \left| I_{ds} \times V_{ds} \right| \tag{5.3}$$

To save computation time, the turn-on surface potential ϕ_s (Phi) is taken to be a constant within each timepoint because a lot of parameters (e.g. X_{dep}) are function of ϕ_s. Each timepoint will use a ϕ_s calculated with the temperature iterated in the previous timepoint. However this approximation may induce error in DC, transient and AC simulation. Therefore, it is a tradeoff between accuracy and speed. The error in DC or transient is minimal if the sweeping step or time step is sufficiently small.
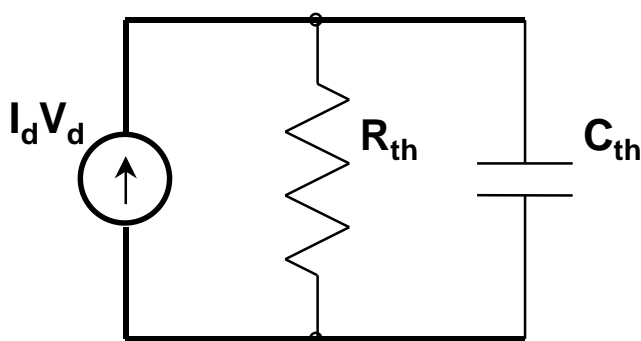
Fig. 5.1   Equivalent circuit for self-heating simulation.

Chapter 6: BSIMSOI –A Unified Model for PD and FD SOI MOSFETs

Using BSIMPD as a foundation, we have developed a unified model for both PD and FD SOI circuit designs based on the concept of *body-source built-in potential lowering* [20, 25].

6.1. BSIMSOI Framework and Built-In Potential Lowering Model

As described in [20], we construct BSIMSOI based on the concept of body-source built-in potential lowering, ΔV_{bi}. There are four modes (soiMod = 0, 1, 2 and 3) in BSIMSOI: BSIMPD (soiMod = 0) can be used to model the PD SOI device, where the body potential is independent of ΔV_{bi} ($V_{BS} > \Delta V_{bi}$). Therefore the calculation of ΔV_{bi} is skipped in this mode. On the other hand, the ideal FD model (soiMod = 2) is for the FD device with body potential equal to ΔV_{bi}. Hence the calculation of body current/charge, which is essential to the PD model, is skipped. For the unified SOI model (soiMod = 1), however, both ΔV_{bi} and body current/charge are calculated to capture the floating-body behavior exhibited in FD devices. As shown in Figure 6.1, this unified model covers both BSIMPD and the ideal FD model. When soiMod = 3, BSIMSOI will select the operation mode based on V_{bs0t} (For details, refer Section 6.3)
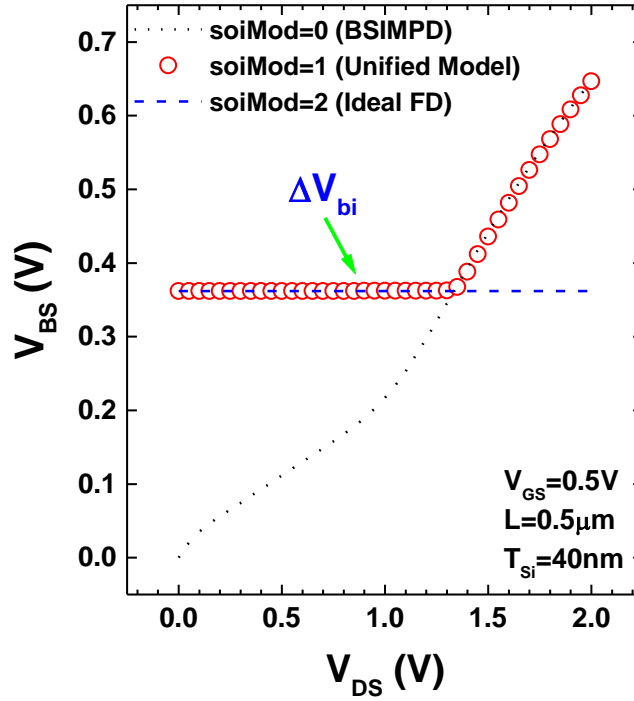
Fig. 6.1 The body potential in the unified model approaches the V_{BS} solved in BSIMPD for PD devices, while returns to ΔV_{bi} for ideal FD devices [20].

This unified model shares the same floating-body module as BSIMPD, with a generalized diode current model considering the body-source built-in potential lowering effect ($I_{BS} \propto \exp(-q\Delta V_{bi}/kT)$). Therefore, an accurate and efficient ΔV_{bi} model is crucial. The following formulation for ΔV_{bi} is mainly based on the Poisson equation and the physical characterization for ΔV_{bi}, as presented in [25].

In order to keep backward compatibility, a new model selector fdMod is introduced. Here, fdMod = 0 is the old ΔV_{bi} formulation, while fdMod = 1 is the new one that is easier to fit.

fdMod = 0

For a given surface band bending ϕ (source reference), ΔV_{bi} can be formulated by applying the Poisson equation in the vertical direction and continuity of normal displacement at the back interface:

$$\Delta V_{bi}(\phi) = \frac{C_{Si}}{C_{Si} + C_{BOX}} \cdot \left(\phi - \frac{qN_{ch}}{2\varepsilon_{Si}} \cdot T_{Si}{}^2 + \Delta V_{DIBL} \right) + \eta_e \left(L_{eff} \right) \frac{C_{BOX}}{C_{Si} + C_{BOX}} \cdot \left(V_{bGS} - V_{FBb} \right)$$

$$C_{Si} = \frac{\varepsilon_{Si}}{T_{Si}}, C_{BOX} = \frac{\varepsilon_{OX}}{T_{BOX}}, C_{OX} = \frac{\varepsilon_{OX}}{T_{OX}}$$

(6.1).

The first term of Equation (6.1) represents the frontgate coupling. T_{Si} is the SOI thickness. N_{ch} accounts for the effective channel doping, which may vary with channel length due to the non-uniform lateral doping effect. Here, $\frac{qN_{ch}}{2\varepsilon_{si}} T_{Si}^2$ is band bending in the body due to depletion charges, which is limited to (Eg-0.1) eV in v4.4. In SOIMOD=2, for any combinations of T_{Si} and N_{ch}, if this term exceeds this limit, N_{ch} is lowered accordingly. The second term of Equation (6.1) represents the backgate coupling (V_{bGS}). V_{FBb} is the backgate flatband voltage. Equation (6.1) shows that the impact of frontgate on ΔV_{bi} reaches maximum when the buried oxide thickness, $T_{BOX,}$ approaches infinity.

In Equation (6.1), ΔV_{DIBL} represents the short channel effect on ΔV_{bi},

$$\Delta V_{DIBL} = D_{vbd0} \left(exp\left(-D_{vbd1} \frac{L_{eff}}{2l} \right) + 2 exp\left(-D_{vbd1} \frac{L_{eff}}{l} \right) \right) \cdot \left(V_{bi} - 2\Phi_B \right)$$

(6.2),

as addressed in [25]. Here l is the characteristic length for the short-channel-effect calculation. D_{vbd0} and D_{vbd1} are model parameters. Similarly, the following equation

$$\eta_e \left(L_{eff} \right) = K_{1b} - K_{2b} \cdot \left(exp\left(-D_{k2b} \frac{L_{eff}}{2l} \right) + 2 exp\left(-D_{k2b} \frac{L_{eff}}{l} \right) \right)$$

(6.3)

is used to account for the short channel effect on the backgate coupling, as described in [25]. D_{K1b}, D_{K2b}, K_{1b} (default 1) and K_{2b} (default 0) are model parameters.

fdMod = 1

However, the two length-dependent functions (i.e., Eqr (6.2) and (6.3)) in ΔV_{bi} model make the parameter extraction difficult. Thus, BSIMSOI4.1 introduces a new ΔV_{bi} equation as following:

$$\Delta V_{bi} = \frac{C_{si}}{C_{si} + C_{BOX} + CDSBS} \cdot \left(\phi - \frac{qN_{ch} \cdot (1 + L_{pe0} / L_{eff})}{2\varepsilon_{Si}} \cdot T_{si}^{2} + V_{nonideal} \right) \tag{6.4}$$

$$+ \frac{C_{BOX}}{C_{si} + C_{BOX} + CDSBS} \cdot \left(V_{bGS} - V_{FBb} \right) + \frac{CDSBS}{C_{si} + C_{BOX} + CDSBS} \cdot \Delta V_{SCE}$$

CDSBS is the new model parameter representing the capacitance of drain to the body-source potential. ΔV_{SCE} is the length dependence of the capacitance coupling from drain. VSCE is the new model parameter for SCE of ΔV_{bi} at zero V_{ds}.

$$\Delta V_{SCE} = DVBD0 \cdot \left(\exp\left(-DVBD1 \frac{L_{eff}}{2l} \right) + 2\exp\left(-DVBD1 \frac{L_{eff}}{l} \right) \right) \cdot \left(V_{ds} + VSCE \right) \tag{6.4}$$

If body contact devices are available, a direct probe of ΔV_{bi} can be achieved by finding the onset of the external body bias after the channel current (threshold voltage) of FD device is modulated.

If body contact devices are not available, the length dependence related parameters of ΔV_{bi} will be set to the value of SCE parameters in V_T equation.

$$Dvbd0 = D_{VT0} \tag{6.5}$$
$$Dvbd1 = D_{VT1}$$

The surface band bending, ϕ, is determined by the frontgate V_{GS} and may be approximated by

$$\phi = \begin{cases} \Phi_{ON} & \text{for } V_{GS} \geq V_T \\ \\ \Phi_{ON} - \dfrac{C_{OX}}{C_{OX} + \left(C_{Si}^{-1} + C_{BOX}^{-1} \right)^{-1}} \cdot \left(V_T - V_{GS} \right) & \text{for } V_{GS} \leq V_T \end{cases} \tag{6.6}.$$

To improve the simulation convergence, the following single continuous function from subthreshold to strong inversion is used:

$$\varphi = \Phi_{ON} - \frac{C_{OX}}{C_{OX} + \left(C_{Si}^{-1} + C_{BOX}^{-1} \right)^{-1}} \cdot N_{OFF,FD} v_t \cdot \ln\left(1 + \exp\left(\frac{V_{T,FD} - V_{gs\_eff} - V_{OFF,FD}}{N_{OFF,FD} v_t} \right) \right) \tag{6.7}.$$

Here V_{gs_eff} is the effective gate bias considering the poly-depletion effect. $V_{T,FD}$ is the threshold voltage at $V_{BS} = \Delta V_{bi}(\phi{=}2\Phi_B)$. $N_{OFF,FD}$ (default 1) and $V_{OFF,FD}$ (default 0) are model parameters introduced to improve the transition between subthreshold and strong inversion. V_t is the thermal voltage. Notice that the frontgate coupling ratio in the subthreshold regime approaches 1 as T_{BOX} approaches infinity.

To accurately model ΔV_{bi} and thus the device output characteristics, the surface band bending at strong inversion, Φ_{ON}, is not pinned at $2\Phi_B$. Instead, the following equation

$$\Phi_{ON} = 2\Phi_B + v_t \ln\left(1 + \frac{V_{gsteff.FD}\left(V_{gsteff,FD} + 2K1\sqrt{2\Phi_B}\right)}{moin \cdot K1 \cdot v_t^2}\right) \tag{6.8}$$

is used to account for the surface potential increment with gate bias in the strong inversion regime [4]. Here *moin* is a model parameter. K1 is the body effect coefficient. Notice that a single continuous function,

$$V_{gsteff,FD} = N_{OFF,FD}V_t \cdot ln\left(1 + exp\left(\frac{V_{gs\_eff} - V_{T,FD} - V_{OFF,FD}}{N_{OFF,FD}V_t}\right)\right) \tag{6.9}$$

has been used to represent the gate overdrive in Equation (6.7).

6.2. Verification

The BSIMPD parameter extraction methodology presented in [20] may still be used under the unified BSIMSOI framework, provided that the link between PD and FD, ΔV_{bi}, can be accurately extracted. As described in [25], a direct probe of ΔV_{bi} can be achieved by finding the onset of the external body bias (through a body contact) after which the threshold voltage and hence the channel current of the FD SOI device is modulated. When the body contact is not available, nevertheless, model parameters related to ΔV_{bi} should be extracted based on the subthreshold

characteristics of the floating-body device. As shown in Figure 6.2, the reduction of ΔV_{bi} with backgate bias is responsible for the transition from the ideal subthreshold swing (~ 60 mV/dec. at room temperature) to the non-ideal one.

Figure 6.2 clearly shows that the PD/FD transition can be captured by the ΔV_{bi} approach. In other words, ΔV_{bi} is indeed an index of the degree of full depletion, as pointed out in [20, 25]. As shown in Figure 6.3, larger floating-body effect can be observed for negative backgate bias due to smaller ΔV_{bi}. In case the ΔV_{bi} value is raised by charge sharing as described in [25], it can be predicted that the short-channel device should exhibit less floating-body effect than the long-channel one due to larger ΔV_{bi}, as verified in Figure 6.4.
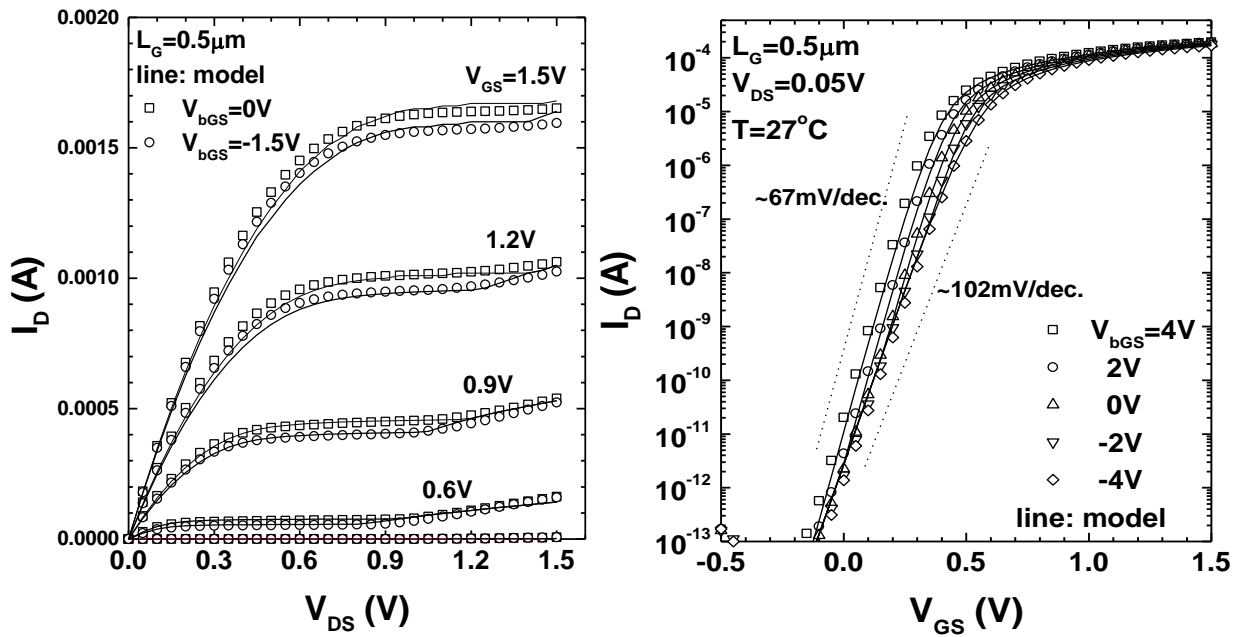
(Left) Fig. 6.2 The PD/FD transition can be captured by modeling ΔV_{bi} [20].

(Right) Fig. 6.3 Larger floating-body effect can be seen for the negative backgate bias (source reference) due to smaller ΔV_{bi} [20].
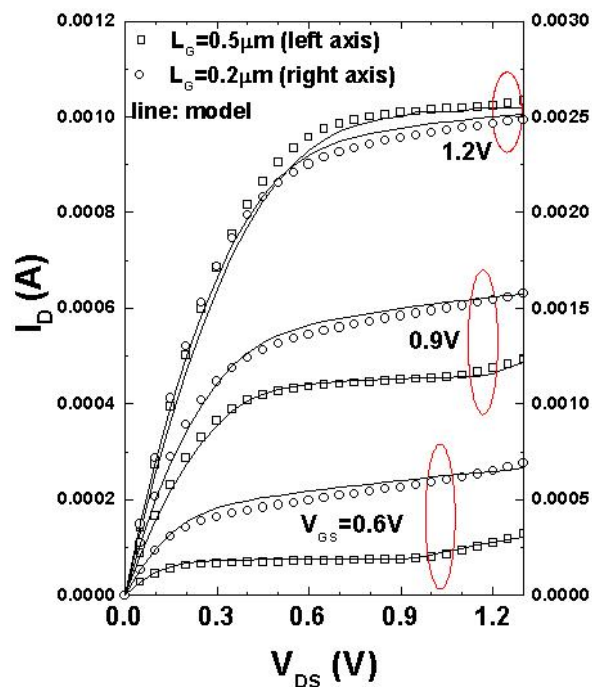
Fig. 6.4 Less floating-body effect can be seen for the short-channel device due to larger ΔV_{bi} [20].

6.3. Model Selector SOIMOD

The model selector, SoiMod, is an instance parameter and a model parameter. SoiMod will determine the operation of BSIMSOI.

If SoiMod=0 (default), the model equation is identical to BSIMPD equation.

If SoiMod=1 (unified model for PD&FD) or SoiMod=2 (ideal FD), the following equations (FD module) are added on top of BSIMPD.

$$V_{bs0} = \frac{C_{Si}}{C_{Si} + C_{BOX}} \cdot \left(phi - \frac{qN_{ch}\left(1 + N_{LX}/L_{eff}\right)}{2\varepsilon_{Si}} \cdot T_{Si}^2 + V_{nonideal} + \Delta V_{DIBL} \right) + \eta_e \frac{C_{BOX}}{C_{Si} + C_{BOX}} \cdot \left(V_{es} - V_{FBb} \right)$$

$$\text{where } C_{Si} = \frac{\varepsilon_{Si}}{T_{Si}}, C_{BOX} = \frac{\varepsilon_{OX}}{T_{BOX}}, C_{OX} = \frac{\varepsilon_{OX}}{T_{OX}}$$

$$\Delta V_{DIBL} = D_{vbd0}\left(exp\left(-D_{vbd1}\frac{L_{eff}}{2l} \right) + 2exp\left(-D_{vbd1}\frac{L_{eff}}{l} \right) \right) \cdot \left(V_{bi} - 2\Phi_B \right)$$

$$\eta_e = K_{1b} - K_{2b} \cdot \left(exp\left(-D_{k2b}\frac{L_{eff}}{2l} \right) + 2exp\left(-D_{k2b}\frac{L_{eff}}{l} \right) \right)$$

$$phi = phi_{ON} - \frac{C_{OX}}{C_{OX} + \left(C_{Si}^{-1} + C_{BOX}^{-1} \right)^{-1}} \cdot N_{OFF,FD}V_t \cdot ln\left(1 + exp\left(\frac{V_{th,FD} - V_{gs\_eff} - V_{OFF,FD}}{N_{OFF,FD}V_t} \right) \right)$$

$$phi_{ON} = 2\Phi_B + V_t\, ln\left(1 + \frac{V_{gsteff,FD}\left(V_{gsteff,FD} + 2K1\sqrt{2\Phi_B} \right)}{MoinFD \cdot K1 \cdot V_t^2} \right),$$

$$V_{gsteff,FD} = N_{OFF,FD}V_t \cdot ln\left(1 + exp\left(\frac{V_{gs\_eff} - V_{th,FD} - V_{OFF,FD}}{N_{OFF,FD}V_t} \right) \right)$$

Here N_{ch} is the channel doping concentration. N_{LX} is the lateral non-uniform doping coefficient to account for the lateral non-uniform doping effect. V_{FBb} is the backgate flatband voltage. $V_{th,FD}$ is the threshold voltage at $V_{bs}=V_{bs0}$(phi=$2\Phi_B$). v_t is thermal voltage. K1 is the body effect coefficient.

If SoiMod=1, the lower bound of V_{bs} (SPICE solution) is set to V_{bs0}. If SoiMod=2, V_{bs} is pinned at V_{bs0}. Notice that there is no body node and body leakage/charge calculation in SoiMod=2.

The zero field body potential that will determine the transistor threshold voltage, V_{bsmos}, is then calculated by

$$\text{if } V_{bs} \leq V_{bs0}\left(T_{OX} \rightarrow \infty\right)$$

$$V_{bsmos} = V_{bs} - \frac{C_{Si}}{2qN_{ch}T_{Si}}\left(V_{bs0}\left(T_{OX} \rightarrow \infty\right) - V_{bs}\right)^2$$

$$\text{else}$$

$$V_{bsmos} = V_{bs}$$

The subsequent clamping of V_{bsmos} will use the same equation that utilized in BSIMPD. Please download the BSIMPD manual at (http://bsim.berkeley.edu/models/bsimsoi).

If SoiMod=3 is specified, BSIMSOI will select the operation mode for the user based on the estimated value of V_{bs0} at phi=2Φ_B (bias independent), V_{bs0t}:

If $V_{bs0t} > V_{bs0fd}$, BSIMSOI will be in the ideal FD mode (SoiMod=2).

If $V_{bs0t} < V_{bs0pd}$, BSIMSOI will be in the BSIMPD mode (SoiMod=0).

Otherwise, BSIMSOI will be operated under SoiMod=1.

Notice that both V_{bs0fd} and V_{bs0pd} are model parameters.

Chapter 7: BSIMSOI RF Model

BSIMSOI4.1 provides the gate resistance model and body resistance model for devices used in RF application.

7.1   Gate Electrode and Intrinsic-Input Resistance (IIR) Model

Users have four options for modeling gate electrode resistance (bias independent) and intrinsic-input resistance (Rii, bias-dependent) by choosing model choice parameter rgateMod.

RgateMod = 0 (zero-resistance):
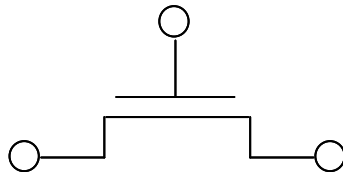
In this case, no gate resistance is generated.

RgateMod = 1 (constant-resistance):
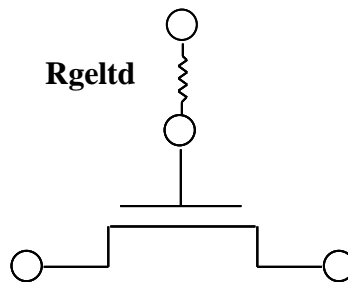
Rgeltd

In this case, only the electrode gate resistance (bias-independent) is generated by adding an internal gate node. The electrode gate resistance Rgeltd is given by

$$Rgeltd = \frac{RSHG \cdot \left(XGW + \dfrac{W_{eff}}{3 \cdot NGCON \cdot NSEG} \right)}{NGCON \cdot \left(L_{drawn} - XGL \right)} \tag{7.1}$$

RgateMod = 2 (RII model with variable resistance):
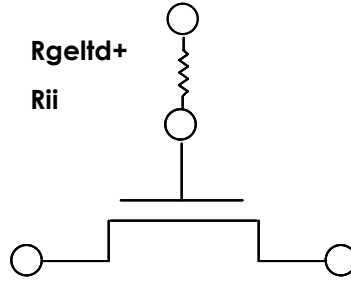
In this case, the gate resistance is the sum of the electrode gate resistance and the intrinsic-input

resistance Rii as given by $\dfrac{1}{Rii} = XRCRG1 \cdot \left(\dfrac{I_{ds}}{V_{dseff}} + XRCRG2 \cdot \dfrac{W_{eff} \mu_{eff} C_{oxeff} k_B T}{q L_{eff}} \right)$

(7.2)

An internal gate node will be generated.

RgateMod = 3 (RII model with two nodes):

In this case, the gate electrode resistance is in series with the intrinsic-input resistance Rii through two internal gate nodes, so that the overlap capacitance current will not pass through the intrinsic-input resistance.
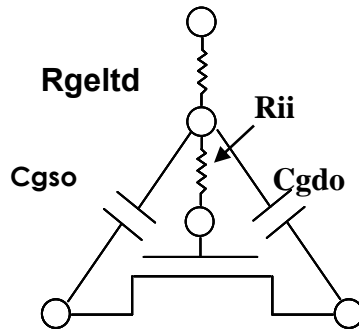
7.2 Body Resistance Network

RbodyMod = 0

In this case, body resistance network turns off. RF data still could be fit for fully depleted SOI device [28].

RbodyMod =1

A two-resistance body resistance network turns on as shown in the following figure.

Two extra nodes sbNode and dbNode are introduced in this case. The body resistor RBSB/RBDB are located between sbNode/dbNode and bNode. As in BSIM4, a minimum conductance, *GBMIN*, is introduced in parallel with each resistance and therefore to prevent infinite resistance values, which would otherwise cause poor convergence.

Note that the intrinsic model body reference point in this case is the internal body node **bNode**, into which the impact ionization current I_{ii} and the GIDL current I_{GIDL} flow.
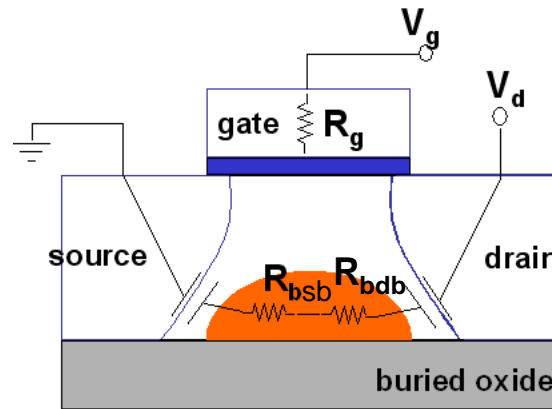
Chapter 8 BSIMSOI Noise Model

8.1 Flicker noise models

BSIMSOI4.1 provides two flicker noise models. When the model selector fnoiMod is set to 0, a simple flicker noise model which is convenient for hand calculation is invoked. A unified physical flicker noise model, which is the default model, will be used if fnoiMod=1. These two modes come from BSIMSOI3.1, but the unified model has many improvements. For instance, it is now smooth over all bias regions and considers the bulk charge effect.

- fnoiMod = 0 (simple model)

The noise density is:

$$S_{id}(f) = \left(\frac{W_{eff}}{W0FLK} \right)^{1-AF} \cdot \frac{KF \cdot I_{ds}^{AF}}{C_{oxe} L_{eff}^{BF} \cdot f^{EF}} \tag{8.1}$$

- fnoiMOd = 1 (unified model)

The physical mechanism for the flicker noise is trapping/de-trapping related charge fluctuation in oxide traps, which results in fluctuations of both mobile carrier numbers and mobility in the channel. The unified flicker noise model captures this physical process.

The noise density in inversion region is given by:

$$S_{id,inv}(f) = \frac{k_B T q^2 \mu_{eff} I_{ds}}{C_{oxe} L_{eff}^2 A_{bulk} f^{ef} \cdot 10^{10}} \left(NOIA \log\left(\frac{N_0 + N^*}{N_l + N^*} \right) + NOIB(N_0 - N_l) + \frac{NOIC}{2}\left(N_0^2 - N_l^2 \right) \right)$$

$$+ \frac{k_B T I_{ds}^2 \Delta L_{clm}}{W_{eff} L_{eff}^2 f^{ef} \cdot 10^{10}} \frac{NOIA + NOIB \cdot N_l + NOIC \cdot N_l^2}{\left(N_l + N^* \right)^2}$$

$$\tag{8.2}$$

Where μ_{eff} is the effective mobility at the given bias condition, and L_{eff} and W_{eff} are the effective length and width respectively. The parameter N_0 is the charge density at the source side given by:

$$N_0 = \frac{C_{ox}V_{gsteff}}{q} \qquad (8.3)$$

The parameter N_l is the charge density at the source side given by:

$$N_l = \frac{C_{ox}V_{gsteff}}{q}\left(1 - \frac{A_{bulk}V_{dseff}}{V_{gsteff} + 2v_t}\right) \qquad (8.4)$$

N^* is given by:

$$N^* = k_B T \cdot (C_{ox} + C_d + CIT) \Big/ q^2 \qquad (8.5)$$

where CIT is a model parameter from DC IV and C_d is the depletion capacitance.

ΔL_{clm} is the channel length reduction due to channel length modulation and given by:

$$\Delta L_{clm} = Litl \cdot \log\left(\frac{\dfrac{V_{ds} - V_{dseff}}{Litl} + EM}{E_{sat}}\right) \qquad (8.6)$$

$$E_{sat} = \frac{2VSAT}{\mu_{eff}}$$

In the subthreshold region, the noise density is written as:

$$S_{id,subVt}(f) = \frac{NOIA \cdot k_B T \cdot I_{ds}^2}{W_{eff} L_{eff} f^{EF} N^{*2} \cdot 10^{10}} \qquad (8.5)$$

The total flicker noise density is given by

$$S_{id}(f) = \frac{S_{id,inv}(f) \times S_{id,subvt}(f)}{S_{id,inv}(f) + S_{id,subvt}(f)} \tag{8.6}$$

8.2 Thermal noise models

There are three channel thermal noise models in BSIMSOI4.0 beta version. One is the charge based model (default) similar to that used in BSIMSOI3.1. The second is the BSIM4 compatible holistic thermal noise model. The simple SPICE2 thermal noise model is also provided in BSIMSOI4.1. These three models can be selected through the model selector tnoiMod.

▪ tnoiMod = 0 (charge based model)

The noise current is given by

$$\overline{i_d^2} = \frac{4k_B T \Delta f}{R_{ds} + \dfrac{L_{eff}^2}{\mu_{eff} |Q_{inv}|}} \cdot NTNOI \tag{8.7}$$

where R_{ds} is the source/drain resistance, and the parameter *NTNOI* is introduced for more accurate fitting of short-channel devices. Q_{inv} is the inversion channel charge computed from the capacitance models

▪ tnoiMod = 1 (holistic model)

In this thermal noise model, all the short-channel effects and velocity saturation effect incorporated in the IV model are automatically included, hence the name "holistic thermal noise model". In addition, the amplification of the channel thermal noise through G_m and G_{mbs} as well as the induced-gate noise with partial correlation to the channel thermal noise are all captured in the new "noise partition" model.

The noise voltage source partitioned to the source side is given by:

$$\overline{v_d^2} = 4k_BT \cdot \theta_{tnoi}^2 \cdot \frac{V_{dseff}\Delta f}{I_{ds}} \tag{8.8}$$

and the noise current source put in the channel region with gate and body amplification is given by:

$$\overline{i_d^2} = 4k_BT \frac{V_{dseff}\Delta f}{I_{ds}} \left[G_{ds} + \beta_{tnoi} \cdot (G_m + G_{mbs})\right]^2 - \overline{v_d^2} \cdot (G_m + G_{ds} + G_{mbs})^2 \tag{8.9}$$

where

$$\theta_{tnoi} = RNOIB \cdot \left[1 + TNOIB \cdot L_{eff} \left(\frac{V_{gsteff}}{E_{sat}L_{eff}}\right)^2\right] \tag{8.10}$$

$$\beta_{tnoi} = RNOIA \cdot \left[1 + TNOIA \cdot L_{eff} \left(\frac{V_{gsteff}}{E_{sat}L_{eff}}\right)^2\right]$$

- tnoiMod = 2 (SPICE2 model)

$$\overline{i_d^2} = \frac{8k_BT\Delta f}{3} \cdot NTNOI \cdot (G_m + G_{mbs} + G_{ds}) \tag{8.11}$$

The parameter NTNOI is added to give the flexibility to tune the magnitude of noise density.

- tnoiMod = 3

Unlike tnoiMod=1, in this thermal noise model both the gate and the drain noise are implemented as current noise sources. The drain current noise flows from drain to source; whereas the induced gate current noise flows from the gate to the source and drain. The correlation between the two noise sources is independently controllable and can be tuned using the parameter RNOIC, although the use of default value 0.395 is recommended when measured data is not available. The relevant formulations of tnoiMod=3 are given below.

$$V_b = \frac{V_{gsteff} + 2v_t}{A_{bulk}} \tag{8.12}$$

$$\eta = 1 - \frac{V_{dseff}}{V_b} \tag{8.13}$$

$$L_{vsat} = L_{eff} \cdot \left[1 + \frac{V_{dseff}}{E_{sat} L_{eff}} \right] \tag{8.14}$$

$$\alpha = A_{bulk} \tag{8.15}$$

$$\gamma = \frac{L}{L_{vsat}} \left[\frac{1 + \eta}{2} + \frac{(1 - \eta)^2}{6 \left[(1 + \eta) + \frac{2V_t \alpha}{V_{gsteff}} \right]} \right] \tag{8.16}$$

$$\delta = \frac{1}{6} \left(\frac{L_{vsat}}{L} \right)^3 \left[\frac{1 + \eta}{\left[(1 + \eta) + \frac{2\alpha V_t}{V_{gsteff}} \right]^2} - \frac{\left[6(1 + \eta) + \frac{2\alpha V_t}{V_{gsteff}} \right] (1 - \eta)^2}{15 \left[(1 + \eta) + \frac{2\alpha V_t}{V_{gsteff}} \right]^4} + \frac{(1 - \eta)^4}{9 \left[(1 + \eta) + \frac{2\alpha V_t}{V_{gsteff}} \right]^5} \right] \tag{8.17}$$

$$\epsilon = \frac{1}{6} \cdot \frac{L_{vsat}}{L} \left[\frac{1 - \eta}{\left[(1 + \eta) + \frac{2\alpha V_t}{V_{gsteff}} \right]} + \frac{(1 - \eta)^3}{3 \left[(1 + \eta) + \frac{2\alpha V_t}{V_{gsteff}} \right]^3} \right] \tag{8.18}$$

$$n_c = RNOIC \cdot \left[1 + TNOIC \cdot L_{eff} \cdot \left(\frac{V_{gsteff}}{E_{sat} L_{eff}} \right)^2 \right] \tag{8.19}$$

$$C_{tnoi} = \frac{\varepsilon}{\sqrt{\gamma \cdot \delta}} \cdot \left(\frac{n_c}{0.395} \right) \tag{8.20}$$

$$n_\beta = RNOIA \cdot \left[1 + TNOIA \cdot L_{eff} \cdot \left(\frac{V_{gsteff}}{E_{sat} L_{eff}} \right)^2 \right] \tag{8.21}$$

$$n_\theta = RNOIB \cdot \left[1 + TNOIB \cdot L_{eff} \cdot \left(\frac{V_{gsteff}}{E_{sat} L_{eff}} \right)^2 \right] \tag{8.22}$$

$$g_{d0} = NF \times \frac{\mu_{eff} C_{oxeff} \frac{W_{eff}}{L_{eff}} V_{gsteff}}{1 + gche \cdot R_{ds}} \tag{8.23}$$

$$S_{id} = 4kT \cdot \gamma \cdot \left(3n_\beta^2 \right) \cdot g_{d0} \tag{8.24}$$

$$C_0 = NF \times C_{oxeff} W_{eff,CV} L_{eff,CV} \tag{8.25}$$

$$sf = \frac{g_{d0}}{\sqrt{\delta \times 3.75 \times n_\theta^2 / \gamma}} \tag{8.26}$$

$$I(di, si) < + white\_noise\left(S_{id} \times \left|1 - C_{tnoi}^2\right|\right) \tag{8.27}$$

$$I(N) < +V(N) \times sf \times SCALEN \tag{8.28}$$

$$I(N) < + white\_noise\left(\frac{S_{id}}{sf^2 \times SCALEN^2}\right) \tag{8.29}$$

$$I(di, si) < + c_{tnoi} \times V(N) \times sf \times SCALEN \tag{8.30}$$

$$I(gi, si) < + ddt\left(0.5 \times C_0 \times SCALEN \times V(N)\right) \tag{8.31}$$

$$I(gi, di) < + ddt\left(0.5 \times C_0 \times SCALEN \times V(N)\right) \tag{8.32}$$

8.3   Other improvement on noise model

In BSIMSOI4.1, some other improvements on noise model are made as following

1. Body contact resistance induced thermal noise is introduced.

2. Thermal noise induced by the body resistance network is introduced as RBODYMOD=1.

3. Shot noises induced by Ibs and Ibd are equal in BSIMSOI3.2 and BSIMPD. In BSIMSOI4.0, these two noises are separated.

Chapter 9   Stress Effect Model

The mechanical stress effect induced by process causes the performance of MOSFET to be function of the active area size (OD: oxide definition) and the location of the device in the active area. The necessity of new models to describe the layout dependence of MOS parameters due to stress effect becomes very urgent in advance CMOS technologies. Influence of stress on mobility has been well known since the 0.13um technology. The stress influence on saturation velocity is also experimentally demonstrated. Stress-induced enhancement or suppression of dopant diffusion during the processing is reported. Since the doping profile may be changed due to different STI sizes and stress, the threshold voltage shift and changes of other second-order effects, such as DIBL and body effect, were shown in process integration.

Experimental analysis shows that there exist at least two different mechanisms within the influence of stress effect on device characteristics. The first one is mobility related which is induced by the band structure modification. The second one is Vth related as a result of doping profile variation. Both of them follow the same 1/LOD trend but reveal different L and W scaling. A BSIM4 compatible phenomenological stress model based on these findings has been developed by modifying some parameters. Note that the following equations have no impact on the iteration time because there are no voltage-controlled components in them.

9.1   Mobility Related Equations

Mobility changes induced by stress effect is modeled by adjusting U_0 and V_{sat} according to different W, L and OD shapes. The relative change of mobility is defined as follows:

$$\rho_{\mu_{eff}} = \frac{\Delta\mu_{eff}}{\mu_{eff0}} = \frac{\mu_{eff} - \mu_{eff0}}{\mu_{eff0}} \tag{9.1}$$

So we have

$$\frac{\mu_{eff}}{\mu_{eff0}} = 1 + \rho_{\mu_{eff}}$$

(9.2)

Figure (9.1) shows the typical layout of a MOSFET on active layout surrounded by STI isolation. SA, SB are the distances between isolation edge to Poly from one and the other side, respectively [27]. 2D simulation shows that stress distribution can be expressed by a simple function of SA and SB. Figure (9.2) shows the schematic stress distribution in the OD region [29].

$$LOD = SA + SB + L \quad \text{OD: gate Oxide Definition}$$
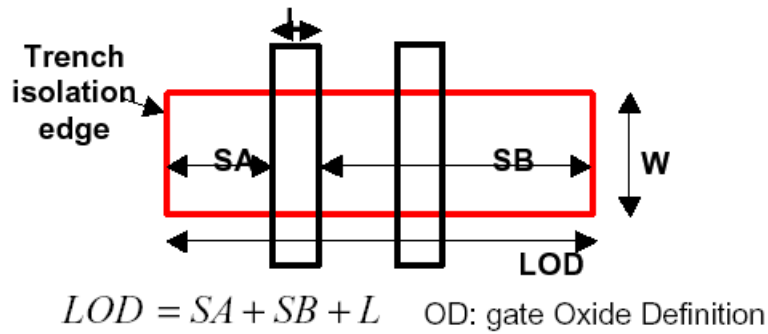
Fig. 9.1 shows the typical layout of a MOSFET [27]
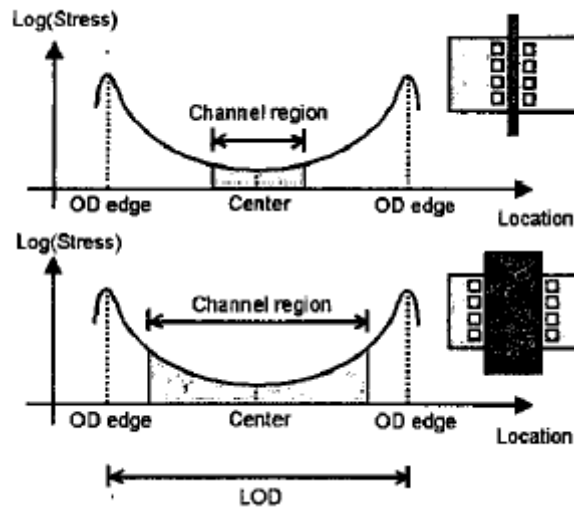
Fig. 9.2 Schematic stress distribution in the OD region [29]

Assuming that mobility relative change is proportional to stress distribution. It can be described as function of SA, SB(LOD effect), L, W, and T dependence.

$$\rho_{\mu_{eff}} = \frac{KU0}{Kstress\_u0} \cdot \left(Inv\_sa + Inv\_sb \right) \tag{9.3}$$

where $Inv\_sa = \dfrac{1}{SA + 0.5 \cdot L_{drawn}}$, $Inv\_sb = \dfrac{1}{SB + 0.5 \cdot L_{drawn}}$,

$$Kstress\_u0 = \left(\begin{array}{l} 1 + \dfrac{LKU0}{(L_{drawn} + XL)^{LLODKU0}} + \dfrac{WKU0}{(W_{drawn} + XW + WLOD)^{WLODKU0}} \\[4mm] + \dfrac{PKU0}{(L_{drawn} + XL)^{LLODKU0} \cdot (W_{drawn} + XW + WLOD)^{WLODKU0}} \cdot \left(1 + TKU0 \cdot \left(\dfrac{Temperature}{TNOM} - 1 \right) \right) \end{array} \right)$$

So that

$$\mu_{eff} = \frac{1 + \rho_{\mu_{eff}}(SA, SB)}{1 + \rho_{\mu_{eff}}(SA_{ref}, SB_{ref})} \mu_{eff0} \tag{9.4}$$

$$v_{sattemp} = \frac{1 + KVSAT \cdot \rho_{\mu_{eff}}(SA, SB)}{1 + KVSAT \cdot \rho_{\mu_{eff}}(SA_{ref}, SB_{ref})} v_{sattemp0} \tag{9.5}$$

where μ_{eff0}, $v_{sattemp0}$ are low field mobility and low field saturation velocity at SA_{ref}, SB_{ref}.

SA_{ref}, SB_{ref} are reference distances between OD edge to poly from one and the other side.

9.2   Vth-related Equations

Vth0, K2 and ETA0 are modified to cover the doping profile change in the devices with different LOD. They use the same 1/LOD formulas as shown in section(13.1.1), but different equations for W and L scaling:

$$VTH0 = VTH0_{original} + \frac{KVTH0}{Kstress\_vth0} \left(Inv\_sa + Inv\_sb - Inv\_sa_{ref} - Inv\_sb_{ref} \right) \tag{9.6}$$

$$K2 = K2_{original} + \frac{STK2}{Kstress\_vth0^{LODK2}} \cdot \left(Inv\_sa + Inv\_sb - Inv\_sa_{ref} - Inv\_sb_{ref} \right) \qquad (9.7)$$

$$ETA0 = ETA0_{original} + \frac{STETA0}{Kstress\_vth0^{LODETA0}} \cdot \left(Inv\_sa + Inv\_sb - Inv\_sa_{ref} - Inv\_sb_{ref} \right) \quad (9.8)$$

$$\text{where } Inv\_sa_{ref} = \frac{1}{SA_{ref} + 0.5 \cdot L_{drawn}}, \qquad Inv\_sb_{ref} = \frac{1}{SB_{ref} + 0.5 \cdot L_{drawn}}$$

$$Kstress\_vth0 = \left(\begin{array}{c} 1 + \dfrac{LKVTH0}{(L_{drawn} + XL)^{LLODKVTH}} + \dfrac{WKVTH0}{(W_{drawn} + XW + WLOD)^{WLODKVTH}} \\[4mm] + \dfrac{PKVTH0}{(L_{drawn} + XL)^{LLODKVTH} \cdot (W_{drawn} + XW + WLOD)^{WLODKVTH}} \end{array} \right) \qquad (9.9)$$

9.3   Multiple Finger Device

For multiple finger devices, as shown the layout in Fig. 9.3, the total LOD effect is the average of LOD effect to every finger. That is:

$$Inv\_sa = \frac{1}{NF} \sum_{i=0}^{NF-1} \frac{1}{SA + 0.5 \cdot L_{drawn} + i \cdot (SD + L_{drawn})}$$

$$Inv\_sb = \frac{1}{NF} \sum_{i=0}^{NF-1} \frac{1}{SB + 0.5 \cdot L_{drawn} + i \cdot (SD + L_{drawn})}$$
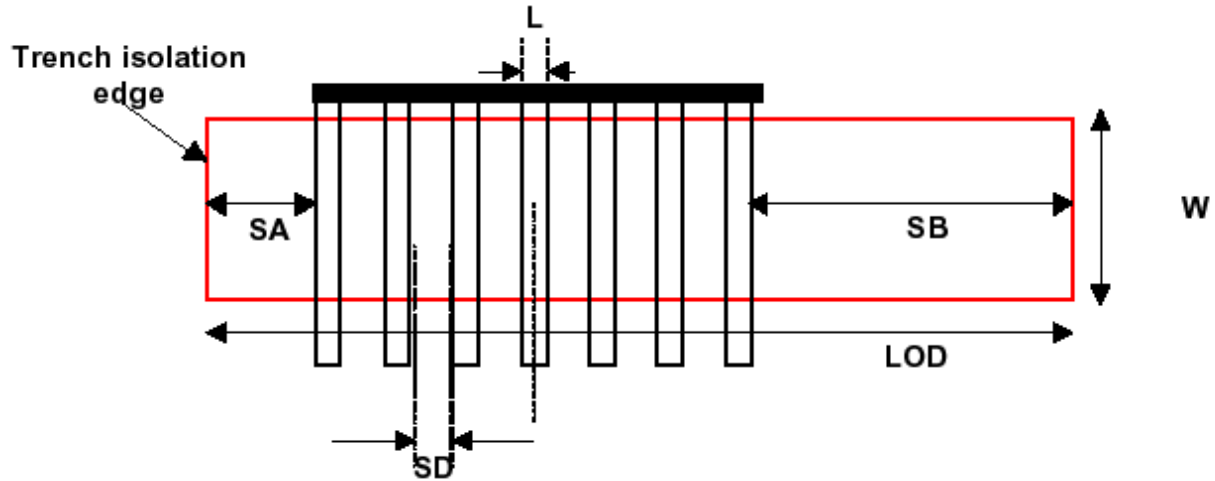
Fig. 9.3 Layout of multiple-finger MOSFET [27]

Chapter 10 New Material Model

In BSIMSOI4.1, a new global selector is introduced to turn on or of the new material models, which are important for the advanced CMOS technology. When users select mtrlMod = 1, the new materials (such as high k/metal gate) could be modeled. The default value (mtrlMod = 0) maintains the backward compatibility.

10.1 Non-Silicon Channel

With the three new parameters, the temperature-dependent band gap and intrinsic carriers in non-silicon channel are described as follow:

$$Eg0 = BG0SUB - \frac{TBGASUB \times Tnom^2}{Tnom + TBGBSUB} \tag{10.1}$$

$$Eg(300.15) = BG0SUB - \frac{TBGASUB \times 300.15^2}{300.15 + TBGBSUB} \tag{10.2}$$

$$n_i = NI0SUB \times \left(\frac{Tnom}{300.15}\right)^{3/2} \times \exp\left(\frac{Eg(300.15) - Eg0}{2v_t}\right) \tag{10.3}$$

$$Eg = BG0SUB - \frac{TBGASUB \times Temp^2}{Temp + TBGBSUB} \tag{10.4}$$

Here, *BG0SUB* is the band-gap of substrate at T=0K; *TBGASUB* and *TBGBSUB* are the first and second parameters of band-gap change due to temperature, respectively.

When capMod=3, the inversion charge layer thickness (X_{DC}) is also modified as follows:

$$X_{DC} = \frac{ADOS \times 1.9 \times 10^{-9}}{1 + \left(\frac{V_{gsteff} + (VTH0 - VFB - \phi_s)}{2TOXP}\right)^{0.7 \times BDOS}} \tag{10.5}$$

Here, the density of states parameters *ADOS* and *BDOS* are introduced to control the charge centroid.

10.2   Non-SiO₂ Gate insulator

For Non-SiO$_2$ gate insulator, the equivalent SiO$_2$ thickness (*EOT*) is a new input parameter, which is measured at *VDDEOT*. Given these new parameters (*EOT* and *VDDEOT*), the physical gate oxide thickness *TOXP* could be calculated as follows:

$$TOXP = EOT - \frac{3.9}{EPSRSUB} \times X_{DC}\Big|_{V_{gs}=VDDEOT,V_{ds}=V_{bs}=0}$$ (10.6)

Here, *EPSRSUB* is the dielectric constant of substrate relative to vacuum.

10.3   Non-Poly Silicon Gate Material

Two new parameters are introduced to describe the non-poly silicon gate material. One is *PHIG*, which is the gate work function. Another is *EPSRGATE*, the dielectric constant of gate relative to vacuum. It is worth pointing out that *EPSRGATE*=0 represents the metal gate and deactivates the ploy depletion effect.

When the gate dielectric and channel are different materials, the flat band voltage at Source/Drain is calculated using the following:

$$V_{fbsd} = PHIG - \left(EASUB + \frac{Eg0}{2} - B4SOItype \times MIN\left(\frac{Eg0}{2}, v_t \ln\left(\frac{NSD}{n_i}\right)\right)\right)$$ (10.7)

Here B4SOItype is defined as +1 for nMOS and -1 for pMOS.

This new flat band equation improves the GIDL/GISL models as following:

$$I_{GIDL} = AGIDL \cdot W_{effCJ} \cdot Nf \cdot \frac{V_{ds} - V_{gse} - EGIDL + V_{fbsd}}{EOT \cdot \dfrac{EPSRSUB}{3.9}}$$ (10.8)

$$\exp\left(-\frac{EOT \cdot \dfrac{EPSRSUB}{3.9} \cdot BGIDL}{V_{ds} - V_{gse} - EGIDL + V_{fbsd}}\right) \cdot \frac{V_{db}^3}{CGIDL + V_{db}^3}$$

$$I_{GIDS} = AGISL \cdot W_{effCJ} \cdot Nf \cdot \frac{V_{ds} - V_{gse} - EGISL + V_{fbsd}}{EOT \cdot \dfrac{EPSRSUB}{3.9}}$$ (10.9)

$$\exp\left(-\frac{EOT \cdot \dfrac{EPSRSUB}{3.9} \cdot BGISL}{V_{ds} - V_{gse} - EGISL + V_{fbsd}}\right) \cdot \frac{V_{db}^3}{CGISL + V_{db}^3}$$

Furthermore, for **mtrlMod=1** the mobility degradation uses the new expression of the vertical field in channel as following:

$$(10.10)$$

$$E_{eff} = \frac{V_{gsteff} + 2V_{th} - 2 \cdot B4SOItype \cdot (PHIG - EASUB - Eg / 2 + 0.45)}{EOT} \times \frac{3.9}{EPSRSUB}$$

Consequently, when **mtrlMod**=1, **mobMod**=1, 2 and 3 are changed, respectively:

mobMod=1

$$\mu_{eff} = \frac{\mu_o}{1 + (U_a + U_c V_{bseff})E_{eff} + U_b E_{eff}^{\ 2}} \tag{10.11}$$

mobMod=2

$$\mu_{eff} = \frac{\mu_o}{1 + (U_a + U_c V_{bseff})(\frac{V_{gsteff} - U_d}{T_{ox}}) + U_b(\frac{V_{gsteff} - U_d}{T_{ox}})^2} \tag{10.12}$$

$$U_d = 2 \cdot B4SOItype \cdot (PHIG - EASUB - Eg / 2 + 0.45)$$

mobMod=3

$$\mu_{eff} = \frac{\mu_0}{1 + [U_a E_{eff} + U_b E_{eff}^{\ 2}](1 + U_c V_{bseff})} \tag{10.13}$$

Appendix A: Model Instance Syntax

```
Mname <D node> <G node> <S node> <E node> [P node]
      [B node] [T node] <model>
      [L=<val>] [W=<val>]
      [AD=<val>] [AS=<val>] [PD=<val>] [PS=<val>]
      [NRS=<val>] [NRD=<val>] [NRB=<val>]
      [OFF][BJTOFF=<val>]
      [IC=<val>,<val>,<val>,<val>,<val>]
      [RTH0=<val>] [CTH0=<val>]
      [DEBUG=<val>]
      [DELVTO=<val>]
      [SA=<val>][SB=<val>][SD=<val>]
      [NF=<val>]
      [NBC=<val>] [NSEG=<val>] [PDBCP=<val>] [PSBCP=<val>]
      [AGBCP=<val>][AEBCP=<val>][VBSUSR=<val>][TNODEOUT]
      [FRBODY=<val>][AGBCPD=<val>][SHMOD=<val>]
```

Description

<D node>	Drain node
<G node>	Gate node
<S node>	Source node
<E node>	Substrate node
[P node]	(Optional) external body contact node
[B node]	(Optional) internal body node
[T node]	(Optional) temperature node
<model>	Level 9 BSIM3SOI model name
[L]	Channel length
[W]	Channel width

[AD]	Drain diffusion area
[AS]	Source diffusion area
[PD]	Drain diffusion perimeter length
[PS]	Source diffusion perimeter length
[NRS]	Number of squares in source series resistance
[NRD]	Number of squares in drain series resistance
[NRB]	Number of squares in body series resistance
[OFF]	Device simulation off
[BJTOFF]	Turn off BJT current if equal to 1
[IC]	Initial guess in the order of (Vds, Vgs, Vbs, Ves, Vps). (Vps will be ignored in the case of 4-terminal device)
[RTH0]	Thermal resistance per unit width
	■ if not specified, RTH0 is extracted from model card.
	■ if specified, it will override the one in model card.
[CTH0]	Thermal capacitance per unit width
	■ if not specified, CTH0 is extracted from model card.
	■ if specified, it will over-ride the one in model card.
[DEBUG]	Please see the debugging notes
[DELVTO]	Zero bias threshold voltage variation
[SA]	Stress effect parameter
[SB]	Stress effect parameter
[SD]	Stress effect parameter
[NF]	Number of fingers
[NBC]	Number of body contact isolation edge
[NSEG]	Number of segments for channel width partitioning [17]
[PDBCP]	Parasitic perimeter length for body contact at drain side
[PSBCP]	Parasitic perimeter length for body contact at source side
[AGBCP]	Parasitic gate-to-body overlap area for body contact (n^+-p)
[AGBCP2]	Parasitic gate-to-body overlap area for body contact (p^+-p)
	For details of AGBCP and AGBCP2, please check Fig.4.4
[AEBCP]	Parasitic body-to-substate overlap area for body contact

[VBSUSR]   Optional initial value of Vbs specified by user for transient analysis

[TNODEOUT]   Temperature node flag indicating the usage of T node

[FRBODY]   Layout-dependent body resistance coefficient

[AGBCPD]   Parasitic gate-to-body overlap area for body contact in DC

[RBDB]   Resistance between bNode and dbNode

[RBSB]   Resistance between bNode and sbNode

A.2.   About Optional Nodes

There are three optional nodes, P, B and T nodes. P and B nodes are used for body contact devices. Let us consider the case when TNODEOUT is not set. If user specifies four nodes, this element is a 4-terminal device, i.e., floating body. If user specifies five nodes, the fifth node represents the external body contact node (P). There is a body resistance between internal body node and P node. In these two cases, an internal body node is created but it is not accessible in the circuit deck. If user specifies six nodes, the fifth node represents the P node and the sixth node represents the internal body node (B). This configuration is useful for distributed body resistance simulation.

If TNODEOUT flag is set, the last node is interpreted as the temperature node. In this case, if user specifies five nodes, it is a floating body case. If user specifies six nodes, it is a body-contacted case. Finally, if user specifies seven nodes, it is a body-contacted case with an accessible internal body node. The temperature node is useful for thermal coupling simulation.

If the NODECHK flag is set, different warning messages are displayed and unsupported nodes are grounded according to the following table.

CASE	BSIM-SOI nodes as seen from the USER (not model) perspective	Nodes supplied on instance call	$port_connected(NODE)			TNODEOUT (instance parameter)	SHMOD	Warning message		
			NODE=P	NODE=B	NODE=T			TNODEOUT Messages	SOIMOD =0,1,3 Messages	SOIMOD=2 Messages
1	D G S E	4	**F**	**F**	**F**	0	0	None	None	None
2	D G S E P	5	**T**	**F**	**F**	0	0	None	None	s1
3	D G S E P B	6	**T**	**T**	**F**	0	0	None	None	s2
4	D G S E P B T	7	**T**	**T**	**T**	0	0	None	None	s2
5	D G S E	4	**F**	**F**	**F**	1	0	None	None	None
6	D G S E T	5	**T**	**F**	**F**	1	0	None	None	None
7	D G S E P T	6	**T**	**T**	**F**	1	0	None	None	s1
8	D G S E P B T	7	**T**	**T**	**T**	1	0	None	None	s2
9	D G S E	4	**F**	**F**	**F**	0	1	None	None	None
10	D G S E P	5	**T**	**F**	**F**	0	1	None	None	s1
11	D G S E P B	6	**T**	**T**	**F**	0	1	None	None	s2
12	D G S E P B T	7	**T**	**T**	**T**	0	1	None	None	s2
13	D G S E	4	**F**	**F**	**F**	1	1	t1	None	None
14	D G S E T	5	**T**	**F**	**F**	1	1	t2	None	None
15	D G S E P T	6	**T**	**T**	**F**	1	1	t3	None	None
16	D G S E P B T	7	**T**	**T**	**T**	1	1	None	None	s2

Table header note: The columns "Spice-syntax netlist (node-order determined terminals)" span CASE and BSIM-SOI nodes; "$port_connected(NODE)" spans NODE=P, NODE=B, NODE=T; "Warning message" spans the final three columns.

List of warning messages:

s1	"Warning: A P node was specified however SOIMOD=2 does not support a P node. Internally this node is tied to global ground"
s2	"Warning: P and B nodes were specified however SOIMOD=2 does not support P or B nodes. Internally these nodes are tied to global ground"
t1	"Warning: TNODEOUT=1 requesting an external temperature node but a 5th node for temperature is not supplied"
t2	""Warning: A 5th node has been specified with TNODEOUT=1. The 5th node will be treated as the temperature node T""
t3	"Warning: 5th and 6th nodes were specified when TNODEOUT=1. The 6th node will be treated as the temperature node T and Internally the 5th node will be tied to global ground"

Implementation Notes:

1) These new warning messages are toggled on/off by a new model parameter INSTANCECHK (analogous to PARAMCHK).

2) $port_connected(NODE) only provides information about whether a node is present in the

node list of the instance in the netlist. $port_connected does not provide any information about whether or where NODE is actually connected in the circuit.

3) If more than 4 nodes are specified but the TNODEOUT, SHMOD, and SOIMOD are not set to use any of the rightmost 5th, 6th, or 7th nodes, these nodes will be ignored and no warning will be issued.

4) TNODEOUT is an integer instance parameter (default 0).

5) When TNODEOUT=1, the right-most node is always interpreted as the temperature node T.

6) When SOIMOD=0,1,3 the P and B node are treated consistently with the BSIM-SOI self-heating model.

7) When SOIMOD=2, the P node is grounded, i.e. (V(p) <+ 0) in cases 2,3,4,7,8,10,11,12,15,16.

8) When SOIMOD=2, the B node grounded, i.e. (V(b) <+ 0) in cases 3,4,8,11,12,16.

9) When SHMOD=0 and TNODEOUT=1 there are no self-heating messages because self-heating is inactive.

10) When SHMOD=1 and TNODEOUT=1 and number of nodes=5, switch SH network to use the 5th node (case 14).

11) When SHMOD=1 and TNODEOUT=1 and number of nodes=6, switch SH network to use the 6th node (case 15).

12) When SHMOD=1 and TNODEOUT=1 and number of nodes=7, switch SH network to use the 7th node (case 16).

A.3. Notes on Debugging

The instance parameter <DEBUG> allows users to turn on debugging information selectively. Internal parameters (e.g. par) for an instance (e.g. m1) can be plotted by this command:

plot m1#par

By default, <DEBUG> is set to zero and two internal parameters will be available for plotting:

#body	V_b value iterated by SPICE
#temp	Device temperature with self-heating mode turned on

If <DEBUG> is set to one or minus one, more internal parameters are available for plotting. This serves debugging purposes when there is a convergence problem. This can also help the user to understand the model more. For <DEBUG> set to minus one, there will be charge calculation even if the user is running DC simulation. Here is the list of internal parameters:

#Vbs	Real V_{bs} value used by the IV calculation
#Vgsteff	Effective gate-overdrive voltage
#Vth	Threshold voltage
#Ids	MOS drain current
#Ic	BJT current
#Ibs	Body to source diode current
#Ibd	Body to drain diode current
#Iii	Impact ionization current
#Igidl	GIDL current
#Itun	Tunneling current
#Ibp	Body contact current
#Gds	Output conductance
#Gm	Transconductance
#Gmb	Drain current derivative wrt Vbs

These parameters are valid only if charge computation is required

#Cbb	Body charge derivative wrt Vbs
#Cbd	Body charge derivative wrt Vds
#Cbe	Body charge derivative wrt Ves
#Cbg	Body charge derivative wrt Vgs
#Qbody	Total body charge

#Qgate   Gate charge

#Qac0   Accumulation charge

#Qsub   Bulk charge

#Qsub0   Bulk charge at zero drain bias

#Qbf   Channel depletion charge

#Qjd   Parasitic drain junction charge

#Qjs   Parasitic source junction charge

Appendix B: Model Parameter List

All model parameters additional to BSIM3v3/BSIM4 will be shown with bold cases.

B.1.   BSIMSOI Model Control Parameters

Symbol used in equation	Symbol used in SPICE	Description	Unit	Default	Notes (below the table)
None	level	Level 10 for BSIMSOI4.1	-	10	-
SoiMod	soiMod	SOI model selector (instance) SoiMod=0: BSIMPD SoiMod=1: unified model for PD&FD. SoiMod=2: ideal FD. SoiMod=3: auto selection by BSIMSOI	-	0	
Shmod	shMod	Flag for self-heating 0 - no self-heating, 1 - self-heating	-	0	
Mobmod	mobmod	Mobility model selector	-	1	-
Capmod	capmod	Flag for the short channel capacitance model	-	2	
Noimod	noimod	Flag for Noise model	-	1	-
IgcMod	IgcMod	Gate-to-channel tunneling current model selector	-	0	
IgbMod	IgbMod	Gate-to-body tunneling current model selector	-	0	
RdsMod	rdsMod	Bias-dependent source/drain resistance model selector	-	0	
RgateMod	rgateMod	Flag for gate resistance model	-	0	-
RbodyMod	rbodyMod	Flag for body resistance model	-	0	-

FnoiMod	fnoiMod	Flicker noise model selector	-	1	
TnoiMod	TnoiMod	Thermal noise model selector	-	0	
MtrlMod	mtrlMod	New material model selector	-	0	
VgstcvMod	*VgstcvMod*	VgsteffCV model selector	-	0	
IiiMod	*IiiMod*	Impact ionization current model selector	-	0	
gidlMod	*gidlMod*	New GIDL/GISL model selector	-	0	
fdMod	*fdMod*	New ΔV_{bi} model selector	-	0	

B.2. Process Parameters

Symbol used in equation	Symbol used in SPICE	Description	Unit	Default	Notes (below the table)
t_{si}	Tsi	Silicon film thickness	m	10^{-7}	-
t_{box}	Tbox	Buried oxide thickness	m	$3x10^{-7}$	-
t_{ox}	tox	Gate oxide thickness	m	$1x10^{-8}$	-
Toxm	toxm	Gate oxide thickness used in extraction	m	tox	
X_j	Xj	S/D junction depth	m	Tsi	-
n_{ch}	Nch	Channel doping concentration	$1/cm^3$	$1.7x10^{17}$	-
n_{sub}	Nsub	Substrate doping concentration	$1/cm^3$	$6x10^{16}$	-
Ngate	ngate	poly gate doping concentration	$1/cm^3$	0	-
Eot	eot	Effective SiO2 thickness	nm	10	
Leffeot	leffeot	Effective length for extraction of EOT	um	1	-
Weffeot	weffeot	Effective width for extraction of EOT	um	10	-
Tempeot	tempeot	Temperature for extraction of EOT	K	300.15	-

Note: Leffeot, Weffeot, Tempeot and Vddeot are the parameters in EOT extraction and used in Toxp calculation (i.e., Eq. (10.6)).

B.3. DC Parameters

Symbol used in equation	Symbol used in SPICE	Description	Unit	Default	Notes (below the table)
V_{th0}	vth0	Threshold voltage @V_{bs}=0 for long and wide device	-	0.7	-
K_1	k1	First order body effect coefficient	$V^{1/2}$	0.6	-
K_{1w1}	k1w1	First body effect width dependent parameter	m	0	-
K_{1w2}	k1w2	Second body effect width dependent parameter	m	0	-
K_2	k2	Second order body effect coefficient	-	0	-
K_3	k3	Narrow width coefficient	-	0	-
K_{3b}	k3b	Body effect coefficient of k3	1/V	0	-
K_{b1}	Kb1	Backgate body charge coefficient	-	1	-
W_0	w0	Narrow width parameter	m	0	-
L_{pe0}	LPE0/ NLX	Lateral non-uniform doping parameter	m	1.74e-7	**If Lpe0 not given, lpe0=nlx if nlx given,; Else take the default Lpe0 was called nlx in BSIMSOI3**
L_{peb}	LPEB	Lateral non-uniform doping effect on K1	m	0.0	-
D_{vt0}	Dvt0	first coefficient of short-channel effect on Vth	-	2.2	-
D_{vt1}	dvt1	Second coefficient of short-channel effect on Vth	-	0.53	-
D_{vt2}	dvt2	Body-bias coefficient of short-channel effect on Vth	1/V	-0.032	-
D_{vt0w}	dvt0w	first coefficient of narrow width effect on Vth for small channel length	-	0	-
D_{vt1w}	dvt1w	Second coefficient of narrow width	-	5.3e6	-

		effect on Vth for small channel length			
D_{vt2w}	dvt2w	Body-bias coefficient of narrow width effect on Vth for small channel length	1/V	-0.032	-
μ_0	u0	Mobility at Temp = Tnom NMOSFET PMOSFET	cm^2/(V-sec)	 670 250	-
U_a	ua	First-order mobility degradation coefficient	m/V	2.25e-9	-
U_b	ub	Second-order mobility degradation coefficient	(m/V)^2	5.9e-19	-
U_c	uc	Body-effect of mobility degradation coefficient	1/V	-.0465	-
U_d	ud	Coulomb scattering factor of mobility	-	0	
Ucs	ucs	Mobility exponent factor in mobMod=4	-	0	
Eu	eu	Mobility exponent factor in mobMod=4	-	0	
v_{sat}	vsat	Saturation velocity at Temp=Tnom	m/sec	8e4	-
$A0$	a0	Bulk charge effect coefficient for channel length	-	1.0	-
A_{gs}	ags	Gate bias coefficient of A$_{bulk}$	1/V	0.0	-
$B0$	b0	Bulk charge effect coefficient for channel width	m	0.0	-
$B1$	b1	Bulk charge effect width offset	m	0.0	-
$Keta$	keta	Body-bias coefficient of bulk charge effect	V^{-1}	0	-
$Ketas$	Ketas	Surface potential adjustment for bulk charge effect	V	0	-
A_1	A1	First non-saturation effect parameter	1/V	0.0	-
A_2	A2	Second non-saturation effect parameter	0	1.0	-
R_{dsw}	rdsw	Parasitic resistance per unit width	Ω-	100	-

				μm^{Wr}		
Prwb	prwb	Body effect coefficient of Rdsw	1/V	0	-
Prwg	prwg	Gate bias effect coefficient of Rdsw	$1/V^{1/2}$	0	-
Wr	wr	Width offset from Weff for Rds calculation	-	1	-
Nfactor	nfactor	Subthreshold swing factor	-	1	-
Wint	wint	Width offset fitting parameter from I-V without bias	m	0.0	-
Lint	lint	Length offset fitting parameter from I-V without bias	m	0.0	-
DWg	dwg	Coefficient of W_{eff}'s gate dependence	m/V	0.0	
DWb	dwb	Coefficient of W_{eff}'s substrate body bias dependence	$m/V^{1/2}$	0.0	
DWbc	Dwbc	Width offset for body contact isolation edge	m	0.0	
V_{off}	voff	Offset voltage in the subthreshold region for large W and L	V	-0.08	-
Eta0	eta0	DIBL coefficient in subthreshold region	-	0.08	-
Eta0CV	eta0cv	DIBL coefficient in subthreshold region for CV	-	*Eta0*	-
Etab	etab	Body-bias coefficient for the subthreshold DIBL effect	1/V	-0.07	-
EtabCV	etabcv	Body-bias coefficient for the subthreshold DIBL effect for CV	1/V	*Etab*	-
D_{sub}	dsub	DIBL coefficient exponent	-	0.56	-
C_{it}	cit	Interface trap capacitance	F/m^2	0.0	-
C_{dsc}	cdsc	Drain/Source to channel coupling capacitance	F/m^2	2.4e-4	-
C_{dscb}	cdscb	Body-bias sensitivty of C_{dsc}	F/m^2	0	-
C_{dscd}	cdscd	Drain-bias sensitivty of C_{dsc}	F/m^2	0	-

P_{clm}	pclm	Channel length modulation parameter	-	1.3	-
P_{dibl1}	pdibl1	First output resistance DIBL effect correction parameter	-	.39	-
P_{dibl2}	pdibl2	Second output resistance DIBL effect correction parameter	-	0.086	-
D_{rout}	drout	L dependence coefficient of the DIBL correction parameter in Rout	-	0.56	-
$Pvag$	pvag	Gate dependence of Early voltage	-	0.0	-
δ	delta	Effective V_{ds} parameter	-	0.01	-
α_0	alpha0	The first parameter of impact ionization current	m/V	0.0	-
F_{bjtii}	fbjtii	Fraction of bipolar current affecting the impact ionization	-	0.0	-
β_0	beta0	First V_{ds} dependent parameter of impact ionization current	V^{-1}	0	-
β_1	beta1	Second V_{ds} dependent parameter of impact ionization current	-	0	-
β_2	beta2	Third V_{ds} dependent parameter of impact ionization current	V	0.1	-
$V_{dsatii0}$	vdsatii0	Nominal drain saturation voltage at threshold for impact ionization current	V	0.9	-
T_{ii}	tii	Temperature dependent parameter for impact ionization current	-	0	-
L_{ii}	lii	Channel length dependent parameter at threshold for impact ionization current	-	0	-
E_{satii}	esatii	Saturation channel electric field for impact ionization current	V/m	1e7	-
S_{ii0}	sii0	First V_{gs} dependent parameter for impact ionization current	V^{-1}	0.5	-
S_{ii1}	sii1	Second V_{gs} dependent parameter for	V^{-1}	0.1	-

		impact ionization current			
S_{ii2}	sii2	Third V_{gs} dependent parameter for impact ionization current	-	0	-
S_{iid}	siid	V_{ds} dependent parameter of drain saturation voltage for impact ionization current	V^{-1}	0	-
$Abjtii$	abjtii	Exponent factor for avalanche current	V^{-1}	0	
$Cbjtii$	cbjtii	Length scaling parameter for II BJT part	m	0	
$Ebjtii$	ebjtii	Impact ionization parameter for BJT part	-	0	
$Mbjtii$	mbjtii	Internal B-C grading coefficient	-	0.4	
$Vbci$	vbci	Internal B-C built-in potential	V	0	
A_{gidl}	Agidl	Pre-exponential GIDL constant	Ω^{-1}	0.0	-
B_{gidl}	Bgidl	GIDL exponential coefficient	V/m	2.3e9	-
C_{gidl}	Cgidl	Parameter for body bias effect on GIDL	V^3	0.5	
E_{gidl}	Egidl/ Ngidl	Fitting parameter for band bending for GIDL	V	1.2	If Egidl not given, Egidl=Ngidl if Ngidl given,; Else take the default Egidl was called Ngidl in BSIMSOI3
A_{gisl}	Agisl	Pre-exponential GISL constant	Ω^{-1}	0.0	-
B_{gisl}	Bgisl	GISL exponential coefficient	V/m	2.3e9	-
C_{gisl}	Cgisl	Parameter for body bias effect on GISL	V^3	0.5	
E_{gisl}	Egisl	Fitting parameter for band bending for GISL	V	1.2	
$Rgidl$	rgidl	Vgs-dependent parameter for GIDL when gidlMod = 1	-	1.0	
$Kgidl$	kgidl	Vds-dependent parameter for GIDL	V	0.0	

		when gidlMod = 1			
Fgidl	fgidl	Vds-dependent parameter for GIDL when gidlMod = 1			
Rgisl	rgisl	Vgs-dependent parameter for GISL when gidlMod = 1	-	1.0	
Kgisl	kgisl	Vbs-dependent parameter for GISL when gidlMod = 1	V	0.0	
Fgisl	fgisl	Vbs-dependent parameter for GISL when gildMod = 1	V	0.0	
n_{diodes}	Ndiode	Diode non-ideality factor for source	-	1.0	-
n_{dioded}	Ndioded	Diode non-ideality factor for drain	-	Default to its source value	-
n_{recf0s}	Nrecf0	Recombination non-ideality factor at forward bias for source	-	2.0	-
n_{recf0d}	Nrecf0d	Recombination non-ideality factor at forward bias for drain	-	Default to its source value	-
n_{recr0s}	Nrecr0	Recombination non-ideality factor at reversed bias for source	-	10	-
n_{recr0d}	Nrecr0d	Recombination non-ideality factor at reversed bias for drain	-	Default to its source value	-
i_{sbjt}	Isbjt	BJT injection saturation current	A/m^2	1e-6	-
I_{dbjt}	Idbjt	BJT injection saturation current	A/m^2	1e-6	-
i_{sdif}	Isdif	Body to source/drain injection saturation current	A/m^2	1e-7	-

I_{ddif}	Iddif	Body to source/drain injection saturation current	A/m^2	1e-7		-
i_{srec}	Isrec	Recombination in depletion saturation current	A/m^2	1e-5		-
I_{drec}	Idrec	Recombination in depletion saturation current	A/m^2	1e-5		-
i_{stun}	Istun	Reverse tunneling saturation current	A/m^2	0.0		-
I_{dtun}	Idtun	Reverse tunneling saturation current	A/m^2	0.0		-
Ln	Ln	Electron/hole diffusion length	m	2e-6		-
V_{rec0s}	Vrec0	Voltage dependent parameter for recombination current for source	V	0		-
V_{rec0d}	Vrec0d	Voltage dependent parameter for recombination current for drain	V	Default to its source value		-
V_{tun0s}	Vtun0	Voltage dependent parameter for tunneling current for source	V	0		-
V_{tun0d}	Vtun0d	Voltage dependent parameter for tunneling current for drain	V	Default to its source value		-
N_{bjt}	Nbjt	Power coefficient of channel length dependency for bipolar current	-	1		-
L_{bjt0}	Lbjt0	Reference channel length for bipolar current	m	0.20e-6		-
V_{abjt}	Vabjt	Early voltage for bipolar current	V	10		-
A_{ely}	Aely	Channel length dependency of early voltage for bipolar current	V/m	0		-
A_{hlis}	Ahli	High level injection parameter for bipolar current for source	-	0		-

A_{hlid}	Ahlid	High level injection parameter for bipolar current for drain	-	Default to its source value	-
$Rbody$	Rbody	Intrinsic body contact sheet resistance	ohm/square	0.0	-
$Rbsh$	Rbsh	Extrinsic body contact sheet resistance	ohm/square	0.0	-
Rsh	rsh	Source drain sheet resistance in ohm per square	ohm/square	0.0	-
$Rhalo$	rhalo	Body halo sheet resistance	ohm/m	1e15	-
Rsw	Rsw	Zero bias lightly-doped source resistance per unit width for RDSMOD=1	Ohm(um)^{WR}	50	
Rdw	Rdw	Zero bias lightly-doped drain resistance per unit width for RDSMOD=1	Ohm(um)^{WR}	50	
$Rswmin$	Rswmin	Lightly-doped source resistance per unit width at high Vgs and zero Vbs for RDSMOD=1	Ohm(um)^{WR}	0	
$Rdwmin$	Rdwmin	Lightly-doped source resistance per unit width at high Vgs and zero Vbs for RDSMOD=1	Ohm(um)^{WR}	0	
$Dvtp0$	Dvtp0	First parameter for Vth shift due to p ocket	m	0.0	
$Dvtp1$	Dvtp1	Second parameter for Vth shift due to p ocket	v^{-1}	0.0	
$Dvtp2$	Dvtp2	Third parameter for Vth shift due to pocket	v^{-1}	0.0	
$Dvtp3$	Dvtp3	Forth parameter for Vth shift due to pocket	v^{-1}	0.0	
$Dvtp4$	Dvtp4	Fifth parameter for Vth shift due to pocket	v^{-1}	0.0	
$Pdits$	Pdits	Coefficient for drain-induced Vth shifts	v^{-1}	1e-20	
$Pditsl$	Pditsl	Length dependence of drain-induced Vt	m^{-1}	0	

		h shifts			
Pditsd	Pditsd	Vds dependence of drain-induced Vth shifts	v^{-1}	0	
Fprout	Fprout	Effect of pocket implant on rout degradation	$V/m^{0.5}$	0.0	
Minv	Minv	Vgsteff fitting parameter for moderate inversion		0.0	

B.4.   Gate-to-body tunneling parameters

B.4. Gate-to-body tunneling parameters

Symbol used in equation	Symbol used in SPICE	Description	Unit	Default
IgMod	igMod	Gate current model selector	-	0
Toxqm	toxqm	Oxide thickness for I_{gb} calculation	m	Tox
Ntox	ntox	Power term of gate current	-	1
Toxref	toxref	Target oxide thickness	m	2.5e-9
φ_g	ebg	Effective bandgap in gate current calculation	V	1.2
α_{gb1}	alphaGB1	First Vox dependent parameter for gate current in inversion	1/V	.35
β_{gb1}	betaGB1	Second Vox dependent parameter for gate current in inversion	$1/V^2$	.03
V_{gb1}	vgb1	Third Vox dependent parameter for gate current in inversion	V	300
V_{EVB}	vevb	Vaux parameter for valence band electron tunneling	-	0.075
α_{gb2}	alphaGB2	First Vox dependent parameter for gate current in accumulation	1/V	.43
β_{gb2}	betaGB2	Second Vox dependent parameter for gate current in accumulation	$1/V^2$	.05
V_{gb2}	vgb2	ThirdVox dependent parameter for gate current in accumulation	V	17
V_{ECB}	vecb	Vaux parameter for conduction band electron tunneling	-	.026
AIGBCP2	aigbcp2	First Vgp dependent parameter for gate current in accumulation in AGBCP2 region	$1/V^2$	0.043
BIGBCP2	bigbcp2	Second Vgp dependent parameter for gate current in accumulation in AGBCP2 region	$1/V^2$	0.0054
CIGBCP2	cigbcp2	Third Vgp dependent parameter for gate current in accumulation in AGBCP2 region	$1/V^2$	0.0075

B.5. AC and Capacitance Parameters

Symbol used in equation	Symbol used in SPICE	Description	Unit	Default	Notes (below the table)
Xpart	xpart	Charge partitioning rate flag	-	0	
CGS0	cgso	Non LDD region source-gate overlap capacitance per channel length	F/m	calcu-lated	**nC-1**
CGD0	cgdo	Non LDD region drain-gate overlap capacitance per channel length	F/m	calcu-lated	**nC-2**
CGEO	cgeo	Gate substrate overlap capacitance per unit channel length	F/m	0.0	-
Cjswgs	cjswg	Source (gate side) sidewall junction capacitance per unit width (normalized to 100nm T_{si})	F/m^2	1e-10	-
Cjswgd	cjswgd	Drain (gate side) sidewall junction capacitance per unit width (normalized to 100nm T_{si})	F/m^2	Default to its source value	-
Pbswgs	pbswg	Source (gate side) sidewall junction capacitance buit in potential	V	.7	-
Pbswgd	pbswgd	Drain (gate side) sidewall junction capacitance buit in potential	V	Default to its source value	-
Mjswgs	mjswg	Source (gate side) sidewall junction capacitance grading coefficient	V	0.5	-
Mjswgd	mjswgd	Drain (gate side) sidewall junction capacitance grading coefficient	V	Default to its	-

				source value	
t_t	tt	Diffusion capacitance transit time coefficient	second	1e-12	-
N_{dif}	Ndif	Power coefficient of channel length dependency for diffusion capacitance	-	-1	-
L_{dif0}	Ldif0	Channel-length dependency coefficient of diffusion cap.	-	1	-
V_{sdfb}	vsdfb	Source/drain bottom diffusion capacitance flatband voltage	V	calcu-lated	nC-3
V_{sdth}	vsdth	Source/drain bottom diffusion capacitance threshold voltage	V	calcu-lated	nC-4
C_{sdmin}	csdmin	Source/drain bottom diffusion minimum capacitance	V	calcu-lated	nC-5
A_{sd}	asd	Source/drain bottom diffusion smoothing parameter	-	0.3	-
C_{sdesw}	csdesw	Source/drain sidewall fringing capacitance per unit length	F/m	0.0	-
$CGSl$	cgsl	Light doped source-gate region overlap capacitance	F/m	0.0	-
$CGDl$	cgdl	Light doped drain-gate region overlap capacitance	F/m	0.0	-
$CKAPPA$	ckappa	Coefficient for lightly doped region overlap capacitance fringing field capacitance	F/m	0.6	-
Cf	cf	Gate to source/drain fringing field capacitance	F/m	calcu-lated	**nC-6**
CLC	clc	Constant term for the short channel model	m	0.1×10^{-7}	-
CLE	cle	Exponential term for the short channel model	none	0.0	-

DLC	dlc	Length offset fitting parameter for gate charge	m	lint	-
DLCB	dlcb	Length offset fitting parameter for body charge	m	0	-
DLBG	dlbg	Length offset fitting parameter for backgate charge	m	0.0	-
DWC	dwc	Width offset fitting parameter from C-V	m	wint	-
DelVt	delvt	Threshold voltage adjust for C-V	V	0.0	-
F_{body}	fbody	Scaling factor for body charge	-	1.0	-
acde	acde	Exponential coefficient for charge thickness in capMod=3 for accumulation and depletion regions.	m/V	1.0	-
moin	moin	Coefficient for the gate-bias dependent surface potential.	$V^{1/2}$	15.0	-
CfrCoeff	cfrcoeff	Sidewall fringe capacitance coefficient	-	1	Max limit = 2

B.6. Temperature Parameters

Symbol used in equation	Symbol used in SPICE	Description	Unit	Default	Note
Tnom	tnom	Temperature at which parameters are expected	°C	27	-
μte	ute	Mobility temperature exponent	none	-1.5	-
Kt1	kt1	Temperature coefficient for threshold voltage	V	-0.11	-
Kt11	kt11	Channel length dependence of the temperature coefficient for threshold voltage	V*m	0.0	
Kt2	kt2	Body-bias coefficient of the Vth	none	0.022	-

		temperature effect			
Ua1	ua1	Temperature coefficient for U_a	m/V	4.31e-9	-
Ub2	ub1	Temperature coefficient for U_b	$(m/V)^2$	-7.61e-18	-
Uc1	uc1	Temperature coefficient for Uc	1/V	-.056	**nT-1**
At	at	Temperature coefficient for saturation velocity	m/sec	3.3e4	-
Tcijswgs	tcjswg	Temperature coefficient of C_{jswgs}	1/K	0	-
Tpbswgs	tpbswg	Temperature coefficient of P_{bswgs}	V/K	0	-
Tcijswgd	tcjswgd	Temperature coefficient of C_{jswgd}	1/K	Default to its source value	-
Tpbswgd	tpbswgd	Temperature coefficient of P_{bswgd}	V/K	Default to its source value	-
Cth0	cth0	Normalized thermal capacity	(W*sec) / m°C	1e-5	-
Prt	prt	Temperature coefficient for Rdsw	Ω-μm	0	-
Rth0	rth0	Normalized thermal resistance	m°C/W	0	-
Nt_{recf}	Ntrecf	Temperature coefficient for N_{recf}	-	0	-
Nt_{recr}	Ntrecr	Temperature coefficient for N_{recr}	-	0	-
X_{bjt}	xbjt	Power dependence of j_{bjt} on temperature	-	1	-
X_{difs}	xdifs	Power dependence of j_{difs} on temperature	-	X_{bjt}	-
X_{recs}	xrecs	Power dependence of j_{recs} on temperature	-	1	-
X_{tuns}	xtuns	Power dependence of j_{tuns} on temperature	-	0	-
X_{difd}	xdifd	Power dependence of j_{difd} on temperature	-	X_{bjt}	-
X_{recd}	xrecd	Power dependence of j_{recd} on temperature	-	1	-
X_{tund}	xtund	Power dependence of j_{tund} on temperature	-	0	-
W_{th0}	Wth0	Minimum width for thermal resistance calculation	m	0	-
Tvbci	tvbci	Temperature coefficient for Vbci	-	0	

B.7. BSIMSOI Built-In Potential Lowering (ΔV$_{bi}$) Model Parameters

Symbol used in equation	Symbol used in SPICE	Description	Unit	Default
SoiMod	soiMod	SOI model selector. SoiMod=0: BSIMPD. SoiMod=1: unified model for PD&FD. SoiMod=2: ideal FD. SoiMod=3: auto selection by BSIMSOI	-	0
$V_{nonideal}$	vbsa	Offset voltage due to non-idealities	V	0
$N_{OFF,FD}$	nofffd	Smoothing parameter in FD module	-	1
$V_{OFF,FD}$	vofffd	Smoothing parameter in FD module	V	0
K_{1b}	K1b	First backgate body effect parameter	-	1
K_{2b}	K2b	Second backgate body effect parameter for short channel effect	-	0
D_{k2b}	dk2b	Third backgate body effect parameter for short channel effect	-	0
D_{vbd0}	dvbd0	First short channel effect parameter in FD module	-	0
D_{vbd1}	dvbd1	Second short channel effect parameter in FD module	-	0
MoinFD	moinfd	Gate bias dependence coefficient of surface potential in FD module	-	1e3
V_{bs0pd}	vbs0pd	Upper bound of built-in potential lowering for BSIMPD operation	V	0.0
V_{bs0fd}	vbs0fd	Lowering bound of built-in potential lowering for ideal FD operation	V	0.5

B.8.   BSIMSOI RF Model Parameters

RgateMod	rgateMod	Gate resistance model selector rgateMod = 0 No gate resistance rgateMod = 1 Constant gate resistance rgateMod = 2 Rii model with variable resistance rgateMod = 3 Rii model with two nodes	-	0
RbodyMod	RbodyMod	RbodyMod=0 No body resistance model RbodyMod=1 Two-resistor body resistance model	-	0
Rshg	Rshg	Gate electrode sheet resistance	Ohm/s quare	0.1
XRCRG1	xrcrg1	Parameter for distributed channel-resistance effect for intrinsic input resistance	-	12.0
XRCRG2	xrcrg2	Parameter to account for the excess channel diffusion resistance for intrinsic input resistance	-	1.0
NGCON	ngcon	Number of gate contacts	-	1
XGW	xgw	Distance from the gate contact to the channel edge	m	0.0
XGL	xgl	Offset of the gate length due to variations in patterning	m	0.0
RBSB	rbsb	Resistance between sbNode and bNode	Ohm	50.0
RBDB	rbdb	Resistance between dbNode and bNode	Ohm	50.0
GBMIN	gbmin	Conductance parallel with RBSB/RBDB	mho	1e-12

B.9. BSIMSOI Noise Model Parameters

FnoiMod	fnoiMod	Flicker noise model selector	-	1
TnoiMod	TnoiMod	Thermal noise model selector	-	0
NTNOI	ntnoi	Noise factor for short-channel devices for TNOIMOD=0 or 2	-	1.0
TNOIA	Tnoia	Coefficient of channel length dependence of total channel thermal noise	-	1.5
TNOIB	Tnoib	Channel length dependence parameter for channel thermal noise partitioning	-	3.5
TNOIC	Tnoic	Length dependent parameter for Correlation Coefficient	-	3.5
RNOIC	Rnoic	Correlation Coefficient parameter	-	0.395
RNOIA	rnoia	Thermal noise parameter	-	0.577
RNOIB	rnoib	Thermal noise parameter	-	0.37
W0FLK	W0flk	Flicker noise width dependence parameter	-	-1
BF	bf	Flicker noise length dependence exponent	-	2.0
SCALEN	SCALEN	Correlated thermal noise scaling parameter		1e5

B.10. BSIMSOI Stress Model Parameters

SA (instance parameter)	sa	Distance between OD edge to poly from one side	m	0.0
SB (instance parameter)	sb	Distance between OD edge to poly from another side	m	0.0
SD (instance parameter)	sd	Distance between neighbouring fingers	m	0.0
SAREF	saref	Reference distance between OD and edge to poly of one side	m	1e-6

SBREF	sbref	Reference distance between OD and edge to poly of another side	m	1e-6
WLOD	Wlod	Width parameter for stress effect	M	0.0
KU0	Ku0	Mobility degradation/enhancement	M	0.0
KVSAT	Kvsat	Saturation velocity degradation/enhancement parameter for stress effect	M	0.0
TKU0	TKU0	Temperature coefficient of KU0		0.0
LKU0	LKU0	Length dependence of KU0		0.0
WKU0	WKU0	width dependence of KU0		0.0
PKU0	PKU0	Cross-term dependence of KU0		0.0
LLODKU0	LLODKU0	Length parameter for u0 stress effect		0.0
WLODKU0	WLODKU0	Width parameter for u0 stress effect		0.0
KVTH0	KVTH0	Threshold shift parameter for stress effect	Vm	0.0
LKVTH0	LKVTH0	Length dependence of KVHT0		0.0
WKVTH0	WKVTH0	Width dependence of KVHT0		0.0
PKVTH0	PKVTH0	Cross term dependence of KVHT0		0.0
LLODVTH	Llodvth	Length parameter for Vth stress effect		0.0
WLODVTH	Wlodvth	Width parameter for Vth stress effect		0.0
STK2	Stk2	K2 shift factor related to Vth0 change	M	0.0
LODK2	LODk2	K2 shift modification factor for stress effect		1.0
STETA0	Steta0	Eta0 shift factor related to vth0 change	M	0.0
STETA0CV	steta0cv	Eta0CV shift factor related to vth0 change	M	STETA0
LODETA0	Lodeta0	Eta0 shift modification factor for stress effect		1.0
LODETA0CV	lodeta0cv	Eta0CV shift modification factor for stress effect		LODETA0

B.11. New parameters added in BSIMSOIv4.5.0 corresponding to the various material properties for mtrlMod=1

Parameter	Description	Default
EGGBCP2	Bandgap in Agbcp2 region	1.12
EGGDEP	Bandgap for gate depletion effect	1.12
AGB1	'A' for Igb1 Tunneling current model	3.7622E-07
BGB1	'B' for Igb1 Tunneling current model	-3.1051E+10
AGB2	'A' for Igb2 Tunneling current model	4.9758E-07
BGB2	'B' for Igb2 Tunneling current model	-2.357E+10
AGBC2N	NMOS 'A' for tunneling current model	3.4254E-07
AGBC2P	PMOS 'A' for tunneling current model	4.9723E-07
BGBC2N	NMOS 'B' for tunneling current model	1.1665E+12
BGBC2P	PMOS 'B' for tunneling current model	7.4567E+11
VTM00	Hard coded 25°C thermal voltage	0.026

B.12. Model Parameter Notes

nI-1. BSIMPD supports *capmod=2* and *3* only. *Capmod=0* and *1* are not supported.

nI-2. In modern SOI technology, source/drain extension or LDD are commonly used. As a result, the source/drain junction depth (X_j) can be different from the silicon film thickness (T_{si}). By default, if X_j is not given, it is set to T_{si}. X_j is not allowed to be greater than T_{si}.

nI-3. BSIMPD refers substrate to the silicon below buried oxide, not the well region in BSIM3. It is used to calculate backgate flatband voltage (V_{fbb}) and parameters related to source/drain diffusion bottom capacitance (V_{sdth}, V_{sdfb}, C_{sdmin}). Positive n_{sub} means the same type of doping as the body and negative n_{sub} means opposite type of doping.

nC-1. If *cgso* is not given then it is calculated using:

if (*dlc* is given and is greater 0) then,

$$cgso = p1 = (dlc*cox) - cgs1$$

if (the previously calculated *cgso* <0), then

$$cgso = 0$$

else $cgso = 0.6 * Tsi * cox$

nC-2. *Cgdo* is calculated in a way similar to *Csdo*

nC-3. If (n_{sub} is positive)

$$V_{sdfb} = -\frac{kT}{q} \log\left(\frac{10^{20} \cdot n_{sub}}{n_i \cdot n_i}\right) - 0.3$$

else

$$V_{sdfb} = -\frac{kT}{q} \log\left(\frac{10^{20}}{n_{sub}}\right) + 0.3$$

nC-4. If (n_{sub} is positive)

$$\phi_{sd} = 2\frac{kT}{q} \log\left(\frac{n_{sub}}{n_i}\right), \quad \gamma_{sd} = \frac{5.753 \times 10^{-12} \sqrt{n_{sub}}}{C_{box}}$$

$$V_{sdth} = V_{sdfb} + \phi_{sd} + \gamma_{sd}\sqrt{\phi_{sd}}$$

else

$$\phi_{sd} = 2\frac{kT}{q} \log\left(-\frac{n_{sub}}{n_i}\right), \quad \gamma_{sd} = \frac{5.753 \times 10^{-12} \sqrt{-n_{sub}}}{C_{box}}$$

$$V_{sdth} = V_{sdfb} - \phi_{sd} - \gamma_{sd}\sqrt{\phi_{sd}}$$

nC-5. $X_{sddep} = \sqrt{\frac{2\varepsilon_{si}\phi_{sd}}{q|n_{sub} \cdot 10^6|}}$, $C_{sddep} = \frac{\varepsilon_{si}}{X_{sddep}}$, $C_{sd\,min} = \frac{C_{sddep}C_{box}}{C_{sddep} + C_{box}}$

nC-6. If cf is not given then it is calculated using

$$CF = \frac{2\varepsilon_{ox}}{\pi} \ln\left(1 + \frac{4 \times 10^{-7}}{T_{ox}}\right)$$

nT-1. For mobmod=1 and 2, the unit is m/V². Default is -5.6E-11. For mobmod=3, unit is 1/V and default is -0.056.

Appendix C: Equation List

C1:   Equation List for BSIMSOI Built-In Potential Lowering Calculation

If SoiMod=0 (default), the model equation is identical to BSIMPD equation.

If SoiMod=1 (unified model for PD&FD) or SoiMod=2 (ideal FD), the following equations (FD module) are added on top of BSIMPD.

fdMod = 0

$$\Delta V_{bi} = \frac{C_{Si}}{C_{Si}+C_{BOX}} \cdot \left(phi - \frac{qN_{ch}}{2\varepsilon_{Si}} \cdot T_{Si}^2 + V_{nonideal} + \Delta V_{DIBL} \right) + \eta_e \frac{C_{BOX}}{C_{Si}+C_{BOX}} \cdot \left(V_{es} - V_{FBb} \right)$$

where $C_{Si} = \dfrac{\varepsilon_{Si}}{T_{Si}}, C_{BOX} = \dfrac{\varepsilon_{OX}}{T_{BOX}}, C_{OX} = \dfrac{\varepsilon_{OX}}{T_{OX}}$

$$\Delta V_{DIBL} = D_{vbd0} \left(\exp\left(-D_{vbd1}\frac{L_{eff}}{2l} \right) + 2\exp\left(-D_{vbd1}\frac{L_{eff}}{l} \right) \right) \cdot \left(V_{bi} - 2\Phi_B \right)$$

$$\eta_e = K_{1b} - K_{2b} \cdot \left(exp\left(-D_{k2b}\frac{L_{eff}}{2l} \right) + 2exp\left(-D_{k2b}\frac{L_{eff}}{l} \right) \right)$$

fdMod = 1

$$\Delta V_{bi} = \frac{C_{si}}{C_{si}+C_{BOX}+CDSBS} \cdot \left(\phi - \frac{qN_{ch} \cdot (1+L_{pe0}/L_{eff})}{2\varepsilon_{Si}} \cdot T_{si}^2 + V_{nonideal} \right)$$
$$+ \frac{C_{BOX}}{C_{si}+C_{BOX}+CDSBS} \cdot \left(V_{bGS} - V_{FBb} \right) + \frac{CDSBS}{C_{si}+C_{BOX}+CDSBS} \cdot \Delta V_{SCE}$$

$$\Delta V_{SCE} = DVBD0 \cdot \left(\exp\left(-DVBD1 \frac{L_{eff}}{2l} \right) + 2\exp\left(-DVBD1 \frac{L_{eff}}{l} \right) \right) \cdot \left(V_{ds} + VSCE \right)$$

$$phi = phi_{ON} - \frac{C_{OX}}{C_{OX} + \left(C_{Si}^{-1} + C_{BOX}^{-1} \right)^{-1}} \cdot N_{OFF,FD} V_t \cdot ln\left(1 + exp\left(\frac{V_{th,FD} - V_{gs\_eff} - V_{OFF,FD}}{N_{OFF,FD} V_t} \right) \right)$$

$$phi_{ON} = 2\Phi_B + V_t \, ln\left(1 + \frac{V_{gsteff.FD}\left(V_{gsteff,FD} + 2K1\sqrt{2\Phi_B} \right)}{MoinFD \cdot K1 \cdot V_t^2} \right),$$

$$V_{gsteff,FD} = N_{OFF,FD} V_t \cdot ln\left(1 + exp\left(\frac{V_{gs\_eff} - V_{th,FD} - V_{OFF,FD}}{N_{OFF,FD} V_t} \right) \right)$$

Here Nch is the channel doping concentration. V_{FBb} is the backgate flatband voltage. $V_{th,FD}$ is the threshold voltage at $V_{bs} = V_{bs0}$(phi=$2\Phi_B$). V_t is thermal voltage. K1 is the body effect coefficient.

If SoiMod=1, the lower bound of V_{bs} (SPICE solution) is set to V_{bs0}. If SoiMod=2, V_{bs} is pinned at V_{bs0}. Notice that there is no body node and body leakage/charge calculation in SoiMod=2.

The zero field body potential that will determine the transistor threshold voltage, V_{bsmos}, is then calculated by

if $V_{bs} \leq V_{bs0}\left(T_{OX} \to \infty\right)$

$$V_{bsmos} = V_{bs} - \frac{C_{Si}}{2qN_{ch}T_{Si}}\left(V_{bs0}\left(T_{OX} \to \infty\right) - V_{bs}\right)^2$$

else

$$V_{bsmos} = V_{bs}$$

The subsequent clamping of V_{bsmos} will use the same equation that utilized in BSIMPD.

If SoiMod=3 is specified, BSIMSOI will select the operation mode for the user based on the estimated value of V_{bs0} at phi=$2\Phi_B$ (bias independent), V_{bs0t}:

If $V_{bs0t} > V_{bs0fd}$, BSIMSOI will be in the ideal FD mode (SoiMod=2).

If $V_{bs0t} < V_{bs0pd}$, BSIMSOI will be in the BSIMPD mode (SoiMod=0).

Otherwise, BSIMSOI will be operated under SoiMod=1.

Notice that both V_{bs0fd} and V_{bs0pd} are model parameters.

C2:   Equation List for BSIMPD IV

Body Voltages

V_{bsh} is equal to the V_{bs} bounded between (V_{bsc}, ϕ_{s1}). V_{bsh} is used in V_{th} and A_{bulk} calculation

$$T_1 = V_{bsc} + 0.5\left[V_{bs} - V_{bsc} - \delta + \sqrt{(V_{bs} - V_{bsc} - \delta)^2 - 4\delta V_{bsc}}\right], \quad V_{bsc} = -5V$$

$$V_{bsh} = \phi_{s1} - 0.5\left[\phi_{s1} - T_1 - \delta + \sqrt{(\phi_{s1} - T_1 - \delta)^2 + 4\delta T_1}\right], \quad \phi_{s1} = 1.5V$$

V_{bsh} is further limited to $0.95\phi_s$ to give V_{bseff}.

$$V_{bseff} = \phi_{s0} - 0.5\left[\phi_{s0} - V_{bsh} - \delta + \sqrt{(\phi_{s0} - V_{bsh} - \delta)^2 + 4\delta V_{bsh}}\right], \quad \phi_{s0} = 0.95\phi_s$$

Effective Channel Length and Width

$$dW' = W_{int} + \frac{W_l}{L^{W_{ln}}} + \frac{W_w}{W^{W_{wn}}} + \frac{W_{wl}}{L^{W_{ln}}W^{W_{wn}}}$$

$$dW = dW' + dW_g V_{gsteff} + dW_b\left(\sqrt{\Phi_s - V_{bseff}} - \sqrt{\Phi_s}\right)$$

$$dL = L_{int} + \frac{L_l}{L^{L_{ln}}} + \frac{L_w}{W^{L_{wn}}} + \frac{L_{wl}}{L^{L_{ln}}W^{L_{wn}}}$$

$$L_{eff} = L_{drawn} - 2dL$$

$$W_{eff} = W_{drawn} - N_{bc}dW_{bc} - (2 - N_{bc})dW$$

$$W_{eff}' = W_{drawn} - N_{bc}dW_{bc} - (2 - N_{bc})dW'$$

$$W_{diod} = \frac{W_{eff}'}{N_{seg}} + P_{dbcp}$$

$$W_{dios} = \frac{W_{eff}'}{N_{seg}} + P_{sbcp}$$

Threshold Voltage

$$V_{th} = V_{tho} + (K_{1ox} sqrtPhisExt - K_{1eff}\sqrt{\Phi_s})\sqrt{1 + \frac{LPEB}{L_{eff}}} - K_{2ox}V_{bseff}$$

$$+ K_{1ox}(\sqrt{1 + \frac{LPE0}{L_{eff}}} - 1)\sqrt{\Phi_s} + (K_3 + K_{3b}V_{bseff})\frac{T_{ox}}{W_{eff}^{'} + W_o}\Phi_s$$

$$- D_{VT0w}(\exp(-D_{VT1w}\frac{W_{eff}^{'}L_{eff}}{2l_{tw}}) + 2\exp(-D_{VT1w}\frac{W_{eff}^{'}L_{eff}}{l_{tw}}))(V_{bi} - \Phi_s)$$

$$- D_{VT0}(\exp(-D_{VT1}\frac{L_{eff}}{2l_t}) + 2\exp(-D_{VT1}\frac{L_{eff}}{l_t}))(V_{bi} - \Phi_s)$$

$$- (\exp(-D_{sub}\frac{L_{eff}}{2l_{to}}) + 2\exp(-D_{sub}\frac{L_{eff}}{l_{to}}))(E_{tao} + E_{tab}V_{bseff})V_{ds}$$

$$- nv_t \cdot \ln\left(\frac{L_{eff}}{L_{eff} + DVTP0 \cdot (1 + e^{-DVTP1 \cdot V_{DS}})}\right)$$

$$- \frac{DVTP2}{L_{eff}^{DVTP3}} \cdot \tanh(DVTP4 \cdot V_{ds})$$

Note: The last term (*DVTP2*, *DVTP3* and *DVTP4*) introduces the flexibility to capture DIBL variation in longer channel. Considering backward compatibility, the old term (*DVTP1* and

DVTP2) is kept.

$$l_t = \sqrt{\varepsilon_{si}X_{dep}/C_{ox}}(1 + D_{VT2}V_{bseff})$$

$$sqrtPhisExt = \sqrt{\phi_s - V_{bseff}} + s(V_{bsh} - V_{bseff}), \quad s = -\frac{1}{2\sqrt{\phi_s - \phi_{s0}}}$$

$$K_{1eff} = K_1\left(1 + \frac{K_{1w1}}{W_{eff}^{'} + K_{1w2}}\right)$$

$$K_{1ox} = K_{1eff}\frac{TOX}{TOXM}$$

$$K_{2ox} = K_2\frac{TOX}{TOXM}$$

$$l_{tw} = \sqrt{\varepsilon_{si}X_{dep}/C_{ox}}(1 + D_{VT2w}V_{bseff}) \qquad l_{to} = \sqrt{\varepsilon_{si}X_{dep0}/C_{ox}}$$

$$X_{dep} = \sqrt{\frac{2\varepsilon_{si}(\Phi_s - V_{bseff})}{qN_{ch}}} \qquad\qquad X_{dep0} = \sqrt{\frac{2\varepsilon_{si}\Phi_s}{qN_{ch}}}$$

$$V_{bi} = v_t \ln(\frac{N_{ch}N_{DS}}{n_i^2})$$

Poly depletion effect

$$\varepsilon_{ox}E_{ox} = \varepsilon_{si}E_{poly} = \sqrt{2q\varepsilon_{si}N_{gate}V_{poly}}$$

$$V_{poly} + \frac{1}{2}X_{poly}E_{poly} = \frac{qN_{gate}X_{poly}^2}{2\varepsilon_{si}}$$

$$V_{gs} - V_{FB} - \phi_x = V_{poly} + V_{ox}$$

$$a(V_{gs} - V_{FB} - \phi_s - V_{poly})^2 - V_{poly} = 0$$

$$a = \frac{\varepsilon_{ox}^2}{2q\varepsilon_{si}N_{gate}T_{ox}^2}$$

$$V_{gs\_eff} = V_{FB} + \phi_s + \frac{q\varepsilon_{si}N_{gate}T_{ox}^2}{\varepsilon_{ox}^2}\left[\sqrt{1 + \frac{2\varepsilon_{ox}^2(V_{gs} - V_{FB} - \phi_s)}{q\varepsilon_{si}N_{gate}T_{ox}^2}} - 1\right]$$

Effective V$_{gst}$ for all region (with Polysilicon Depletion Effect)

$$V_{gsteff} = \frac{nv_t \ln[1 + \exp(\frac{m*(V_{gs\_eff} - Vth)}{nv_t})]}{m* + nCox\sqrt{\frac{2\Phi_s}{q\varepsilon_{si}N_{dep}}}\exp(-\frac{(1-m*)(V_{gs\_eff} - Vth) - Voff}{nv_t})}$$

$$m* = 0.5 + \frac{arctan(MINV)}{\pi}$$

$$n = 1 + N_{factor}\frac{\varepsilon_{si}/X_{dep}}{C_{ox}} + \frac{(C_{dsc} + C_{dscd}V_{ds} + C_{dscb}V_{bseff})\left[\exp(-D_{VT1}\frac{L_{eff}}{2l_t}) + 2\exp(-D_{VT1}\frac{L_{eff}}{l_t})\right]}{C_{ox}} + \frac{C_{it}}{C_{ox}}$$

Effective Bulk Charge Factor

$$A_{bulk} = 1 + \left(\frac{K_{1ox} \cdot \sqrt{1 + LPEB/L_{eff}}}{2\sqrt{(\phi_s + Ketas) - \frac{V_{bsh}}{1 + Keta \cdot V_{bsh}}}} \left(\frac{A_0 L_{eff}}{L_{eff} + 2\sqrt{T_{si} X_{dep}}} \left(1 - A_{gs} V_{gsteff} \left(\frac{L_{eff}}{L_{eff} + 2\sqrt{T_{si} X_{dep}}} \right)^2 \right) + \frac{B_0}{W_{eff}' + B_1} \right) \right)$$

$$A_{bulk0} = A_{bulk} \left(V_{gsteff} = 0 \right)$$

Mobility and Saturation Velocity

mtrlMod = 0

For Mobmod=1

$$\mu_{eff} = \frac{\mu_o}{1 + (U_a + U_c V_{bseff})(\frac{V_{gsteff} + 2V_{th}}{T_{ox}}) + U_b(\frac{V_{gsteff} + 2V_{th}}{T_{ox}})^2}$$

For Mobmod=2

$$\mu_{eff} = \frac{\mu_o}{1 + (U_a + U_c V_{bseff})(\frac{V_{gsteff}}{T_{ox}}) + U_b(\frac{V_{gsteff}}{T_{ox}})^2}$$

For Mobmod=3

$$\mu_{eff} = \frac{\mu_0}{1 + [U_a(\frac{V_{gstef} + 2V_{th}}{T_{ox}}) + U_b(\frac{V_{gsteff} + 2V_{th}}{T_{ox}})^2](1 + U_c V_{bseff})}$$

For Mobmod=4

$$\mu_{eff} = \frac{U0}{1 + \left(UA + UC \cdot V_{bseff} \right) \left[\frac{V_{gsteff} + C_0 \cdot \left(VTH0 - VFB - \Phi_s \right)}{TOXE} \right]^{EU} + \frac{UD}{\left[1 + V_{gsteff} / V_{gsteff, Vth} \right]^{UCS}}}$$

$$V_{gsteff, Vth} = V_{gsteff} \left(V_{gse} = V_{th}, V_{ds} = V_{bs} = 0 \right)$$

mtrlMod = 1

$$E_{eff} = \frac{V_{gsteff} + 2V_{th} - 2 \cdot BSIM4type \cdot (PHIG - EASUB - Eg/2 + 0.45)}{EOT} \times \frac{3.9}{EPSRSUB}$$

For MobMod = 1

$$\mu_{eff} = \frac{\mu_o}{1 + (U_a + U_c V_{bseff}) E_{eff} + U_b E_{eff}^2}$$

For MobMod = 2

$$\mu_{eff} = \frac{\mu_o}{1 + (U_a + U_c V_{bseff})(\frac{V_{gsteff} - U_d}{T_{ox}}) + U_b(\frac{V_{gsteff} - U_d}{T_{ox}})^2}$$

$$U_d = 2 \cdot BSIM4type \cdot (PHIG - EASUB - Eg/2 + 0.45)$$

For MobMod = 3

$$\mu_{eff} = \frac{\mu_0}{1 + [U_a E_{eff} + U_b E_{eff}^2](1 + U_c V_{bseff})}$$

For MobMod = 4

$$\mu_{eff} = \frac{U0}{1 + (UA + UC \cdot V_{bseff})\left[\frac{V_{gsteff} + C_0 \cdot (VTH0 - VFB - \Phi_s)}{TOXE}\right]^{EU} + \frac{UD}{\left[1 + V_{gsteff}/V_{gsteff,Vth}\right]^{UCS}}}$$

$$V_{gsteff,Vth} = V_{gsteff}\left(V_{gse} = V_{th}, V_{ds} = V_{bs} = 0\right)$$

Drain Saturation Voltage

For $R_{ds} > 0$ or $\lambda \neq 1$:

$$V_{dsat} = \frac{-b - \sqrt{b^2 - 4ac}}{2a}$$

$$a = A_{bulk}^2 W_{eff} v_{sat} C_{ox} R_{ds} + (\frac{1}{\lambda} - 1)A_{bulk}$$

$$b = -\left[(V_{gsteff} + 2v_t)(\frac{2}{\lambda} - 1) + A_{bulk} E_{sat} L_{eff} + 3A_{bulk}(V_{gsteff} + 2v_t)W_{eff} v_{sat} C_{ox} R_{ds}\right]$$

$$c = (V_{gsteff} + 2v_t)E_{sat}L_{eff} + 2(V_{gsteff} + 2v_t)^2 W_{eff} v_{sat} C_{ox} R_{ds}$$

$$\lambda = A_1 V_{gsteff} + A_2$$

For R_{ds}=0, λ=1:

$$V_{dsat} = \frac{E_{sat}L_{eff}(V_{gsteff} + 2v_t)}{A_{bulk}E_{sat}L_{eff} + (V_{gsteff} + 2v_t)}$$

$$E_{sat} = \frac{2v_{sat}}{\mu_{eff}}$$

V_{dseff}

$$V_{dseff} = V_{dsat} - \frac{1}{2}\left[V_{dsat} - V_{ds} - \delta + \sqrt{(V_{dsat} - V_{ds} - \delta)^2 + 4\delta V_{dsat}}\right]$$

Drain current expression

$$I_{ds,MOSFET} = \frac{1}{N_{seg}} \frac{I_{ds0}(V_{dseff})}{1 + \frac{R_{ds}I_{dso}(V_{dseff})}{V_{dseff}}}(1 + \frac{V_{ds} - V_{dseff}}{V_A})$$

$$\beta = \mu_{eff} C_{ox} \frac{W_{eff}}{L_{eff}}$$

$$I_{dso} = \frac{\beta V_{gsteff}\left(1 - A_{bulk}\frac{V_{dseff}}{2(V_{gsteff} + 2v_t)}\right)V_{dseff}}{1 + \frac{V_{dseff}}{E_{sat}L_{eff}}}$$

$$V_A = V_{Asat} + \left(1 + \frac{P_{vag}V_{gsteff}}{E_{sat}L_{eff}}\right)(\frac{1}{V_{ACLM}} + \frac{1}{V_{ADIBLC}})^{-1}$$

$$V_{ACLM} = \frac{A_{bulk}E_{sat}L_{eff} + V_{gsteff}}{P_{clm}A_{bulk}E_{sat}litl}(V_{ds} - V_{dseff})$$

$$V_{ADIBLC} = \frac{(V_{gsteff} + 2v_t)}{\theta_{rout}(1 + P_{DIBLCB}V_{bseff})}(1 - \frac{A_{bulk}V_{dsat}}{A_{bulk}V_{dsat} + 2v_t})$$

$$\theta_{rout} = P_{DIBLC1}[\exp(-D_{ROUT}\frac{L_{eff}}{2l_{t0}} + 2\exp(-D_{ROUT}\frac{L_{eff}}{l_{t0}})] + P_{DIBLC2}$$

$$V_{Asat} = \frac{E_{sat}L_{eff} + V_{dsat} + 2R_{ds}\nu_{sat}C_{ox}W_{eff}V_{gsteff}[1 - \frac{A_{bulk}V_{dsat}}{2(V_{gsteff} + 2\nu_t)}]}{2/\lambda - 1 + R_{ds}\nu_{sat}C_{ox}W_{eff}A_{bulk}}$$

$$litl = \sqrt{\frac{\varepsilon_{si}T_{ox}T_{Si}}{\varepsilon_{ox}}}$$

Drain/Source Resistance

• *rdsMod* = 0 (Bias Independent External Series Resistance, Bias Dependent Internal Resistance)

$$R_{ds}(V) = R_{dsw}\frac{1 + P_{rwg}\cdot V_{gsteff} + P_{rwb}\cdot\left(\sqrt{\emptyset_s - V_{bseff}} - \sqrt{\emptyset_s}\right)}{\left(10^6 W'_{eff}\right)^{WR}}$$

$$R_s = R_{s,geo}, R_d = R_{d,geo}$$

• *rdsMod* = 1 (External *Rd*(V) and *Rs*(V))

$$R_s(V) = \frac{RSWMIN + RSW\cdot\left[-PRWB\cdot V_{bs} + \frac{1}{1 + PRWG\cdot\left(V_{gs} - V_{fbsd}\right)}\right]}{\left(1e6\cdot W_{eff}\right)^{WR}\cdot NF}$$

$$R_d(V) = \frac{RDWMIN + RDW\cdot\left[-PRWB\cdot V_{bd} + \frac{1}{1 + PRWG\cdot\left(V_{gd} - V_{fbsd}\right)}\right]}{\left(1e6\cdot W_{eff}\right)^{WR}\cdot NF}$$

Where, $V_{fbsd} = \frac{k_B T}{q}\ln\left(\frac{N_{gate}}{10^{20}}\right)$ for NGATE larger than 0, otherwise, $V_{fbsd} = 0$.

• *rdsMod* = 2 (Bias Dependent Internal Resistance, $R_{ds}(V)$)

$$R_{ds}(V) = R_{s,geo} + R_{dsw}\frac{1 + P_{rwg}\cdot V_{gsteff} + P_{rwb}\left(\sqrt{\emptyset_s - V_{bseff}} - \sqrt{\emptyset_s}\right)}{\left(10^6\cdot W'_{eff}\right)^{WR}} + R_{d,geo}$$

Where, The resistance $R_{s,geo}$ and $R_{d,geo}$ are simply calculated as the sheet resistance (RSH) times the number of squares (NRS, NRD):

$R_{s,geo}$ = NRS*RSH

$R_{d,geo}$ = NRD*RSH

Impact Ionization Current

$$I_{ii} = \alpha_0 (I_{ds,MOSFET} + F_{bjtii} I_c) \exp\left(\frac{V_{diff}}{\beta_2 + \beta_1 V_{diff} + \beta_0 V_{diff}^2} \right)$$

$$V_{diff} = V_{ds} - V_{dsatii}$$

$$V_{dsatii} = VgsStep + \left[V_{dsatii0} \left(1 + T_{ii} \left(\frac{T}{T_{nom}} - 1 \right) \right) - \frac{L_{ii}}{L_{eff}} \right]$$

$$VgsStep = \left(\frac{E_{satii} L_{eff}}{1 + E_{satii} L_{eff}} \right) \left(\frac{1}{1 + S_{ii1} V_{gsteff}} + S_{ii2} \right) \left(\frac{S_{ii0} V_{gst}}{1 + S_{iid} V_{ds}} \right)$$

Gate-Induced-Drain-Leakage (GIDL)

gidlMod = 0

$$I_{GIDL} = AGIDL \cdot W_{diod} \cdot Nf \cdot \frac{V_{ds} - V_{gse} - EGIDL + V_{fbsd}}{3 \cdot T_{oxe}} \cdot \exp\left(-\frac{3 \cdot T_{oxe} \cdot BGIDL}{V_{ds} - V_{gse} - EGIDL} \right) \cdot \frac{V_{db}^3}{CGIDL + V_{db}^3}$$

$$I_{GISL} = AGISL \cdot W_{dios} \cdot Nf \cdot \frac{-V_{ds} - V_{gse} - EGISL + V_{fbsd}}{3 \cdot T_{oxe}} \cdot \exp\left(-\frac{3 \cdot T_{oxe} \cdot BGISL}{-V_{ds} - V_{gse} - EGISL} \right) \cdot \frac{V_{sb}^3}{CGISL + V_{sb}^3}$$

gidlMod = 1

$$I_{gidl} = AGIDL \cdot W_{diod} \cdot Nf \cdot \frac{V_{ds} - RGIDL \cdot V_{gse} - EGIDL + V_{fbsd}}{3 \cdot T_{oxe}} \cdot \exp\left(-\frac{3 \cdot T_{oxe} \cdot BGIDL}{V_{ds} - V_{gse} - EGIDL} \right) \cdot \exp\left(\frac{KGIDL}{V_{bd} - FGIDL} \right)$$

$$I_{gisl} = AGISL \cdot W_{dios} \cdot Nf \cdot \frac{-V_{ds} - RGISL \cdot V_{gse} - EGISL + V_{fbsd}}{3 \cdot T_{oxe}} \cdot \exp\left(-\frac{3 \cdot T_{oxe} \cdot BGISL}{-V_{ds} - V_{gse} - EGISL} \right) \cdot \exp\left(\frac{KGISL}{V_{bs} - FGISL} \right)$$

Here $V_{fbsd} = 0$ when mtrlMod = 0.

Oxide tunneling current

In inversion,

$$J_{gb} = A \frac{V_{gb} V_{aux}}{T_{ox}^2} \left(\frac{T_{oxref}}{T_{oxqm}} \right)^{N_{tox}} exp\left(\frac{-B\left(\alpha_{gb1} - \beta_{gb1} |V_{ox}|\right) T_{ox}}{1 - |V_{ox}|/V_{gb1}} \right)$$

$$V_{aux} = V_{EVB} \, ln\left(1 + exp\left(\frac{|V_{ox}| - \varphi_g}{V_{EVB}} \right) \right)$$

$$A = \frac{q^3}{8\pi h \phi_b}$$

$$B = \frac{8\pi \sqrt{2m_{ox}} \, \phi_b^{3/2}}{3hq}$$

$$\phi_b = 4.2eV$$

$$m_{ox} = 0.3m_0$$

In accumulation,

$$J_{gb} = A \frac{V_{gb} V_{aux}}{T_{ox}^2} \left(\frac{T_{oxref}}{T_{oxqm}} \right)^{N_{tox}} exp\left(\frac{-B\left(\alpha_{gb2} - \beta_{gb2} |V_{ox}|\right) T_{ox}}{1 - |V_{ox}|/V_{gb2}} \right)$$

$$V_{aux} = V_{ECB} V_t \, ln\left(1 + exp\left(-\frac{V_{gb} - V_{fb}}{V_{ECB}} \right) \right)$$

$$A = \frac{q^3}{8\pi h \phi_b}$$

$$B = \frac{8\pi \sqrt{2m_{ox}} \, \phi_b^{3/2}}{3hq}$$

$$\phi_b = 3.1eV$$

$$m_{ox} = 0.4m_0$$

$$I_{g\_agbcp2} = A \times A_{agbcp2} \, \min(V_{gp} - V_{fb2}, 0) \times V_{gp\_eff} T_{oxRatio}$$

$$exp\left[-B \times T_{oxqm} \left(AIGBCP2 - BIGBCP2 \times V_{gp\_eff} \right) \left(1 + CIGBCP2 \times V_{gp\_eff} \right) \right]$$

$$V_{gp\_eff} = 0.5 \times \left[\sqrt{\left(V_{gp} - V_{fb2} \right)^2 + \delta^2} - \left(V_{gp} - V_{fb2} \right) - \delta \right]$$

$$\delta = 0.01$$

Body contact current

$$R_{bp} = \left(R_{body} \frac{W'_{eff}/N_{seg}}{L_{eff}} \right) // \left(R_{halo} \frac{W'_{eff}/N_{seg}}{2} \right), \quad R_{bodyext} = R_{bsh} N_{rb}$$

For 4-T device, $I_{bp} = 0$

For 5-T device,

$$I_{bp} = \frac{V_{bp}}{R_{bp} + R_{bodyext}}$$

Diode and BJT currents

Bipolar Transport Factor

$$\alpha_{bjt} = \exp\left[-0.5\left(\frac{L_{eff}}{L_n}\right)^2\right]$$

Body-to-Source/drain diffusion

$$I_{bs1} = W_{dios}T_{si}j_{difs}\left(\exp\left(\frac{V_{bs}}{n_{diode}V_t}\right) - 1\right)$$

$$I_{bd1} = W_{diod}T_{si}j_{difd}\left(\exp\left(\frac{V_{bd}}{n_{dioded}V_t}\right) - 1\right)$$

Recombination/trap-assisted tunneling current in depletion region

$$I_{bs2} = W_{dios}T_{si}j_{recs}\left(\exp\left(\frac{V_{bs}}{0.026n_{recf}}\right) - \exp\left(\frac{V_{sb}}{0.026n_{recr}}\frac{V_{rec0}}{V_{rec0} + V_{sb}}\right)\right)$$

$$I_{bd2} = W_{diod}T_{si}j_{recd}\left(\exp\left(\frac{V_{bd}}{0.026n_{recfd}}\right) - \exp\left(\frac{V_{db}}{0.026n_{recrd}}\frac{V_{rec0d}}{V_{rec0d} + V_{db}}\right)\right)$$

Reversed bias tunneling leakage

$$I_{bs4} = W_{dios}T_{si}j_{tuns}\left(1 - \exp\left(\frac{V_{sb}}{0.026n_{tun}}\frac{V_{tun0}}{V_{tun0} + V_{sb}}\right)\right)$$

$$I_{bd4} = W_{diod}T_{si}j_{tund}\left(1 - \exp\left(\frac{V_{db}}{0.026n_{tund}}\frac{V_{tun0d}}{V_{tun0d} + V_{db}}\right)\right)$$

Recombination current in neutral body

$$I_{bs3} = \left(1 - \alpha_{bjt}\right)I_{en}\left[\exp\left(\frac{V_{bs}}{n_{diode}V_t}\right) - 1\right]\frac{1}{\sqrt{E_{hli} + 1}}$$

$$I_{bd3} = \left(1 - \alpha_{bjt}\right)I_{en}\left[\exp\left(\frac{V_{bd}}{n_{dioded}V_t}\right) - 1\right]\frac{1}{\sqrt{E_{hlid} + 1}}$$

$$I_{ens} = \frac{W'_{eff}}{N_{seg}}T_{si}j_{sbjt}\left[L_{bjt0}\left(\frac{1}{L_{eff}} + \frac{1}{L_n}\right)\right]^{N_{bjt}}$$

$$I_{end} = \frac{W'_{eff}}{N_{seg}}T_{si}j_{dbjt}\left[L_{bjt0}\left(\frac{1}{L_{eff}} + \frac{1}{L_n}\right)\right]^{N_{bjt}}$$

$$E_{hlis} = A_{hli\_eff}\left[\exp\left(\frac{V_{bs}}{n_{diode}V_t}\right) - 1\right]$$

$$E_{hlid} = A_{hli\_eff}\left[\exp\left(\frac{V_{bd}}{n_{dioded}V_t}\right) - 1\right]$$

$$A_{hlis\_eff} = A_{hli}\exp\left[\frac{-E_g(300K)}{n_{diode}V_t}X_{bjt}\left(1 - \frac{T}{T_{nom}}\right)\right]$$

$$A_{hlid\_eff} = A_{hlid}\exp\left[\frac{-E_g(300K)}{n_{dioded}V_t}X_{bjt}\left(1 - \frac{T}{T_{nom}}\right)\right]$$

BJT collector current

$$I_c = \alpha_{bjt}I_{en}\left\{\exp\left[\frac{V_{bs}}{n_{diodes}V_t}\right] - \exp\left[\frac{V_{bd}}{n_{dioded}V_t}\right]\right\}\frac{1}{E_{2nd}}$$

$$E_{2nd} = \frac{E_{ely} + \sqrt{E_{ely}^2 + 4E_{hli}}}{2}$$

$$E_{ely} = 1 + \frac{V_{bs} + V_{bd}}{V_{Abjt} + A_{ely}L_{eff}}$$

$$E_{hli} = E_{hlis} + E_{hlid}$$

Total body-source/drain current

$$I_{bs} = I_{bs1} + I_{bs2} + I_{bs3} + I_{bs4}$$

$$I_{bd} = I_{bd1} + I_{bd2} + I_{bd3} + I_{bd4}$$

Total body current

$$I_{ii} + I_{dgidl} + I_{sgisl} + I_{gb} - I_{bs} - I_{bd} - I_{bp} = 0$$

Temperature effects

$$V_{th(T)} = V_{th(Tnom)} + (K_{T1} + K_{t1l} / L_{eff} + K_{T2}V_{bseff})(T / T_{nom} - 1)$$

$$\mu_{o(T)} = \mu_{o(Tnom)}(\frac{T}{T_{nom}})^{\mu te} \quad v_{sat(T)} = v_{sat(Tnom)} - A_T(T / T_{nom} - 1)$$

$$R_{dsw(T)} = R_{dsw(Tnom)} + P_{rt}(\frac{T}{T_{nom}} - 1)$$

$$U_{a(T)} = U_{a(Tnom)} + U_{a1}(T / T_{nom} - 1)$$

$$U_{b(T)} = U_{b(Tnom)} + U_{b1}(T / T_{nom} - 1)$$

$$U_{c(T)} = U_{c(Tnom)} + U_{c1}(T / T_{nom} - 1)$$

$$R_{th} = \frac{R_{th0}}{\left(W_{eff}^{'} + W_{th0}\right)/N_{seg}} \quad , \quad C_{th} = C_{th0} \frac{W_{eff}^{'} + W_{th0}}{N_{seg}}$$

$$j_{sbjt} = i_{sbjt} \exp\left[\frac{-E_g(300K)}{n_{diode}V_t} X_{bjt}\left(1 - \frac{T}{T_{nom}}\right)\right]$$

$$j_{dbjt} = i_{dbjt} \exp\left[\frac{-E_g(300K)}{n_{dioded}V_t} X_{bjt}\left(1 - \frac{T}{T_{nom}}\right)\right]$$

$$j_{sdif} = i_{sdif} \exp\left[\frac{-E_g(300K)}{n_{diode}V_t} X_{dif}\left(1 - \frac{T}{T_{nom}}\right)\right]$$

$$j_{ddif} = i_{ddif} \exp\left[\frac{-E_g(300K)}{n_{dioded}V_t} X_{difd}\left(1 - \frac{T}{T_{nom}}\right)\right]$$

$$j_{srec} = i_{srec} \exp\left[\frac{-E_g(300K)}{n_{recf0}V_t} X_{rec}\left(1 - \frac{T}{T_{nom}}\right)\right]$$

$$j_{drec} = i_{drec} \exp\left[\frac{-E_g(300K)}{n_{recf0d}V_t} X_{recd}\left(1 - \frac{T}{T_{nom}}\right)\right]$$

$$j_{stun} = i_{stun} \exp\left[X_{tun}\left(\frac{T}{T_{nom}} - 1\right)\right]$$

$$j_{dtun} = i_{dtun} \exp\left[X_{tund}\left(\frac{T}{T_{nom}} - 1\right)\right]$$

$$n_{recfs} = n_{recf0}\left[1 + nt_{recf}\left(\frac{T}{T_{nom}} - 1\right)\right]$$

$$n_{recfd} = n_{recf0d}\left[1 + nt_{recf}\left(\frac{T}{T_{nom}} - 1\right)\right]$$

$$n_{recrs} = n_{recr0}\left[1 + nt_{recr}\left(\frac{T}{T_{nom}} - 1\right)\right]$$

$$n_{recrd} = n_{recr0d}\left[1 + nt_{recr}\left(\frac{T}{T_{nom}} - 1\right)\right]$$

E_g is the energy gap energy.

Equation List for BSIMPD CV

Dimension Dependence

$$\delta W_{eff} = DWC + \frac{W_{lc}}{L^{W_{ln}}} + \frac{W_{wc}}{W^{W_{wn}}} + \frac{W_{wlc}}{L^{W_{ln}}W^{W_{wn}}}$$

$$\delta L_{eff} = DLC + \frac{L_{lc}}{L^{L_{ln}}} + \frac{L_{wc}}{W^{L_{wn}}} + \frac{L_{wlc}}{L^{L_{ln}}W^{L_{wn}}}$$

$$L_{active} = L_{drawn} - 2\delta L_{eff}$$
$$L_{activeB} = L_{active} - DLCB$$
$$L_{activeBG} = L_{activeB} + 2\delta L_{bg}$$

$$W_{active} = W_{drawn} - N_{bc}dW_{bc} - (2 - N_{bc})\delta W_{eff}$$

$$W_{diosCV} = \frac{W_{active}}{N_{seg}} + P_{sbcp}$$

$$W_{diodCV} = \frac{W_{active}}{N_{seg}} + P_{dbcp}$$

Charge Conservation

$$Q_{Bf} = Q_{acc} + Q_{sub0} + Q_{subs}$$

$$Q_{inv} = Q_{inv,s} + Q_{inv,d}$$

$$Q_g = -\left(Q_{inv} + Q_{Bf}\right)$$

$$Q_b = Q_{Bf} - Q_e + Q_{js} + Q_{jd}$$

$$Q_s = Q_{inv,s} - Q_{js}$$

$$Q_d = Q_{inv,d} - Q_{jd}$$

$$Q_g + Q_e + Q_b + Q_s + Q_d = 0$$

Intrinsic Charges

$$(1)\ capMod = 2$$

Front Gate Body Charge

Accumulation Charge

$$V_{FBeff} = V_{fb} - 0.5\left((V_{fb} - V_{gb} - \delta) + \sqrt{\left(V_{fb} - V_{gb} - \delta\right)^2 + \delta^2}\right)$$

where $V_{gb} = V_{gs} - V_{bseff}$

$$V_{fb} = V_{th} - \phi_s - K_{1eff}\sqrt{\phi_s - V_{bseff}} + delvt$$

$$Q_{acc} = -F_{body}\left(\frac{W_{active}L_{activeB}}{N_{seg}} + A_{gbcp}\right)C_{ox}(V_{FBeff} - V_{fb})$$

vgstcvMod = 0 and 1

$$V_{gsteffCV} = nv_t \ln\left(1 + \exp\left[\frac{V_{gs} - V_{th}}{nv_t}\right] \cdot \exp\left[-\frac{delvt}{nv_t}\right]\right)$$

vgstcvMod = 2

$$V_{gsteffCV} = \frac{nv_t \ln\left[1+\exp(\frac{m^{*CV}(V_{gs\_eff}-V_{th}-delvt)}{nv_t})\right]}{m^{*CV}+nC_{ox}\sqrt{\frac{2\Phi_s}{q\varepsilon_{si}N_{dep}}}\exp(-\frac{(1-m^*)(V_{gs\_eff}-V_{th}-delvt)-V_{offCV}}{nv_t})}$$

$$m^{*CV} = 0.5 + \frac{\arctan(MINVCV)}{\pi}$$

Gate Induced Depletion Charge

$$Q_{sub0} = -F_{body}\left(\frac{W_{active}L_{activeB}}{N_{seg}}+A_{gbcp}\right)C_{ox}\frac{K_{1eff}^2}{2}\left(-1+\sqrt{1+\frac{4(V_{gs}-V_{FBeff}-V_{gsteffCV}-V_{bseff})}{K_{1eff}^2}}\right)$$

Drain Induced Depletion Charge

$$V_{dsatCV} = V_{gsteffCV}/A_{bulkCV}, \ A_{bulkCV} = A_{bulk0}\left[1+\left(\frac{CLC}{L_{activeB}}\right)^{CLE}\right]$$

$$V_{dsCV} = V_{dsatCV} - \frac{1}{2}(V_{dsatCV}-V_{ds}-\delta+\sqrt{(V_{dsatCV}-V_{ds}-\delta)^2+4\delta V_{dsatCV}})$$

$$Q_{subs} = F_{body}\left(\frac{W_{active}L_{activeB}}{N_{seg}}+A_{gbcp}\right)K_{1eff}C_{ox}\left(A_{bulkCV}-1\right)\left[\frac{V_{dsCV}}{2}-\frac{A_{bulkCV}V_{dsCV}^2}{12\left(V_{gsteffCV}-A_{bulkCV}V_{dsCV}/2\right)}\right]$$

Back Gate Body Charge

$$Q_e = k_{b1}F_{body}\left(\frac{W_{active}L_{activeBG}}{N_{seg}}+A_{ebcp}\right)C_{box}\left(V_{es}-V_{fbb}-V_{bseff}\right)$$

Inversion Charge

$$V_{cveff} = V_{dsat,CV} - 0.5\left(V_4+\sqrt{V_4^2+4\delta_4 V_{dsat,CV}}\right) where V_4 = V_{dsat,CV}-V_{ds}-\delta_4; \delta_4 = 0.02$$

$$Q_{inv} = -\left(\frac{W_{active}L_{active}}{N_{seg}}+A_{gbcp}\right)C_{ox}\left(\left(V_{gsteffCV}-\frac{A_{bulkCV}}{2}V_{cveff}\right)+\frac{A_{bulkCV}^2 V_{cveff}^2}{12\left(V_{gsteffCV}-\frac{A_{bulkCV}}{2}V_{cveff}\right)}\right)$$

50/50 Charge Partition

$$Q_{inv,s} = Q_{inv,d} = 0.5 Q_{inv}$$

40/60 Charge Partition

$$Q_{inv,s} = -\frac{\left(\frac{W_{active}L_{active}}{N_{seg}} + A_{gbcp}\right)C_{ox}}{2\left(V_{gsteffCV} - \frac{A_{bulkCV}}{2}V_{cvefff}\right)^2}\left(V_{gsteffCV}^3 - \frac{4}{3}V_{gsteffCV}^2\left(A_{bulkCV}V_{cveff}\right) + \frac{2}{3}V_{gsteff}\left(A_{bulkCV}V_{cveff}\right)^2 - \frac{2}{15}\left(A_{bulkCV}V_{cveff}\right)^3\right)$$

$$Q_{inv,d} = -\frac{\left(\frac{W_{active}L_{active}}{N_{seg}} + A_{gbcp}\right)C_{ox}}{2\left(V_{gsteffCV} - \frac{A_{bulkCV}}{2}V_{cvefff}\right)^2}\left(V_{gsteffCV}^3 - \frac{5}{3}V_{gsteffCV}^2\left(A_{bulkCV}V_{cveff}\right) + V_{gsteff}\left(A_{bulkCV}V_{cveff}\right)^2 - \frac{1}{5}\left(A_{bulkCV}V_{cveff}\right)^3\right)$$

0/100 Charge Partition

$$Q_{inv,s} = -\frac{W_{active}L_{active} + A_{gbcp}}{N_{seg}}C_{ox}\left(\frac{V_{gsteffCV}}{2} + \frac{A_{bulkCV}V_{cveff}}{4} - \frac{\left(A_{bulkCV}V_{cveff}\right)^2}{24\left(V_{gsteffCV} - \frac{A_{bulkCV}}{2}V_{cveff}\right)}\right)$$

$$Q_{inv,d} = -\frac{W_{active}L_{active} + A_{gbcp}}{N_{seg}}C_{ox}\left(\frac{V_{gsteffCV}}{2} - \frac{3A_{bulkCV}V_{cveff}}{4} + \frac{\left(A_{bulkCV}V_{cveff}\right)^2}{8\left(V_{gsteffCV} - \frac{A_{bulkCV}}{2}V_{cveff}\right)}\right)$$

(2) capMod = 3 (Charge-Thickness Model)

capMod = 3 only supports zero-bias flat band voltage, which is calculated from bias-independent threshold voltage. This is different from capMod = 2. For the finite thickness (X_{DC}) formulation, refer to Chapter 4 of BSIM3v3.2 Users's Manual.

Front Gate Body Charge

Accumulation Charge

$$V_{FBeff} = V_{fb} - 0.5\left(\left(V_{fb} - V_{gb} - \delta\right) + \sqrt{\left(V_{fb} - V_{gb} - \delta\right)^2 + \delta^2}\right)$$

where $V_{gb} = V_{gs} - V_{bseff}$

$$V_{fb} = V_{th} - \phi_s - K_{1eff}\sqrt{\phi_s - V_{bseff}}$$

$$Q_{acc} = -F_{body}\left(\frac{W_{active}L_{activeB}}{N_{seg}} + A_{gbcp}\right)C_{oxeff}V_{gbacc}$$

$$V_{gbacc} = 0.5\left(V_0 + \sqrt{V_0^2 + 4\delta V_{fb}}\right)$$

$$V_0 = V_{fb} + V_{bseff} - V_{gs} - \delta$$

$$C_{oxeff} = \frac{C_{ox}C_{cen}}{C_{ox} + C_{cen}}$$

$$C_{cen} = \varepsilon_{Si}/X_{DC}$$

Gate Induced Depletion Charge

$$Q_{sub0} = -F_{body}\left(\frac{W_{active}L_{activeB}}{N_{seg}} + A_{gbcp}\right)C_{oxeff}\frac{K_{1eff}^2}{2}\left(-1 + \sqrt{1 + \frac{4(V_{gs} - V_{FBeff} - V_{gsteffCV} - V_{bseff})}{K_{1eff}^2}}\right)$$

Drain Induced Depletion Charge

$$V_{dsatCV} = (V_{gsteffCV} - \Phi_\delta)/A_{bulkCV}$$

$$\Phi_\delta = \Phi_s - 2\Phi_B = v_t \ln\left[1 + \frac{V_{gsteffCV}(V_{gstefCV} + 2K_{1eff}\sqrt{2\Phi_B})}{moinK_{1eff}v_t^2}\right]$$

$$V_{dsCV} = V_{dsatCV} - \frac{1}{2}(V_{dsatCV} - V_{ds} - \delta + \sqrt{(V_{dsatCV} - V_{ds} - \delta)^2 + 4\delta V_{dsatCV}})$$

$$Q_{subs} = F_{body}\left(\frac{W_{active}L_{activeB}}{N_{seg}} + A_{gbcp}\right)K_{1eff}C_{oxeff}(A_{bulkCV} - 1)\left[\frac{V_{dsCV}}{2} - \frac{A_{bulkCV}V_{dsCV}^2}{12(V_{gsteffCV} - \Phi_\delta - A_{bulkCV}V_{dsCV}/2)}\right]$$

Back Gate Body Charge

$$Q_e = k_{b1}F_{body}\left(\frac{W_{active}L_{activeBG}}{N_{seg}} + A_{ebcp}\right)C_{box}(V_{es} - V_{fbb} - V_{bseff})$$

Inversion Charge

$$V_{cveff} = V_{dsat,CV} - 0.5\left(V_4 + \sqrt{V_4^2 + 4\delta_4 V_{dsat,CV}}\right) where V_4 = V_{dsat,CV} - V_{ds} - \delta_4; \delta_4 = 0.02$$

$$Q_{inv} = -\left(\frac{W_{active}L_{active}}{N_{seg}} + A_{gbcp}\right)C_{oxeff}\left(\left(V_{gsteffCV} - \Phi_\delta - \frac{A_{bulkCV}}{2}V_{cveff}\right) + \frac{A_{bulkCV}^2 V_{cveff}^2}{12\left(V_{gsteffCV} - \Phi_\delta - \frac{A_{bulkCV}^2}{2}V_{cveff}\right)}\right)$$

50/50 Charge Partition

$$Q_{inv,s} = Q_{inv,.d} = 0.5Q_{inv}$$

40/60 Charge Partition

$$Q_{inv,s} = -\frac{\left(\frac{W_{active}L_{active}}{N_{seg}} + A_{gbcp}\right)C_{oxeff}}{2\left(V_{gsteffCV} - \Phi_\delta - \frac{A_{bulkCV}}{2}V_{cvefff}\right)^2}\left(\left(V_{gsteffCV} - \Phi_\delta\right)^3 - \frac{4}{3}\left(V_{gsteffCV} - \Phi_\delta\right)^2\left(A_{bulkCV}V_{cveff}\right) + \frac{2}{3}\left(V_{gsteff} - \Phi_\delta\right)\left(A_{bulkCV}V_{cveff}\right)^2 - \frac{2}{15}\left(A_{bulkCV}V_{cveff}\right)^3\right)$$

$$Q_{inv,d} = -\frac{\left(\frac{W_{active}L_{active}}{N_{seg}} + A_{gbcp}\right)C_{oxef}}{2\left(V_{gsteffCV} - \Phi_\delta - \frac{A_{bulkCV}}{2}V_{cvefff}\right)^2}\left(\left(V_{gsteffCV} - \Phi_\delta\right)^3 - \frac{5}{3}\left(V_{gsteffCV} - \Phi_\delta\right)^2\left(A_{bulkCV}V_{cveff}\right) + \left(V_{gstefCVf} - \Phi_\delta\right)\left(A_{bulkCV}V_{cveff}\right)^2 - \frac{1}{5}\left(A_{bulkCV}V_{cveff}\right)^3\right)$$

0/100 Charge Partition

$$Q_{inv,s} = -\frac{W_{active}L_{active} + A_{gbcp}}{N_{seg}}C_{oxeff}\left(\frac{V_{gsteffCV} - \Phi_\delta}{2} + \frac{A_{bulkCV}V_{cveff}}{4} - \frac{\left(A_{bulkCV}V_{cveff}\right)^2}{24\left(V_{gsteffCV} - \Phi_\delta - \frac{A_{bulkCV}}{2}V_{cveff}\right)}\right)$$

$$Q_{inv,d} = -\frac{W_{active}L_{active} + A_{gbcp}}{N_{seg}}C_{oxeff}\left(\frac{V_{gsteffCV} - \Phi_\delta}{2} - \frac{3A_{bulkCV}V_{cveff}}{4} + \frac{\left(A_{bulkCV}V_{cveff}\right)^2}{8\left(V_{gsteffCV} - \Phi_\delta - \frac{A_{bulkCV}}{2}V_{cveff}\right)}\right)$$

Overlap Capacitance

Source Overlap Charge

$$V_{gs\_overlap} = \frac{1}{2}\left\{\left(V_{gs} + \delta\right) + \sqrt{\left(V_{gs} + \delta\right)^2 + 4\delta}\right\}$$

$$\frac{Q_{overlap,s}}{W_{diosCV}} = CGS0 \cdot V_{gs} + CGS1\left\{V_{gs} - V_{gs\_overlap} + \frac{CKAPPA}{2}\left(-1 + \sqrt{1 + \frac{4V_{gs\_overlap}}{CKAPPA}}\right)\right\}$$

Drain Overlap Charge

$$V_{gd\_overlap} = \frac{1}{2}\left\{\left(V_{gd} + \delta\right) + \sqrt{\left(V_{gd} + \delta\right)^2 + 4\delta}\right\}$$

$$\frac{Q_{overlap,d}}{W_{diodCV}} = CGD0 \cdot V_{gd} + CGD1\left\{V_{gd} - V_{gd\_overlap} + \frac{CKAPPA}{2}\left(-1 + \sqrt{1 + \frac{4V_{gd\_overlap}}{CKAPPA}}\right)\right\}$$

Gate Overlap Charge

$$Q_{overlap,g} = -\left(Q_{overlap,s} + Q_{overlap,d}\right)$$

Source/Drain Junction Charge

       For $V_{bs} < 0.95\phi_s$

       else

$$Q_{jswg} = C_{bsdep}(0.95\phi_s)(V_{bs} - 0.95\phi_s) + Q_{bsdif}$$

For $V_{bd} < 0.95\phi_s$

       else

$$Q_{jdwg} = C_{bddep}(0.95\phi_s)(V_{bd} - 0.95\phi_s) + Q_{bddif}$$

where

$$Q_{bsdep} = W_{dioCV} C_{jswgs} \frac{T_{si}}{10^{-7}} \frac{P_{bswgs}}{1 - M_{jswgs}} \left[1 - \left(1 - \frac{V_{bs}}{P_{bswgs}} \right)^{1-M_{jswgs}} \right]$$

$$Q_{bddep} = W_{dioCV} C_{jswgd} \frac{T_{si}}{10^{-7}} \frac{P_{bswgd}}{1 - M_{jswgd}} \left[1 - \left(1 - \frac{V_{bd}}{P_{bswgd}} \right)^{1-M_{jswgd}} \right]$$

$$C_{jswgs} = C_{jswgs0} \left[1 + t_{cjswgs} (T - T_{nom}) \right]$$
$$C_{jswgd} = C_{jswgd0} \left[1 + t_{cjswgd} (T - T_{nom}) \right]$$
$$P_{bswgs} = P_{bswgs0} - t_{pbswgs} (T - T_{nom})$$
$$P_{bswgd} = P_{bswgd0} - t_{pbswgd} (T - T_{nom})$$

$$Q_{bsdif} = \tau \frac{W_{eff}'}{N_{seg}} T_{si} J_{sbjt} \left[1 + L_{dif0} \left(L_{bj0} \left(\frac{1}{L_{eff}} + \frac{1}{L_n} \right) \right) \right]^{N_{dif}} \left[\exp \left(\frac{V_{bs}}{n_{dios} V_t} \right) - 1 \right] \frac{1}{\sqrt{E_{hlis} + 1}}$$

$$Q_{bddif} = \tau \frac{W_{eff}'}{N_{seg}} T_{si} J_{dbjt} \left[1 + L_{dif0} \left(L_{bj0} \left(\frac{1}{L_{eff}} + \frac{1}{L_n} \right) \right) \right]^{N_{dif}} \left[\exp \left(\frac{V_{bd}}{n_{diod} V_t} \right) - 1 \right] \frac{1}{\sqrt{E_{hlid} + 1}}$$

Extrinsic Capacitance

Bottom S/D to Substrate Capacitance (per unit area)

$$C_{esb} = \begin{cases} C_{box} & \text{if} & V_{s/d,e} < V_{sdfb} \\ C_{box} - \frac{1}{A_{sd}} (C_{box} - C_{min}) \left(\frac{V_{s/d,e} - V_{sdfb}}{V_{sdth} - V_{sdfb}} \right)^2 & \text{elseif} & V_{s/d,e} < V_{sdfb} + A_{sd} (V_{sdth} - V_{sdfb}) \\ C_{min} + \frac{1}{1 - A_{sd}} (C_{box} - C_{min}) \left(\frac{V_{s/d,e} - V_{sdth}}{V_{sdth} - V_{sdfb}} \right)^2 & \text{elseif} & V_{s/d,e} < V_{sdth} \\ C_{min} & \text{else} \end{cases}$$

Sidewall S/D to Substrate Capacitance (per unit length)

$$C_{s/d,esw} = C_{sdesw} \log \left(1 + \frac{T_{si}}{T_{box}} \right)$$

Finite Thickness Formulation

When capMod = 3, the finite thickness model is selected.

mtrlMod = 0

$$C_{oxeff} = \frac{C_{oxp} \cdot C_{cen}}{C_{oxp} + C_{cen}}$$

$$C_{cen} = \varepsilon_{si} / X_{DC}$$

(i) X_{DC} for accumulation and depletion

$$X_{DC} = \frac{1}{3} L_{debye} \exp\left[ACDE \cdot \left(\frac{NDEP}{2 \times 10^{16}} \right)^{-0.25} \cdot \frac{V_{gse} - V_{bseff} - V_{FBeff}}{TOXP} \right]$$

For numerical stability,

$$X_{DC} = X_{max} - \frac{1}{2}\left(X_0 + \sqrt{X_0^2 + 4\delta_x X_{max}} \right)$$

$$X_0 = X_{max} - X_{DC} - \delta_x$$

(ii) X_{DC} of inversion charge

$$X_{DC} = \frac{ADOS \times 1.9 \times 10^{-9} \text{ m}}{1 + \left(\dfrac{V_{gsteff} + 4(VTH0 - VFB - \Phi_s)}{2TOXP} \right)^{0.7 \times BDOS}}$$

(iii) Body charge thickness in inversion

$$\varphi_\delta = \Phi_s - 2\Phi_B = v_t \ln\left(1 + \frac{V_{gsteffCV} \cdot (V_{gsteffCV} + 2K_{1ox}\sqrt{2\Phi_B})}{MOIN \cdot K_{1ox}^2 v_t} \right)$$

$$q_{inv} = -C_{oxeff} \cdot \left(V_{gsteff,CV} - \varphi_\delta \right)_{eff}$$

mtrlMod = 1

In this case, *TOXP* has to be calculated first:

$$TOXP = EOT - \frac{3.9}{EPSRSUB} \times X_{DC}\Big|_{V_{gs}=VDDEOT, V_{ds}=V_{bs}=0}$$

Then, other procedures are same in mtrlMod = 0.

Appendix D: Parameter Extraction

D.1.   Extraction Strategy

The complicated physics in SOI MOSFETs makes parameter extraction quite involved [20]. It is always preferable to have more measurements so that the parameters extracted can have more valid physical meaning. Similar to conventional bulk devices, two basic extraction strategies can be used: single device extraction, and group device extraction. The group device extraction is more popular because of several reasons. In analog circuit, channel length and width scalability is very important. In digital circuit, statistical modeling is often used to predict the circuit performance due to process variation. Hence channel length scalability is also important. Besides, model parameters extracted from group device extraction have better physical meaning than that from single device extraction. In this work, we shall emphasize on group device extraction.

Parameter extraction using body contact devices is highly recommended because parameters related to body effect, impact ionization and leakage currents can be directly extracted [18, 19]. This yields less ambiguity in extracting technology parameters for I-V fitting purposes. In the followings, we suggest a set of measurement suitable for PD devices.

D.2.   Suggested I-V Measurement

Measurement set A is used to extract basic MOS I-V parameters. For each body-contacted device :

$\quad$ (A1)$\quad$ I_{ds} vs. V_{gs} @ small V_{ds} with different V_{bs}, V_{es}=0V.

$\quad$ (A2)$\quad$ I_{ds} vs. V_{gs} @ V_{ds}=V_{dd} with different V_{bs}, V_{es}=0V.

$\quad$ (A3)$\quad$ I_{ds} vs. V_{ds} with different V_{gs} and different V_{bs}, V_{es}=0V.

Parameters extracted include threshold voltage, body coefficient, delta L and W, series resistance, mobility, short channel effect, and subthreshold swing. (A2) is used to extract DIBL

parameters at subthreshold. (A3) is used to extract saturation velocity, body charge effect, output resistance, body contact resistance and self-heating parameters.

Measurement set C is used to extract impact ionization current parameters. For each body-contacted device :

(C1) I_b vs. V_{gs} @ different V_{ds}, V_{bs}=0V, V_{es}=0V.

(C2) I_b vs. V_{ds} @ different V_{gs}, V_{bs}=0V, V_{es}=0V.

Measurement set D is used to extract MOS temperature dependent parameter. For a long channel body-contacted device:

(D1) I_{ds} vs. V_{gs} @ small V_{ds}, V_{bs}=0V, V_{es}=0V, repeat with several temperatures.

(D2) I_{ds} vs. V_{ds} @ different V_{gs}, V_{bs}=0V, V_{es}=0V, repeat with several temperatures.

Notice that the self-heating parameters have to be extracted from set A.

Measurement set E is used to extract diode parameters. For a long channel body-contacted device or gated diode :

(E1) I_{diode} vs. V_{bs} @ V_{gs}=-1V, V_{es}=0V, repeat with several temperature

Measurement set F is used to extract BJT parameters. For each body-contacted device:

(F1) I_{ds} vs. I_b @ V_{gs}=-1V, V_{es}=0V, V_{ds}=1V.

Measurement set G is used to verify the floating body device data. For each floating-body device :

(G1) I_{ds} vs. V_{gs} @ small V_{ds}.

(G2) I_{ds} vs. V_{gs} @ V_{ds}=V_{dd}.

(G3) I_{ds} vs. V_{ds} @ different V_{gs}.

Appendix E: Model Parameter Binning

Below is the information on parameter binning regarding which model parameters can or cannot be binned. All those parameters which can be binned follow this implementation:

$$P = P_0 + \frac{P_L}{L_{eff}} + \frac{P_W}{W_{eff}} + \frac{P_P}{L_{eff} \times W_{eff}}$$

For example, for the parameter k1: P_0 = k1, P_L = lk1, P_W = wk1, P_P = pk1. binUnit is a bining unit selector. If binUnit = 1, the units of L_{eff} and W_{eff} used in the binning equation above have the units of microns; otherwise in meters.

For example, for a device with L_{eff} = 0.5µm and W_{eff} = 10µm. If binUnit = 1, the parameter values for *vsat* are 1e5, 1e4, 2e4, and 3e4 for *vsat*, *lvsat*, *wvsat*, and *pvsat*, respectively. Therefore, the effective value of *vsat* for this device is

$$vsat = 1e5 + 1e4/0.5 + 2e4/10 + 3e4/(0.5*10) = 1.28e5$$

To get the same effective value of *vsat* for binUnit = 0, the values of *vsat*, *lvsat*, *wvsat*, and *pvsat* would be 1e5, 1e-2, 2e-2, 3e-8, respectively. Thus,

$$vsat = 1e5 + 1e-2/0.5e-6 + 2e-2/10e-6 + 3e-8/(0.5e-6 * 10e-6) = 1.28e5$$

Model parameters that have been binned in B4SOI are listed as follows:

E.1. DC Parameters

Symbol used in equation	Symbol used in SPICE	Description
V_{th0}	vth0	Threshold voltage @V_{bs}=0 for long and wide device
K_1	k1	First order body effect coefficient
K_{1w1}	k1w1	First body effect width dependent parameter
K_{1w2}	k1w2	Second body effect width dependent parameter
K_2	k2	Second order body effect coefficient
K_3	k3	Narrow width coefficient
K_{3b}	k3b	Body effect coefficient of k3
K_{b1}	Kb1	Backgate body charge coefficient
W_0	w0	Narrow width parameter
N_{LX}	nlx	Lateral non-uniform doping parameter
D_{vt0}	Dvt0	first coefficient of short-channel effect on Vth
D_{vt1}	dvt1	Second coefficient of short-channel effect on Vth
D_{vt2}	dvt2	Body-bias coefficient of short-channel effect on Vth
D_{vt0w}	dvt0w	first coefficient of narrow width effect on Vth for small channel length
D_{vt1w}	dvt1w	Second coefficient of narrow width effect on Vth for small channel length
D_{vt2w}	dvt2w	Body-bias coefficient of narrow width effect on Vth for small channel length
μ_0	u0	Mobility at Temp = Tnom
U_a	ua	First-order mobility degradation coefficient
U_b	ub	Second-order mobility degradation coefficient
U_c	uc	Body-effect of mobility degradation coefficient
v_{sat}	vsat	Saturation velocity at Temp=Tnom
$A0$	a0	Bulk charge effect coefficient for channel length

A_{gs}	ags	Gate bias coefficient of A_{bulk}
$B0$	b0	Bulk charge effect coefficient for channel width
$B1$	b1	Bulk charge effect width offset
$Keta$	keta	Body-bias coefficient of bulk charge effect
$Ketas$	Ketas	Surface potential adjustment for bulk charge effect
A_1	A1	First non-saturation effect parameter
A_2	A2	Second non-saturation effect parameter
R_{dsw}	rdsw	Parasitic resistance per unit width
$Prwb$	prwb	Body effect coefficient of Rdsw
$Prwg$	prwg	Gate bias effect coefficient of Rdsw
Wr	wr	Width offset from Weff for Rds calculation
$Nfactor$	nfactor	Subthreshold swing factor
$Wint$	wint	Width offset fitting parameter from I-V without bias
$Lint$	lint	Length offset fitting parameter from I-V without bias
DWg	dwg	Coefficient of W_{eff}'s gate dependence
DWb	dwb	Coefficient of W_{eff}'s substrate body bias dependence
V_{off}	voff	Offset voltage in the subthreshold region for large W and L
$Eta0$	eta0	DIBL coefficient in subthreshold region
$Etab$	etab	Body-bias coefficient for the subthreshold DIBL effect
$EtabCV$	etabcv	Body-bias coefficient for the subthreshold DIBL effect for CV
D_{sub}	dsub	DIBL coefficient exponent
C_{it}	cit	Interface trap capacitance
C_{dsc}	cdsc	Drain/Source to channel coupling capacitance
C_{dscb}	cdscb	Body-bias sensitivty of C_{dsc}
C_{dscd}	cdscd	Drain-bias sensitivty of C_{dsc}
P_{clm}	pclm	Channel length modulation parameter
P_{dibl1}	pdibl1	First output resistance DIBL effect correction parameter
P_{dibl2}	pdibl2	Second output resistance DIBL effect correction parameter
D_{rout}	drout	L dependence coefficient of the DIBL correction parameter in Rout

$Pvag$	pvag	Gate dependence of Early voltage
δ	delta	Effective V_{ds} parameter
α_0	alpha0	The first parameter of impact ionization current
F_{bjtii}	fbjtii	Fraction of bipolar current affecting the impact ionization
β_0	beta0	First V_{ds} dependent parameter of impact ionization current
β_1	beta1	Second V_{ds} dependent parameter of impact ionization current
β_2	beta2	Third V_{ds} dependent parameter of impact ionization current
$V_{dsatii0}$	vdsatii0	Nominal drain saturation voltage at threshold for impact ionization current
T_{ii}	tii	Temperature dependent parameter for impact ionization current
L_{ii}	lii	Channel length dependent parameter at threshold for impact ionization current
E_{satii}	esatii	Saturation channel electric field for impact ionization current
S_{ii0}	sii0	First V_{gs} dependent parameter for impact ionization current
S_{ii1}	sii1	Second V_{gs} dependent parameter for impact ionization current
S_{ii2}	sii2	Third V_{gs} dependent parameter for impact ionization current
S_{iid}	siid	V_{ds} dependent parameter of drain saturation voltage for impact ionization current
α_{gidl}	Agidl	GIDL constant
β_{gidl}	Bgidl	GIDL exponential coefficient
χ	Ngidl	GIDL V_{ds} enhancement coefficient
n_{tun}	Ntun	Reverse tunneling non-ideality factor
n_{diode}	Ndiode	Diode non-ideality factor
n_{recf0}	Nrecf0	Recombination non-ideality factor at forward bias
n_{recr0}	Nrecr0	Recombination non-ideality factor at reversed bias
i_{sbjt}	Isbjt	BJT injection saturation current
i_{sdif}	Isdif	Body to source/drain injection saturation current
i_{srec}	Isrec	Recombination in depletion saturation current
i_{stun}	Istun	Reverse tunneling saturation current

V_{rec0}	Vrec0	Voltage dependent parameter for recombination current
V_{tun0}	Vtun0	Voltage dependent parameter for tunneling current
N_{bjt}	Nbjt	Power coefficient of channel length dependency for bipolar current
L_{bjt0}	Lbjt0	Reference channel length for bipolar current
V_{abjt}	Vabjt	Early voltage for bipolar current
A_{ely}	Aely	Channel length dependency of early voltage for bipolar current
A_{hli}	Ahli	High level injection parameter for bipolar current
V_{bsa}	vbsa	"vbsa offset voltage"
V_{sce}	vsce	SCE parameter for improved dVbi model
C_{dsbs}	cdsbs	coupling from Vd to Vbs for improved dVbi model
V_{offfd}	vofffd	smoothing parameter in FD module
N_{offfd}	nofffd	smoothing parameter in FD module
M_{oinfd}	moinfd	Coefficient for the gate-bias dependent surface potential in FD
K_{1b}	k1b	First backgate body effect parameter
K_{2b}	k2b	Second backgate body effect parameter
D_{k2b}	dk2b	Third backgate body effect parameter for short channel effect
D_{vbd0}	dvbd0	First short-channel effect parameter in FD module
D_{vbd1}	dvbd1	Second short-channel effect parameter in FD module
V_{bs0pd}	vbs0pd	Upper bound of built-in potential lowering for PD operation
V_{bs0fd}	vbs0fd	Lower bound of built-in potential lowering for PD operation

E.2. AC and Capacitance Parameters

Symbol used in equation	Symbol used in SPICE	Description
V_{sdfb}	vsdfb	Source/drain bottom diffusion capacitance flatband voltage
V_{sdth}	vsdth	Source/drain bottom diffusion capacitance threshold voltage
$DelVt$	delvt	Threshold voltage adjust for C-V
$acde$	acde	Exponential coefficient for charge thickness in capMod=3 for accumulation and depletion regions.
$moin$	moin	Coefficient for the gate-bias dependent surface potential.

References

[1]   Y. Cheng, M. C. Jeng, Z. H. Liu, J. Huang M. Chan, P. K. Ko, and C. Hu, "A Physical   and Scalable I-V Model in BSIM3v3 for Analog/Digital Circuit Simulation", *IEEE Trans. On Elec. Dev.,* vol. 42, p. 2, Feb 1997.

[2]   BSIM3SOIv1.3 Users' Manual, UC Berkeley, Department of EECS.

[3]   W. Jin, P. C. H. Chan, S. K. H. Fung, P. K. Ko, "A Physically-Based Low-Frequency Noise Model for NFD SOI MOSFET's", *IEEE Intl. SOI conf.,* pp. 23-24, 1998.

[4]   BSIM3v3.2 Users' Manual, UC Berkeley, Department of EECS.

[5]   D. Suh, J. G. Fossum, "A physical charge-based model for non-fully depleted SOI MOSFET's and its use in assessing floating-body effects in SOI CMOS circuits", *IEEE Tran. on Electron Devices,* vol. 42, no. 4, pp. 728-37, April 1995.

[6]   M. S. L. Lee, W. Redman-White, B. M. Tenbroek, M. Robinson, "Modelling of thin film SOI devices for circuit simulation including per-instance dynamic self-heating effects", *IEEE Intl. SOI conf.,* pp. 150-151, 1993.

[7]   D. Sinitsky, S. Tang, A. Jangity, F. Assaderaghi, G. Shahidi, C. Hu, "Simulation of SOI Devices and Circuits using BSIM3SOI", *IEEE Electron Device Letters,* vol. 19, no. 9, pp. 323-325, September 1998.

[8]   G. S. Gildenblat, VLSI Electronics: Microstructure Science, p. 11, vol. 18, 1989.

[9]   M. C. Jeng, "Design and Modeling of Deep-Submicrometer MOSFETs", Ph. D. Dissertation, UC Berkeley.

[10]   D. Sinitsky, S. Fung, S. Tang, P. Su, M. Chan, P. Ko, C. Hu, "A Dynamic Depletion SOI MOSFET Model for SPICE", in *Dig. Tech. Papers, Symp. VLSI Technology*, 1998.

[11]   D. Sinitsky, R. Tu, C. Liang, M. Chan, J. Bokor and C. Hu, "AC output conductance of SOI MOSFETs and impact on analog applications", *IEEE Electron Device Letters,* vol.18, no.2, pp. 36-38, Feb 1997.

[12]   T. Y. Chan, P. K. Ko and C. Hu, "A Simple Method to Characterize Substrate Current in MOSFETs", *IEEE Electron Dev. Letts*., EDL-5, Dec 1984, p. 505.

[13]   S. A. Parke, J. E. Moon, H. C. Wann, P. K. Ko and C. Hu, "Design for suppression of gate-induced drain leakage in LDD MOSFETs using a quasi-two-dimensional analytical model", *IEEE Trans. On Electron Device,* vol. 39, no. 7, pp. 1697-703, July 1992.

[14]   J. Gautier and J. Y.-C. Sun, "On the transient operation of partially depleted SOI NMOSFET's", *IEEE Electron device letters,* vol.16, no.11, pp. 497-499, Nov 1995.

[15]   L. T. Su, D. A. Antoniadis, M. I. Flik, J. E. Chung, "Measurement and modeling of self- heating effects in SOI nMOSFETs", *IEDM tech. Digest,* pp. 357-360, 1994.

[16]   R. H. Tu, C. Wann, J. C. King, P. K. Ko, C. Hu, "An AC Conductance Technique for Measuring Self-Heating in SOI MOSFET's", *IEEE Electron device letters,* vol.16, no.2, pp. 67-69, Feb. 1995.

[17]   P. Su, S. K. H. Fung, F. Assaderaghi, C. Hu, "A Body-Contact SOI MOSFET Model for Circuit Simulation", *Proceedings of the 1999 IEEE Intl. SOI Conference*, pp.50-51.

[18]   P. Su, S. K. H. Fung, S. Tang, F. Assaderaghi and C. Hu, "BSIMPD: A Partial-Depletion SOI MOSFET Model for Deep-Submicron CMOS Designs", *Proceedings of the IEEE 2000 Custom Integrated Circuits Conference*, pp.197-200.

References

[19] H. Nakayama, P. Su , C. Hu, M. Nakamura, H. Komatsu, K. Takeshita, Y. Komatsu, "Methodology of Self-Heating Free Parameter Extraction and Circuit Simulation for SOI CMOS", *Proceedings of the IEEE 2001 Custom Integrated Circuits Conference*, pp.381-384.

[20] P. Su, "An International Standard Model for SOI Circuit Design," Ph. D. Dissertation, Department of EECS, University of California at Berkeley, December 2002. (http://www.eecs.berkeley.edu/~pinsu)

[21] http://www.eigroup.org/cmc

[22] P. Su, S. Fung, H. Wan, A. Niknejad, M. Chan and C. Hu, "An impact ionization model for SOI circuit simulation," *2002 IEEE International SOI Conference Proceedings*, Williamsburg, VA, Oct. 2002, pp. 201-202.

[23] P. Su, K. Goto, T. Sugii and C. Hu, "A thermal activation view of low voltage impact ionization in MOSFETs," *IEEE Electron Device Letters*, vol. 23, no. 9, September 2002.

[24] P. Su, K. Goto, T. Sugii and C. Hu, "Enhanced substrate current in SOI MOSFETs," *IEEE Electron Device Letters*, vol. 23, no. 5, pp. 282-284, May 2002.

[25] P. Su et al., "On the body-source built-in potential lowering of SOI MOSFETs," *IEEE Electron Device Letters*, February 2003.

[26] BSIMSOI3.2 Users' Manual, UC Berkeley, Department of EECS.

[27] BSIM4.5.0 Users' Manual, UC Berkeley, Department of EECS.

[28] H. Wan, P. Su, S.K.H. Fung, C.L. Chen, P.W. Wyatt, A.M. Niknejad, C. Hu, "RF Modeling for FDSOI MOSFET and Self Heating Effect on RF Parameter Extraction", *Eighth International Conference on Modeling and Simulation of Microsystems*, May 2005.

[29]   K.W. Su**,** K.H. Chen, T.X. Chung, et. al, "Modeling Isolation-induced Mechanical Stress Effect on SO1 MOS Devices", *IEEE International SOI conference Proceedings*, pp 80-82, 2003.

[30]   Xuemei Xi, Fei Li, Bogdan Tudor, Wenyuan Wang, Weidong Liu, Frank Lee, Ping Wang, Niraj Subba, Jung-Suk Goo, "An Improved Impact Ionization Model for SOI Circuit Simulation", *Eleventh International Conference on Modeling and Simulation of Microsystems*, *June 2008.*